

UNIVERSIDADE DE SÃO PAULO
INSTITUTO DE FÍSICA DE SÃO CARLOS

MOHAMMAD SADRAEIAN

Production and Characterization of Pulchellin A
chain conjugated to HIV mAbs, and study its
selective cytotoxicity against cells expressing HIV
envelope

São Carlos

2017

MOHAMMAD SADRAEIAN

Production and Characterization of Pulchellin A
chain conjugated to HIV mAbs, and study its
selective cytotoxicity against cells expressing HIV
envelope

Dissertation or Thesis presented to the
Graduate Program in Physics at the Instituto
de Física de São Carlos, Universidade de São
Paulo to obtain the degree of Master or Doctor
of Science.

Concentration area: Applied Physics
Option: Biomolecular Physics

Advisor: Prof. Dr. Francisco E. G. Guimaraes.

Corrected Version
(Original version available on the Program Unit)

São Carlos

2017

I AUTHORIZE THE REPRODUCTION AND DISSEMINATION OF TOTAL OR PARTIAL COPIES OF THIS DOCUMENT, BY CONVENCIONAL OR ELECTRONIC MEDIA FOR STUDY OR RESEARCH PURPOSE, SINCE IT IS REFERENCED.

Cataloguing data revised by the Library and Information Service
of the IFSC, with information provided by the author

Sadraeian, Mohammad

Production and Characterization of Pulchellin A chain conjugated to HIV mAbs, and study its selective cytotoxicity against cells expressing HIV envelope / Mohammad Sadraeian; advisor Francisco Eduardo Gontijo Guimarães - revised version -- São Carlos 2017.

112 p.

Dissertation (Master's degree - Graduate Program in Biomolecular Physics) -- Instituto de Física de São Carlos, Universidade de São Paulo - Brasil , 2017.

1. Pulchellin. 2. HIV monoclonal Antibody. 3. Cytotoxicity assay. 4. Confocal microscopy. 5. Flow cytometry. I. Guimarães, Francisco Eduardo Gontijo, advisor. II. Title.

“Whoever has taught me one letter has made me his/her slave.”

ACKNOWLEDGEMENTS

I would like to acknowledge the people responsible for guiding and assisting me throughout this process, without support from each one I would not be where I am today. First, I must thank, Drs. Francisco Guimaraes and Seth Pincus, who tirelessly gave of their time and expertise to guide me in the right direction. I'd also like to thank the other professors for their assistance: Drs. Ana Paula Araujo and Dr. Igor Polikarpov. Also, I would like to thank my friends in the lab, at HIV lab in Children's Hospital in USA and IFSC, USP in Brazil. Finally, I need to thank my wonderful family for their support throughout the last four years and the thirty before.

“The purpose in life is to "be among those who renew the world...to make the world progress towards perfection". Its basic maxims include: Good Thoughts, Good Words, Good Deeds.”

Zoroaster

ABSTRACT

SADRAEIAN, M. **Production and Characterization of Pulchellin A chain conjugated to HIV mAbs, and study its selective cytotoxicity against cells expressing HIV envelope.** 2017. 112 p. Thesis (Doctor of Sciences) – Instituto de Física de São Carlos, Universidade de São Paulo, São Carlos, 2017.

Immunotoxins (ITs), which consist of antibodies conjugated to toxins, have been proposed as a treatment for cancer and chronic infections. To develop and improve the ITs, different toxins such as ricin, have been used, aiming for higher efficacy against target cells. The toxin pulchellin, isolated from the *Abrus pulchellus* plant, has similar structure and function as ricin. Here we have compared two plant toxins, recombinant A chains from ricin (RAC) and pulchellin (PAC) toxins, for their ability to kill HIV Env-expressing cells. Briefly, RAC and PAC were produced in *E. coli*, and chromatographically purified, then chemically conjugated to two different anti-HIV monoclonal antibodies (MAbs), anti-gp120 MAb 924 or anti-gp41 MAb 7B2. These conjugates were characterized biochemically by microcapillary electrophoresis and BCA assay and immunologically by a variety of ELISA tests. We performed a side-by-side comparison of their ability to bind, enter and kill HIV infected cells (H9/NL4-3) or Env-transfected 293T cells, as well as their non-specific toxicity on uninfected or non-transfected parental cells. Cell binding and internalization were studied by flow cytometry and confocal microscopy. Results showed that PAC can function within an effective IT. The ITs demonstrated specific binding against native antigens on persistently HIV-infected cells and recombinant antigens on Env-transfected cells. An irrelevant antibody conjugated to either RAC or PAC had no effect. PAC cytotoxicity appears somewhat less than RAC, the standard for comparison. This is the first report that PAC may have utility for the design and construction of therapeutic ITs, highlighting the potential role for specific cell targeting not only for AIDS also for cancer therapy.

Keywords: Pulchellin. HIV monoclonal Antibody. Cytotoxicity assay. Confocal microscopy. Flow cytometry.

RESUMO

SADRAEIAN, M. **Produção e Caracterização da cadeia de Pulchellin A conjugada com mAbs de HIV e estudo da citotoxicidade seletiva contra células que expressam o envelope de HIV.** 2017. 112 p. e (Doutorado em Ciências) – Instituto de Física de São Carlos, Universidade de São Paulo, São Carlos, 2017.

As toxinas imunológicas (TIs), que consistem em anticorpos conjugados com toxinas, foram propostas como tratamento para câncer e infecções crônicas. Para desenvolver e melhorar as TI, diferentes toxinas, como a ricina, foram usadas, visando uma maior eficácia contra células alvo. A toxina pulchellina, isolada da planta de *Abrus Pulchellus*, tem estrutura e função semelhantes à da ricina. Aqui, comparamos duas toxinas de plantas, cadeias A recombinantes de toxinas de ricina (RAC) e pulchellina (PAC), por sua capacidade de matar células que expressam HIV. Resumidamente, RAC e PAC foram produzidos em *E. coli* e purificados por cromatografia, depois conjugados quimicamente com dois anticorpos monoclonais anti corpo-HIV diferentes (MAcs), MAc 924 anti-gp120 ou MAc 7B2 anti-gp41. Estes conjugados foram caracterizados bioquimicamente por eletroforese microcapilar e teste BCA e imunologicamente por uma variedade de testes ELISA. Realizamos uma comparação lado-a-lado de sua capacidade de ligar, entrar e matar células infectadas pelo HIV (H9 / NL4-3) ou células 293T transfectadas com Env, bem como a sua toxicidade não específica em parentes não infectados ou não transfectados Células. A ligação celular e a internalização foram estudadas por citometria de fluxo e microscopia confocal. Os resultados mostraram que PAC pode funcionar dentro de uma TI efetiva. As TI demonstraram ligação específica contra antígenos nativos em células persistentemente infectadas pelo HIV e antígenos recombinantes em células transfectadas com Env. Um anticorpo irrelevante conjugado com RAC ou PAC não teve efeito. A citotoxicidade de PAC aparece um pouco menor que o RAC, o padrão de comparação. Este é o primeiro relatório que o PAC pode ter utilidade para o projeto e a construção de TI terapêuticas, destacando o papel potencial para o direcionamento celular específico, não apenas para a AIDS, também para a terapia do câncer.

Palavras-chave: Pulchellin. Anticorpo monoclonal do HIV. Ensaio de citotoxicidade. Microscopia confocal. Citometria de fluxo.

LIST OF FIGURES

- Figure 1 – Mechanism of action of ribosome-inactivating proteins (RIPs). A specific N-glycosidase activity cleaves adenine (A4324), which is located in the sarcin–ricin loop of the ribosomal RNA of the large subunit. 32
- Figure 2 – Schematic structure of RIPs type II 33
- Figure 3 – Schematic representation of the intoxication pathways followed by Ricin (A)... 35
- Figure 4 - Antibody structure; Labels indicate heavy (blue) and light (red) chains, variable (light) and constant (dark) regions, and antigen binding site. 39
- Figure 5 - Schematic structure of Antibody Drug Conjugates. 46
- Figure 6 - HIV genome organization and virus structure **A**, Genome organization showing major genes of HIV. **B**, 3D structure of HIV virions (HIV-derived proteins shown in orange, human in grey)..... 49
- Figure 7 – Illustration of HIV life cycle [Shattock, 2012. CSHPM] 53
- Figure 8 – Env structure with earliest neutralizing antibody epitopes 54
- Figure 9 - Crystal structure of b12-Fv bound to gp120; Secondary structures reveal the CDR loops and Ig domain- folds of b12, and the bridging sheet, inner, and outer domains of gp120. 56
- Figure 10 - 2F5 and 4E10 epitopes overlaid on SIV gp160. a, Peptide epitope superimposed on Env shell with gp41 anchor residues shown. b and c, Overlay of Fv structures of 2F5 (b) and 4E10 (c) on peptide epitopes and Env shell..... 57
- Figure 11 - Shell of gp120 with broadly neutralizing antibody epitope. Illustration shows a transparent glycosylated Env trimer anchored into viral membrane with binding sites for major recently discovered bnAbs to gp120 and gp41 59
- Figure 12 - Organization of the HIV-1 virion. Env consists of two smaller glycoproteins: gp41 forms the stem and gp120 the tip. A great deal of study has focused on one part of the gp120 glycoprotein known as the V3 (variable region #3) loop. The V3 loop is involved in both the virus's infection of host cells and in recognition of HIV by the immune system..... 62
- Figure 13 - A. Schematic picture of the sequence of rPAC after generation by PCR. Herein, the target sequence was subcloned into pET28a(+) vector (Novagen). B. Schematic constructs of rPAC and rRAC, demonstrating the position of Thioredoxin and TEV in pET28a(+) vector. 72
- Figure 14 – Espectros de transmissão no infravermelho das amostras de vidros Teluritos/Germanatos. A banda de absorção centrada em torno de 3 μm é devido à presença dos radicais OH \cdot . Percebe-se a queda mais acentuada na transmissão para essa banda conforme a quantidade de GeO $_2$ incorporada à

matriz vítrea é incrementada. O valor máximo de transmissão para cada amostra nesse intervalo está indicado na escala das ordenadas. 73

Figure 15 – Schematic representation of the delivery of cytotoxic immunotoxins based on pulchellin A chain to the relevant antigens. The overall structures of two antibodies conjugated to PAC are shown. Cell lines are depicted in different morphology representing suspension H9 lymphoma cells (A) and adherent 293T (B) cells. A. 924 MAb specifically targets HIV infected cells expressing native Env on the surface. After internalization of 924-PAC, the toxin compartment has separated from MAb, and PAC kills the cell. B. 293T cell lines are stably transfected with gp160, expressing gp120 and gp41 on the surface. Anti-gp120 (CD4) has a positive cooperativity on the binding of 7B2-PAC to the hairpin loop of gp41. Neither ITs nor CD4 bind to non-transfected 293T cells. 77

Figure 16 – SDS-PAGE analysis of purified His6 tag-removed products of rPAC (A) and rRAC (D) after cleavage by TEV protease by Sephacryl S-200 column; lane A, Protein marker; lane B, rRAC; lane C, Control rRAC; lane D, rRAC. The arrow indicates the similar molecular weight of 27 kDa for both rPAC and rRAC. 77

Figure 17 – Microcapillary electrophoresis of reduced and non-reduced protein preparations with 10, 20 or 40-fold molar excess of antibody-biolinker. Results show the conjugates with 40-fold molar excess of LC-SPDP biolinker give major bands of the predicted molecular weights for one, two and three toxin A chains per antibody molecule. Red arrows indicate the conjugate harboring three toxin A chains. The star symbol (*) means under reducing conditions by using 2-Mercaptoethano. 80

Figure 18 – Characterization of immunoconjugates (ICs). A. The table shows components of ICs with different concentrations of LC-SPDP biolinker. The final products include 10 ICs as well as 2 conjugates with irrelevant MAb, as control. B. Microcapillary electrophoresis of reduced and non-reduced ICs. Results are displayed in the familiar format of a coumassie stained gels. Size standards are indicated on the side of each “gel”. PAC, RAC and light chain of 924 MAb represent the same molecular size on the gel. The star symbol (*) means under reducing conditions by using 2-Mercaptoethanol. The ICs represent the conjugation with 40-fold molar excess of LC-SPDP biolinker. C. Electropherogram of 924-PAC IC, after passing from Ultra-100K centrifugal filter, demonstrates the negligible presence of free MAb as well as MAbs conjugated with 1, 2, 3 or even 4 PAC. D. Peak table of RAC and PAC ICs show the percentage of MAbs conjugated with A chains. 82

Figure 19 – Fluorescence correlation spectroscopy (FCS) to confirm the conjugation of 924-PAC with Alexa Fluor 488. Red line shows a significant shift to the right side, as a result of labeling between mAb-PAC and Alexa Fluor 488. 83

Figure 20 – 924 based-ITs bind to recombinant antigens and native antigens on the HIV infected cells. A. ELISA plates are coated with a synthetic V3 loop peptide,

recombinant gp120 and gp41 peptide as a control ligand. The results show the binding of 924 MAb and 924-ICs to the either gp120 or V3 peptide, but not the unrelated isotype controls. B. ELISA plates are coated with recombinant RAC, PAC and recombinant gp120 as a control ligand. The results demonstrate the binding of anti-ricin A chain MAb (RAC18) to rPAC and rRAC, but not the unrelated isotype control. In panels A and B, the Ab binding is detected with AP-conjugated goat anti-mouse IgG. Where no error bars are visible they are obscured by the symbol. Results are representative of means of duplicate values with at least three different assays (varying by Ab, ITs, or Ag tested)..... 83

Figure 21 – Binding ability of 7B2 based-ITs to gp41 antigen by using ELISA and flow cytometry. A. ELISA plates coated with gp41 Ag, as a peptide representing 7B2's epitope. Binding of the 7B2 based-ITs is detected by AP-conjugated goat anti-human IgG. Results are representative of means of triplicate values with three individual experiments. 84

Figure 22 – The concentration of LC-SPDP biolinker did not have a significant effect on the antigen binding ability of immunoconjugates. The graphs show ELISA assay of the conjugates based on either 924 MAb (A) or 7B2 MAb (B) with different fold molars of biolinker (10X, 20X or 40X). A. ELISA binding of 924-ITs to recombinant gp120 antigen were compared side by side. B. 7B2-ITs with 10X or 20X molar excess of biolinker were compared for binding ability to gp41 antigen. Results are representative of at least three independent experiments..... 84

Figure 23 – Flow cytometry histograms for binding of 924 MAb and 924 based-ITs to uninfected H9 cells, as control, and persistently-infected H9/NL4-3 cells. Binding was detected with Alexa488 conjugated goat anti-mouse IgG. On the right, IT binding to H9/NL4-3 cells is plotted as median fluorescence versus IT concentration. The results are representative of three independent experiments. Isotype control is shown as red shaded histogram. 85

Figure 24 – A. Using FITC-secondary immunofluorescence, we detect binding of ITs to Env-transfected 293T cells in the presence (darker line) or absence (lighter line) of sCD4 (CD4-183). Isotype control is shown as red shaded histogram. B. IT binding to 293T cells and transfected 293T cells with 92UG037.8 gp160 (293T/92UG). 86

Figure 25 – Distinguishing the internalized ITs from those bound on the cell surface by using quenching effect of Trypan Blue (TB). All the flow cytometry and microscopic experiments are in the presence of sCD4-183 (300 ng/ml) **A**. Before incubation with ITs, the viability of cells was 96%. The diagrams show percentage of 7B2-PAC-Alexa488 that remained fluorescent after the addition an increasing concentration of TB (1, 2 and 3 mg/ml). In the presence of NaAz, 7B2-PAC can only attach to the cell membrane, without cell internalization. As the right diagram demonstrates, the addition of an increasing concentration of TB shows that a concentration of 3 mg/ml of TB is sufficient to quench the extracellular fluorescence. In the absence of NaAz, due to the IT internalization, the fluorescence intensity of ITs remain intact from quenching by TB (**B, C**). Dot plots of cells incubated with 7B2-PAC-

Alexa488 (**B**) or 7B2-RAC-Alexa488 (**C**) in the absence of NaAz, analyzed by flow cytometry before TB addition and 2 hr after that. Before TB addition, the dot plots of the cell population incubated with Alexa-ITs, either adherent to plasma membrane or internalized, are emitting green fluorescence (FL1). TB cannot enter the live cells, therefore, after TB addition the green fluorescence emission (FL1) is not quenched, while we observe the upshift of cell population corresponding to the cells with damaged membrane (ie. 4% dead cells) and Alexa-ITs adherent to the membrane which emitted red fluorescence (FL3) after quenching. Results are representative of two independent experiments. (**D**) Live confocal microscopy by taking images from a series of different regions started with time after the addition of Abs, generally 50 observations during the 90 min period. Live cells incubated with 7B2-PAC-Alexa488 demonstrate the presence of IT on the cell surface after 15 min. Following 90 min, 7B2-PAC is observable both internalized and on the cell surface. By imaging the same region, after 5 min TB addition, only the green fluorescence on the cell surface is quenched and emitting red fluorescence (shown by white arrow). The green and red fluorescences are detected by band-pass filters 530 ± 30 nm and 650 ± 13 nm, respectively..... 88

Figure 26 – Binding, internalization and intracellular localization of fluorescent ITs. (A). Env-transfected 293T cells were incubated with cold PBS in the presence or absence of 0.02% sodium azide. 45 min later, Alexa488-ITs were separately added to each set of slides in the presence of sCD4-IgG2. The slides were counterstained with BFA-bodipy, incubated an additional 60 min under the same conditions. Five min later, cells were washed 3X with cold PBS in the presence or absence of azide. The cells were fixed in 2% paraformaldehyde or one drop SlowFade Gold Mountant DAPI. Cells were observed with a 62X oil-immersion objective. Z-stack images collected at 1 μ m sections. The bottom of cells represents the closest plane to the slide. ITs are green, ER and Golgi are red. Some samples have nuclei stained with Hoechst Dye (Blue). Colocalization of red and green dyes appears yellow. The white bar indicates 10 μ m. (B,C). A comparison between Env-transfected 293T cells (B) and 293T cells (C) incubated with the same description in panel (A) but in the absence of sodium azide, in order to show the specific targeting the transfected cells. BFA-bodipy was used to demonstrate accumulation of ITs on the ER and Golgi..... 90

Figure 27 – Binding, internalization and intracellular localization of fluorescent ITs. (A). Env-transfected 293T cells were incubated with cold PBS in the presence or absence of 0.02% sodium azide. 45 min later, Alexa488-ITs were separately added to each set of slides in the presence of sCD4-IgG2. The slides were counterstained with BFA-bodipy, incubated an additional 60 min under the same conditions. Five min later, cells were washed 3X with cold PBS in the presence or absence of azide. The cells were fixed in 2% paraformaldehyde or one drop SlowFade Gold Mountant DAPI. Cells were observed with a 62X oil-immersion objective. Z-stack images collected at 1 μ m sections. The bottom of cells represents the closest plane to the slide. ITs are green, ER and Golgi are red. Some samples have nuclei stained with Hoechst Dye (Blue). Colocalization of red and green dyes appears yellow. The white bar indicates 10 μ m. (B,C). A comparison between Env-transfected 293T cells (B) and 293T cells (C) incubated with the same description in panel (A) but in the

absence of sodium azide, in order to show the specific targeting the transfected cells. BFA-bodipy was used to demonstrate accumulation of ITs on the ER and Golgi.92

LIST OF TABLES

Error! Reference source not found.	41
Error! Reference source not found.	48

LIST OF ABBREVIATIONS

ELISA – Enzyme-linked immunosorbent assay

HEK 293 Cell – Human embryonic kidney cells 293

HIV – Human immunodeficiency virus

IC – Immuno-conjugation

Ig – Immunoglobulin

IT – Immunotoxin

mAb – Monoclonal antibody

PAC – Pulchellin A chain

RAC – Ricin A chain

RAC18 – Anti-Ricin A chain mAb

SUMMARY

1	LITRATURE REVIEW	27
1.1	Ribosome-inactivating proteins (RIPs)	28
1.1.1	Bacterial and plant RIPs	29
1.1.2	Defensive role of RIPs in plants	30
1.1.3	RIPs as Immunotoxins	31
1.1.4	Mechanism of ITs function	32
1.1.5	Structure of Immunotoxins	32
1.1.6	Antitumor activity of RIPs	34
1.1.7	Transport of protein RIPs into cells	35
1.2	Pulchellin	36
1.2.1	Structure of Pulchellin	36
1.2.2	Isoforms of Pulchellin	37
1.3	Historical overview on antibody therapy	37
1.3.1	The Variable Domain	41
1.3.2	The Constant Domain	41
1.3.3	Fc-Mediated Functions	42
1.4	Therapeutic Antibodies	43
1.4.1	Antibodies against Infectious Diseases or as Immunomodulatory Agents	43
1.4.2	Antibodies for Treatment of Cancer	43
1.4.3	Antibody Drug Conjugates (ADC)	47
1.4.4	Antibodies as Immunoconjugates	48

1.5	Human Immunodeficiency Virus	49
1.5.1	Background and Significance of HIV	49
1.5.2	HIV Vaccine (T cell immunity vs. B cell immunity).....	51
1.5.3	HIV Envelope Protein and the Immune Response	53
1.5.4	Early Discovery of Broadly Neutralizing Antibodies	55
1.5.5	Recent Discovery of Broadly Neutralizing Antibodies.....	58
1.5.6	Anti-HIV Immunoconjugates	60
1.5.7	Antigenic determinants as target on the HIV-infected cell.....	62
1.5.8	Antigenic determinants as target on the HIV-infected cell.....	63
1.6	Human Immunodeficiency Virus	65
1.6.1	mAb-IT, directed against PND region on gp120.....	65
1.6.2	mAb-Ricin A, directed against a CD4-binding region on gp120.....	65
1.6.3	Human polyclonal /monoclonal Abs coupled to RTA	66
1.6.4	Implications for mAb therapies to eradicate HIV infection	57
2	OBJECTIVES	69
3	MATERIALS AND METHODS	71
3.1	Cells and reagents.....	71
3.2	Antibodies.....	71
3.3	Cloning, expression and purification of recombinant toxin A chains.....	72
3.4	Conjugation of Abs to RAC and PAC	73
3.5	ELISA	74
3.6	Immunofluorescence assay	75
3.7	Alexa Fluor 488 labeling of ITs.....	75
3.8	Measurement of internalization by flow cytometry	75

3.9	Live confocal imaging	75
3.10	Confocal microscopy for cell binding and internalization	76
3.11	Cytotoxicity measurements for immunoconjugates	76
3.12	Statistical analyses	78
4	RESULTS.....	79
4.1	Production, characterization and conjugation of toxin A chains to MAbs	79
4.2	Binding of immunotoxins to recombinant antigen	82
4.3	ITs bind to Env expressed on the surface of infected and transfected cells	84
4.4	Cell binding and internalization of immunotoxins	86
4.5	Live imaging of ITs during binding and internalization.....	87
4.6	Confocal microscopy of binding, internalization, intracellular localization IT..	89
4.7	Immunotoxins based on PAC effectively and specifically kill transfected cells .	90
5	DISCUSSION.....	93
6	PUBLICATIONS EXTRACTED FROM THIS STUDY	97
7	ACKNOWLEDGEMENT	99
	REFERENCES	101

1 LITERATURE REVIEW

It is widely accepted that the human immunodeficiency virus (HIV) is the etiological agent responsible for AIDS. (1) This virus is a complex retrovirus belonging to the subclass of lenti viruses and consisting of two known HIV subtypes, HIV-1 and HIV-2, of which HIV-1 is most frequently found in infected populations. (1-2)

The virus particle is surrounded by a lipid envelope containing glycoproteins gp160 (extracellular gp120 and transmembrane gp41) protruding from the surface. Within the virus particle, core proteins surround the HIV genome, which is comprised of two identical single strands of RNA. The first step of HIV-infection is selective binding of gp120 to the human CD4 antigen, a glycoprotein expressed on T-helper cells and to a lesser extent on monocytes/macrophages. After conformational changes of CD4 and the glycoprotein, the lipid envelope membrane of the virus fuses with the membrane of the target cell. (3-4) The virus is then uncoated within the cytoplasm and reverse transcriptase (RT) uses the viral RNA as a template to form proviral DNA. The virus DNA is integrated into the human genome and can remain in a latent form for years. After activation of the HIV-infected cell, factors are released which activate the promoter of HIV and transcribe the viral genome into mRNA, where subsequent translation to viral proteins can take place. The new RNA genome is assembled and the virus buds out from the cell surface that contains the newly expressed gp120 and gp41. (4)

Ribosome-inactivating proteins (RIPs) are widely distributed in nature but are found predominantly in plants, bacteria and fungi. RIPs, such as Ricin and Pulchellin consist of an A chain and B chain linked by a disulphide bridge. (5-7) Besides their activity on rRNA, certain RIPs display a variety of antimicrobial activities *in vitro*, such as antifungal, antibacterial, and broad-spectrum anti-viral activities against both human and animal viruses, including the human immunodeficiency virus, HIV. It is predicted that to prevent nonspecific cell binding of an Immunotoxin containing pulchelline, the galactoside binding sites of the pulchelline B chain are blocked or the B chain is removed. Pulchelline A chain is the cytotoxic compound. (7)

The number of HIV-infected cells is small, however continuous reduction of infected and healthy CD4-positive cells occurs, which is thought to be the most likely reason for AIDS. (1-2) The mechanism by which HIV causes this reduction is not completely understood but it is probably a combination between direct and indirect mechanisms such as the cytopathicity of

HIV-infection, syncytium formation between infected and uninfected cells, immune response against gp120 and the functional impairment of CD4-positive cells. (1-2,4)

1.1 Ribosome-inactivating proteins (RIPs)

RIPs are toxins able to specifically and irreversibly inhibit protein translation. RIPs exert their toxic effects through binding to the large 60S ribosomal subunit on which they act as an N-glycosidase by specifically cleaving the adenine base A4324 in the 28S ribosomal rRNA subunit Figure 1. The most promising way to exploit plant RIPs as weapons against cancer cells is either by designing molecules in which the toxic domains are linked to selective tumor targeting domains or directly delivered as suicide genes for cancer gene therapy. (5,8)

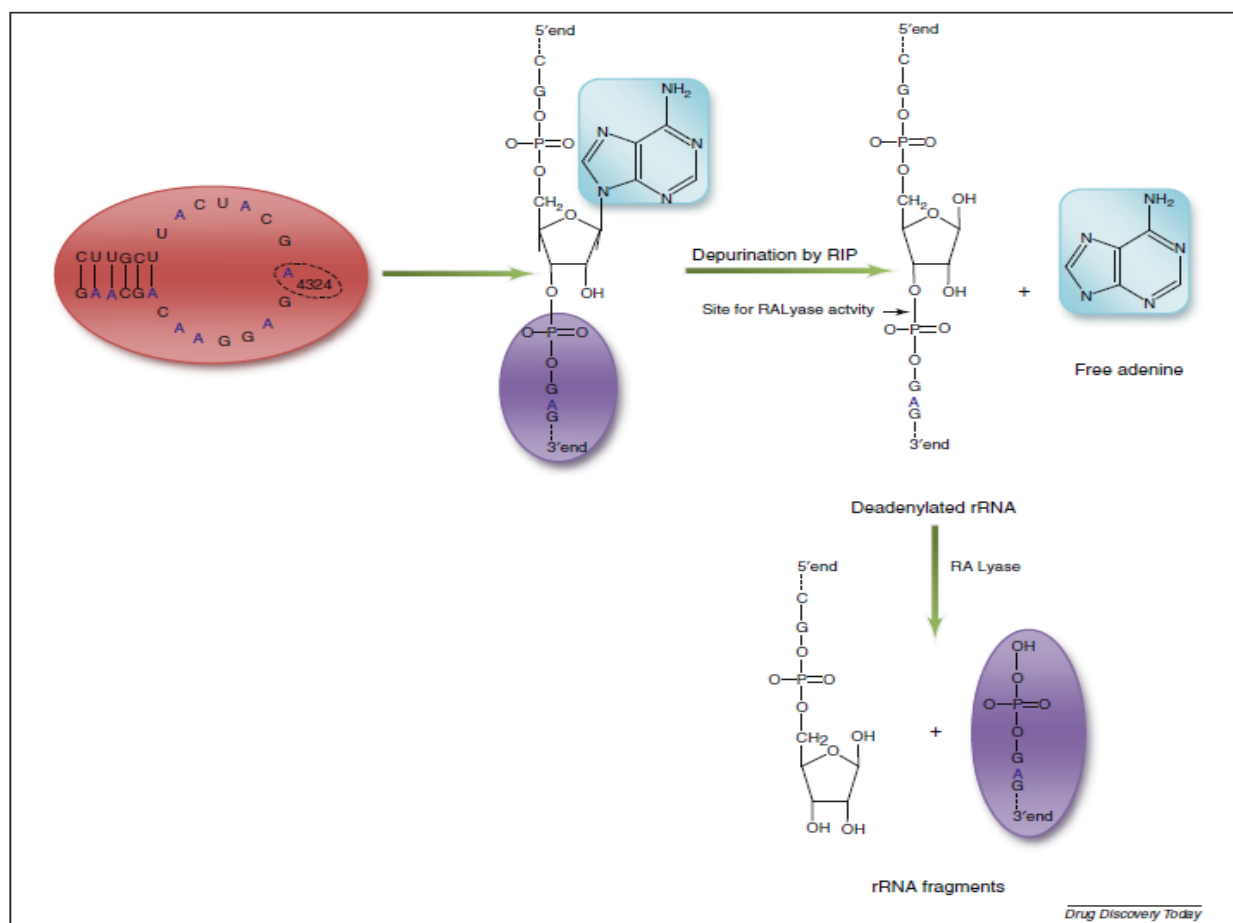


Figure 1-Mechanism of action of ribosome-inactivating proteins (RIPs). A specific N-glycosidase activity cleaves adenine (A4324), which is located in the sarcin-ricin loop of the ribosomal RNA of the large subunit.

Source: PURI et al. (9)

1.1.1 Bacterial and plant RIPs

Most plants and bacterial RIPs, such as Shiga and Shiga-like toxins from the bacteria *Shigella dysenteriae* and the Shiga toxigenic group of *Escherichia coli* (which include other Enterohemorrhagic *E. coli* strains), exert their toxic effects through binding to the large 60S ribosomal subunit. (5-7,9) This results in the inability of the ribosome to bind elongation factor 2, thus blocking protein translation. Besides their activity on rRNA, certain RIPs display a variety of antimicrobial activities *in vitro*, such as antifungal, antibacterial, and broad-spectrum anti-viral activities (10) against both human and animal viruses, including the human immunodeficiency virus, HIV. (11)

RIPs from plants have been classified into three main types: Type I is composed of a single polypeptide chain of approximately 30 kDa, Type II is a heterodimer consisting of an A chain, functionally equivalent to the Type I polypeptide, linked to a B subunit, endowed with lectin-binding properties (Figure 2), while Type III are synthesized as inactive precursors (ProRIPs) that require proteolytic processing events to form an active RIP and are not in use for therapeutic purposes. Besides their well characterized activity of depurinating ribosomes at the “sarcin/ricin loop” *in vitro*, their physiological function(s) are not yet completely understood and the questions to why some plants should synthesize RIPs remains still open. Different RIPs have been reported from about 50 plant species covering 17 families. Some families include many RIP-producing species, particularly Cucurbitaceae, Euphorbiaceae, Poaceae, and families belonging to the superorder Caryophyllales. (12)

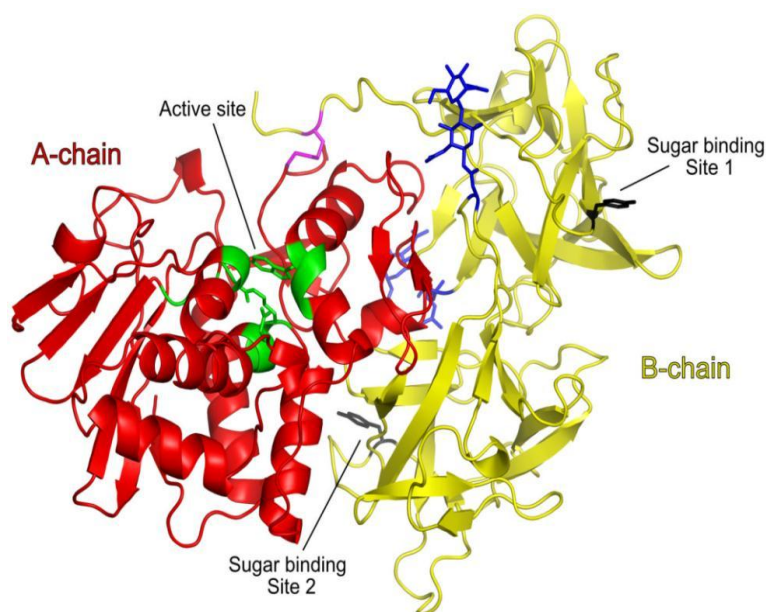


Figure 2 -Schematic structure of RIPs type II
Source: STIRPE (12)

1.1.2 Defensive role of RIPs in plants

The antiviral role of RIPs in plants is postulated on the basis of the enzymatic activity and selective compartmentalization. RIPs may potentially inactivate ribosomes in the same cells in which they are synthesized and they are found sequestered into vacuoles, protein bodies, or cell walls. It is suggested that when plants are wounded, for instance during viral infection, RIPs may be released from their intracellular compartments. This would prevent viral replication at an early stage by inactivating the cell protein synthesis machinery and leading to autonomous cell death. However, the exact role of RIPs in plants still remains elusive, since also not all plant species express these toxins. (7-8) In addition, most RIP-expressing plants present multi gene families that seem to be under a clear selective pressure. A recent publication from the Craig Venter Institute revealed that whereas oil metabolism genes were found in single copy, the ricin gene family was even more extensive than previously thought, implying a strong selective pressure to maintain these ricin-like genes. Among 25 geographically different castor bean plants, the presence of six ricin-like loci was confirmed, which shared 62.9–96.3% nucleotide identity with intact A-chains of the preproricin gene. Replacement mutations preserved the 12 amino acids known to affect catalysis and electrostatic interactions of the native protein toxin, suggesting that functional divergence among alleles was only minimal. Nucleotide polymorphism was maintained but included an excess of rare silent mutations much greater than what would be predicted by a neutral equilibrium model. (8)

Synthesizing an endoplasmic reticulum (ER)-targeted inactive precursor polypeptide is most likely the mechanism by which *Ricinus communis*, cells can avoid intoxication by the endogenously synthesized toxin. In addition, it has been shown that tobacco protoplasts can also safely synthesize the full-length ricin precursor without any detrimental effect on host protein synthesis. In contrast, the expression of an orphan secretory ricin toxic A chain (RTA) polypeptide results in the hetero-translocation of RTA to the cytosol followed by inhibition of protein synthesis in the tobacco protoplasts, making RTA the most studied plant ER-associated degradation (ERAD) substrate, with the AAA-ATPase Cdc48/p97 being recently identified as an extraction motor for this toxin from the plant ER. (6,13) Little is known about the synthesis of Type-I precursor polypeptides in plant. Since several Type I RIPs are active towards “conspicuous” ribosomes, and because of this observation, the inefficient targeting or translocation of Type I RIPs can potentially lead to self-intoxication, and therefore, mechanisms must be in place to prevent the unregulated accumulation of the active enzymes

in the cytosolic compartment. In addition, this characteristic has led to the idea that these enzymes could play an important role in blocking the spread of certain pathogens by causing the death of infected cells. Following the local suicide hypothesis, plant cells undergoing plasma membrane breaching by a virus would allow entry of apoplast-located toxins. This localized cell death would concomitantly block replication and the systemic spread of the virus load throughout the plant. In such a model, prior accumulation of the RIPs within the apoplast would be crucial. However, this mechanism was criticized because protein synthesis in damaged cells would be stopped during viral infection. As an alternative, it has been suggested that specific mechanisms might regulate the access of a particular RIP to cytosolic ribosomes only when the plant cell becomes infected. The Iris RIPs, as an example, protect plants from local but not from systemic infections, indicating that the antiviral activity is effective only in the initially infected cells. (14) Specific signals may lead to a change in the subcellular localization of the toxin, or to the degradation of a putative RIP inhibitor. One of these mechanisms might be embedded in the plant signal peptide, as we have recently demonstrated in the case of saporin where cleavage of the signal peptide was found to represent an activation step in the saporin biosynthetic pathway. (15-16) *In vivo*, mutations affecting signal peptide cleavage could clearly reduce (although not fully eliminate) host cell toxicity.

Stress-sensitive abortion of co-translational translocation may provide a novel pre-emptive quality control pathway to regulate protein entry into the secretory compartment and would lead in the case of saporin to activate the newly synthesized saporin precursor, allowing for its partial insertion into the ER to undergo signal peptide cleavage, and thus toxin activation. (14)

1.1.3 RIPs as Immunotoxins

The commonly used cytotoxic agents in ITs directed against HIV-infected cells are the plant toxins ricin and pokeweed antiviral protein (PAP), and the bacterial toxins *Pseudomonas* exotoxin (PE) and Diphtheria toxin (DT). All these toxins belong to the ribosome-inhibiting proteins (RIPs). PE, DT and ricin are type II RIPs and contain three functional elements responsible for cell binding, membrane translocation to the cytosol, and catalytic inhibition of protein synthesis, respectively. PAP is a type I RIP lacking the cell-binding function. (7,9)

1.1.4 Mechanism of ITs function

In the cytosol of eukaryotic cells, all these toxins selectively and irreversibly inactivate the 60S ribosomal subunit and inhibit peptide elongation during protein synthesis (5-6) PE and DT possess ADP-ribosyl transferase activity and catalyze the transfer of ADP-ribose from NAD to elongation factor EF-2, thereby inactivating EF-2. EF-2 is responsible for the GTP hydrolysis-dependent translocation of ribosomes during polypeptide formation. Ricin and PAP act as N-glycosidases that cleave a single N-glycosidic bond of a specific adenine from 28S ribosomal RNA thereby preventing binding of EF-2 to this ribosomal subunit. Both modes of action result in cell death. (13,17)

1.1.5 Structure of Immunotoxins

To be active the toxins have to bind the target cell, be internalized and translocated to the cytosol. The routes by which the toxins are transported intracellularly vary for each toxin inducing a differential sensitivity dependent on the targeted cell type.

Ricin consists of an A chain and B chain linked by a disulphide bridge. The toxin binds via the B-chain to galactose-containing glycoproteins and glycolipids that are present on the surface of all cell types. To prevent nonspecific cell binding of an IT containing ricin, the galactoside binding sites of the ricin B chain are blocked or the B chain is removed. Ricin A is the cytotoxic compound. To prevent clearance of the ricin A in the liver due to recognition of sugar groups in the toxin, the A chain has been chemically deglycosylated or genetically engineered resulting in an absence of glycosylation. (6,13,15,18)

PE is naturally produced as a single-chain protein consisting of three domains (I, II and III). PE binds via the N-terminal region of domain I to the 2-macroglobulin receptor present on the surface of most cells. To avoid nonspecific binding, PE has been genetically engineered in order to eliminate the binding domain I (e.g. PE40). This truncated form of PE still contains domains II and III that are responsible for translocation and ADP-ribosylation, respectively.

Cholera toxin (CT) constitutes one of the most powerful non-replicative mucosal adjuvants together with the heat-labile enterotoxin from *Escherichia coli* (LT). CT is able to induce local systemic immunity against coadministered Ags when given at the same time by the same mucosal route, but due to its toxicity, CT is not usable in clinical trials. (6) CT has an AB₅ structure composed of two distinct subunits: a single toxic A subunit and a nontoxic

homo pentamer B subunit (nontoxic B subunit of CT(CTB)), with strong affinity for GM1 gangliosides present on all mammalian nucleated cells, which is responsible for the anchor of the toxin onto host cells. (6)

Shiga toxin from *Shigella dysenteriae* is composed of an A subunit that mediates toxicity and a B subunit (nontoxic B subunit of Shiga toxin (STxB)), a nontoxic homopentameric protein responsible for toxin binding and internalization into target cells by interacting with the glycolipid Gb3. (19) We have previously shown that STxB efficiently targets exogenous peptides into the MHC class I and II pathways and delivers Ag *in vivo* directly to DCs (20), which preferentially expressed the Gb3 receptor. (6,15)

Diphtheria toxin (DT) is a disulphide-bonded two-chain molecule. The B-chain binds to an epidermal growth factor-like receptor that is expressed by most mammalian cell types. To overcome this receptor-mediated binding, the native receptor-binding domain has been genetically eliminated (e.g. DAB486). In contrast to ricin and PE, cytotoxicity of DT was not inhibited by AZT. This might be explained by differences in the mechanisms by which AZT influence toxicity of the toxins. AZT acts within the cytosol to inhibit the enzymatic action of PE, whereas the inhibition of ricin cytotoxicity might be the result of an alteration in ricin translocation. Nevertheless, as a consequence DT might be used in combination therapies with Azidothymidine (AZT). (17)

PAP lacks a cell-binding domain and only enters cells with increased permeability, like virally infected cells. Besides the protein synthesis inhibition of such cells PAP has the ability to inhibit the replication of viruses. PAP could inhibit the replication of HIV and also of other passive viruses in HIV-infected individuals like cytomegalovirus and herpes simplex virus. The mechanism of the antiviral capacity of PAP is unknown. (14) Both inhibition mechanisms render unmodified PAP suitable for HIV therapy.

Two other type I RIPs, trichosanthin and Bryodin, which might be active against HIV-infected cells have been investigated. Both RIPs were *in vitro* effective against infected cells in about the same dose range. (14)

To specifically direct toxins to a target, they have to be linked to the ligands. Ricin A and PAP are often linked to the carrier protein with hetero bifunctional linkers that introduce a disulphide bond between the carrier and the toxin. The toxin can be released after endocytose by reduction of the disulphide bond. (9,14,21-22) ITs composed of recombinant PE or DT have been prepared by splicing the genes encoding truncated DT or PE to the gene encoding the carrier protein and expressing the entire IT as a fusion protein.

1.1.6 Antitumor activity of RIPs

The RIPs from many plants have shown antitumor activity both *in vitro* and *in vivo*. MAP30 exhibits antitumor activity against certain human tumor cell lines originating from renal, non-small cell lung and breast cancer tumors. Antitumor activity of rec-MAP30 has also been studied in several human tumor cell lines, such as brain glioblastoma, breast carcinoma, epidermoid carcinoma, liver hepatoma, melanoma, myeloma, neuroblastoma and prostate carcinoma. The antitumor activity of rec-MAP30 and nMAP30 was identical with respect to their sensitivity to particular tumor types. The most sensitive tumor cell lines were breast, central nervous system, melanoma and myeloma tumors with EC50 values of 0.21–0.38 nM. Prostate and epidermoid carcinomas were less responsive, with ID50 values of 3.42 and 1.88 nM, respectively. (23)

Moreover, in our previous studies, we showed some antiviral and immunoadjuvancy effects of STxb (19-20), Ricin toxin B (10,24) and Cholera toxin B (25), against cervical cancer caused by HPV.

1.1.7 Transport of protein RIPs into cells

RIPs enter the cell by first binding to cell surface carbohydrates, then crossing the cell wall via endocytosis and finally entering the cytosol via translocation from intracellular endocytic compartments. This occurs after retrograde transport through the Golgi apparatus to the endoplasmic reticulum (ER). In the ER, the catalytic moieties exploit the ER-associated degradation (ERAD) pathway to reach their cytosolic targets. Most of the observations concern type IIRIPs and suggest that more than one mechanism of internalization is involved. (6,15,18) The cell–RIP interaction shows common features, including:

- (i) only some of the toxin molecules taken up by the cells are transferred into the cytosol and so reach their target;
- (ii) inhibition of protein synthesis can only be detected in cells at least 30 min after it occurred;
- (iii) a single RIP molecule might be sufficient to induce cell death.

Internalization of type II RIPs, such as Ricin (13), has evolved a mechanism for efficiently entering mammalian cells (Figure 3).

Other type II RIPs, such as Pulchellin, from plants are structurally and functionally equivalent to ricin. Recently, studies of endocytosis and intracellular transport of Pulchellin

have been done in the Institute of Physics in Sao Carlos, University of Sao Paulo. (26-28) It is assumed that the mechanism of Pulchellin for entering target cells would be similar to ricin.

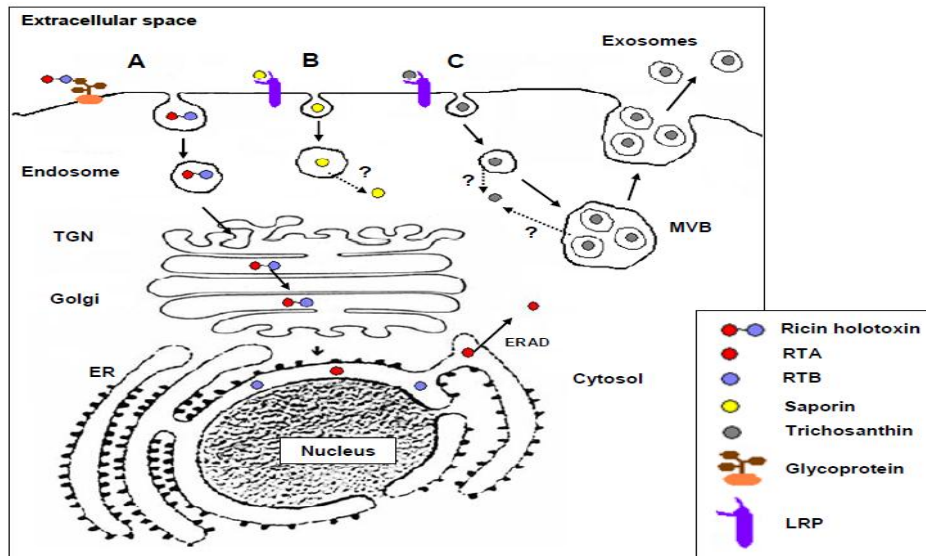


Figure 3 – Schematic representation of the intoxication pathways followed by Ricin (A), saporin (B) and trichosanthin (C)

Source: SANDVIG et al. (13)

1.2 Pulchellin toxin

1.2.1 Structure of Pulchellin

Abrus pulchellus, sub-species *tenuiflorus*, belonging to the family Leguminosae, domesticated in Brazil, contains a seed lectin (pulchellin), specific for galactose and galactose-containing sugars, showing haem-agglutinating and toxic activities. Pulchellin is a ribosome inactivating protein (RIP) type 2 which are a combination of lectin B subunit and toxic A subunit held together via a disulfide bond. Each subunit plays a distinct role during their action on eukaryotic cells. (26-28) The B subunit, which contains two galactose binding sites, binds the toxin to cell surface glycoproteins and/or glycolipids containing terminal galactose and helps endocytosis and subsequent transport of the A subunit into cytosol. Pulchellin B-chain exhibits affinity for β -D-galactose substrate. (26)

It exhibits specificity for galactose and galactose-containing structures, can agglutinate human and rabbit erythrocytes, and kills mice and the microcrustacean *Artemia salina* at very low concentrations. Similar to the RIP in *A. precatorius* seeds, this toxic activity is presented by a mixture of closely related isoforms. (29)

The A subunit is an enzyme that, when free in cytosol, depurinates a single base, adenine 4324, of the 28S rRNA in mice, thereby inactivating protein synthesis. (29) Analogously to ricin and abrin, pulchellin displays strong cytotoxic effects on mammalian cells at low protein concentrations. Pulchellin enters cells through lectin–carbohydrate interactions at the cell surface followed by endocytic uptake and subsequent retrograde transport. For type2 RIPs the toxic A-chain, after being reduced from its B-chain, enters the cell cytoplasm by exploiting the ER-associated protein degradation pathway (ERAD). (29-30)

In the recent studies at IFSC, University of Sao Paulo, four pulchellin isoforms have been isolated, and their amino acids sequences deduced by cDNA cloning and verified by Mass Spectrometry. (26) They also showed the recombinant pulchellin B-chain (rPBC) was produced as inclusion bodies in *E. coli* that were successfully refolded recovering biological activity. (31) In further studies, they demonstrated that rPAC interacts with negatively charged phospholipids using Langmuir monolayers as membrane models. Using Polarization Modulated-Infrared Reflection Absorption Spectroscopy (PM-IRRAS) they observed that at a bare air/water interface rPAC comprised mainly α -helix structures, the C-terminal region had unordered structures when interacting with DPPG. For rPAC236 the α -helices were preserved even in the presence of DPPG. The results confirm the importance of the C-terminal region for PAC-ER membrane interaction. The partial unfolding only with preserved C-terminal appears a key step for the protein to reach the cytosol and develop its toxic activity. (29)

1.2.2 Isoforms of Pulchellin

The whole protein is categorized in four types, based on the half maximal inhibitory concentration (IC₅₀) and median lethal dose (LD₅₀) values from HeLa cells and mice: the more toxic forms (P I and P II) and the less toxic forms (P III and P IV). From a comparison of deduced amino acid sequences within each subgroup, it is striking that the members of each subgroup show closest identity in domain 2 of the B-chain. (26) In the four pulchellin A-chains, the residues involved in the active site cleft are the same as in abrin and ricin A-chains. This suggests that the catalytic reaction is exactly the same. The sugar binding pulchellin B-chains are 264 (P I and P II) or 263 (P III and P IV) amino acids in length and contain two N-glycosylation sites. Moreover, deduced amino acid sequences from the cDNA clones of P I, P II, P III and P IV aligned to ricin (pdb 2AAI) show high homology for residues involved in the active site cleft of A chains. (26,30)

1.3 Historical overview on antibody therapy

The study of antibodies has yielded in many critical advances in our overall understanding of protein structure and the genetic mechanisms used to encode proteins, as well as discoveries to combat human diseases including infections, cancer, inflammation, and even metabolic diseases. Antibody-based therapies include vaccines, serum therapy in the preantibiotic era, and currently monoclonal and recombinant antibodies, with seven of the top ten best selling drugs in the U.S. being antibodies. (32)

In the late 1800s, following Edward Jenner's discovery of a smallpox-preventing vaccine and Louis Pasteur's creation of a live, "attenuated" rabies vaccine, Emil von Behring and Kitasato Shibasaburo proved that serum from infected animals could protect uninfected animals from disease, unveiling the arm of the human immune system that would come to be known as humoral immunity. (32) In 1901, the first Nobel Prize in Medicine or Physiology was awarded to von Behring for his work on "serum therapy, especially its application against diphtheria, by which he has opened a new road in the domain of medical science and thereby placed in the hands of the physician a victorious weapon against illness and deaths". (33) In fact, there have been at least 8 Nobel Prizes awarded for research on Ig structure and function, with more certainly to come.

Not long after the discovery that factors in serum were able to protect against infection, structural studies began. Paul Ehrlich was the first to use the term antibody, and he formulated the famous "side chain theory of immunity" to explain antibody-antigen interactions. (34) For this, he shared the 1908 Nobel Prize with Ilya Metchnikoff, often regarded as the father of studies in innate immunity. Ehrlich focused most of his revolutionary work on the immune response to toxins and therapy for infectious diseases. Along with the work of Ehrlich, the technical procedures Tiselius and Kabat undertook in the 1930s allowed them to analyze serum and isolate Igs adding a much better understanding of the blood component of the immune system. (35)

This ushered in the great era of serum-therapy for infection. Before effective antibiotics were available, often the only way to treat serious infections was by the administration of hyperimmune sera, and it saved the lives of countless people, most famously in Nome, Alaska when serum was delivered by a sled dog relay during a diphtheria outbreak in the winter of 1925, and now commemorated in the annual Iditarod dogsled race. More routinely, it was used to treat pneumococcal pneumonia and meningococcal outbreaks. However, it came with a cost. People treated with crudely purified serum from immunized animals would often

develop serum sickness as they made antibodies against the foreign Igs. Serum sickness was manifest by fevers, arthritis, and potentially lethal nephritis, all resulting from immune complex formation and deposition. With the introduction of antibiotics, interest in serum therapy waned, yet gamma-globulin was commonly used for prevention of hepatitis B until the 1980's when an effective vaccine was developed. Even today, hyperimmune human gammaglobulin, highly purified and disaggregated, is used for postexposure prevention of tetanus, varicella zoster, and rabies in at risk patients. (36-37)

A major breakthrough in the study of antibodies came with the understanding that myeloma proteins were actually Igs. Myeloma is a cancer of plasma cells resulting in production of extremely large amounts of a single monoclonal antibody (mAb) in patients. Using the new technology of electrophoresis to separate plasma proteins, Kunkel was the first to show that these serum proteins were actually gamma-globulins. Patients' blood was collected and antibodies isolated in quantities needed for functional and structural studies. It was in the 1960s that the native structure of antibodies was revealed. Gerald Edelman (38) and Rodney Porter (39-41) won the 1972 Nobel Prize in Medicine for their elegant description of the structure of antibodies. Their work with reducing agents like β -mercaptoethanol proved that disulfide bonds hold the heavy and light chains together, which led to the discovery that antigen binding domains required both chains. Later, Edelman described and expounded on the function of the products created by digestion with pepsin or papain. Then he went on to publish the first sequence of a human Ig and preliminarily classify key regions on both the heavy and light chains. Once sufficient sequences were obtained, variable and constant regions were identified. Poljak incorporated crystallographic evidence with Ig sequences to create the first three-dimensional structure (42) which led to more refined models of the antigen binding site by a combination of nuclear magnetic resonance (NMR), electron spin resonance, and affinity labeling. (43) Kohler and Milstein used myeloma cell lines as the basis of their hybridoma technology, which earned them a Nobel Prize for "the discovery of the principle for production of monoclonal antibodies." Also awarded a share of that prize was Niels Jerne, who described the clonal selection hypothesis, the cellular basis underlying the production of antibodies. In fact, Kohler and Milstein were seeking to test this selection hypothesis when they invented hybridoma technology. Susumu Tonegawa used myeloma cells as an enriched source of antibody-encoding mRNA to develop the probes he then used to study the structure and organization of Ig genes, work for which he received a Nobel Prize in 1987. (44)

The introduction of mAbs eventually led to their use as immunotherapy against infectious, inflammatory, hematologic, and autoimmune diseases. One of the first mAbs approved for treatment of infectious diseases was Palivizumab, for prevention of respiratory syncytial virus (RSV) by binding a neutralizing epitope on the viral surface. Many cancers are susceptible to killing by antibody-mediated mechanisms. These cancers usually overexpress a cell surface marker that can be targeted by antibodies. Commonly cancers are driven by proliferation signals, and stimulation of receptors for growth factors like VEGF, EGF, or HER2 can be blocked by antibodies. The third major class of disease treated by mAb therapy is autoimmune disorders like lupus, rheumatoid arthritis, and multiple sclerosis. These Abs target a wide range of molecules involved in TNF signaling (45), integrin-mediated extravasation (46), and IL-2-mediated transplant rejection. (47) Anti-TNF therapeutics have altered the basic treatment of rheumatoid arthritis, inflammatory bowel disease, and other common autoimmune conditions; and for his work that led to the discovery of TNF, Bruce Beutler was awarded the 2011 Nobel Prize for Physiology or Medicine.

Antibodies (Abs) can be divided into regions based on sequence variability and function. IgG Abs, the most common class, are ~150 kDa proteins made of two heavy (gamma) chains with 450 amino acids and two light (kappa or lambda) chains, averaging 225 amino acids, joined by disulfide bonds. (48) Each chain contains a variable domain at the amino terminus followed by a constant region (Fig. 4).

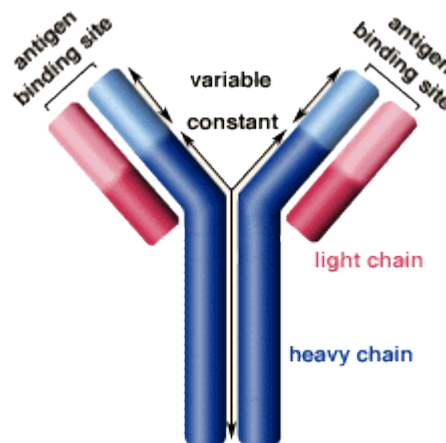


Figure 4 – Antibody structure; Labels indicate heavy (blue) and light (red) chains, variable (light) and constant (dark) regions, and antigen binding site.

Source: By the author.

Each heavy or light chain variable domain is approximately 110 amino acids long and is responsible for forming the antigen-binding pocket when the two chains are paired. The

constant domain is the more genetically conserved region, responsible for binding to immune cells or complement proteins to generate an effector response. The distinctive structure is known as an Immunoglobulin (Ig) fold and is made of β -sheets joined by intra-domain disulfide bonds between conserved cysteine residues to form a β -barrel. As the β -sheets fold back they leave hairpin loops exposed, which in the variable domain contain the hypervariable regions involved in antigen contact. Other molecules share this basic domain structure, including B-cell receptors (Abs and CD19), NK cell Ig-like receptors (KIRs), T-cell receptors (CD3, CD4, and CD8) and major histocompatibility complex (MHC) proteins. These can all be classified under the Ig superfamily and play similar roles in immune signaling and antigen presentation. (48)

1.3.1 The Variable Domain

A variable domain from each chain comes together to determine epitope specificity of the Ab. The variability is a reflection of the genetic events responsible for generating such a large repertoire of Abs ($>10^{11}$), such as combinatorial and junctional diversity and somatic hypermutation. Within each variable domain, there are relatively constant sections known as framework regions, interspersed with areas of extraordinarily high amino acid variability known as hypervariable regions. These hypervariable loops come together in three-dimensional space to form the antigen-binding site, and are thus referred to as complementarity determining regions (CDRs). The framework regions form β -sheets to stabilize the overall Ig structure and maintain the spatial orientation of the CDRs.

In the 1940s, researchers began experimenting with enzymatic digestion of Abs. (49) After years of work with papain and pepsin, cleavage products were characterized and became known as the Fab (Fragment of antigen binding) and the Fc (Fragment crystallizable) portions. More recently, Fab fragments have undergone extensive genetic engineering to develop therapeutic drugs. By linking the variable domains from one heavy and one light chain into a single polypeptide chain, single-chain Fragment variable domains (scFv) were created. The advantage of the small size of scFvs is that they can penetrate tissue or target small, restricted epitopes for diseases that are historically resistant to Ab therapy. (48-49)

1.3.2 The Constant Domain

The other main portion of an Ab is called the constant region. It is the more genetically conserved region that makes up the tail of the Ab. The heavy chain constant regions function to bind and signal the effector proteins and cells of the host immune system. Each heavy chain is made of several subdomains in the constant region, called C_H domains. The number and amino acid sequence of C_H domains within the Fc region determines the isotype of an Ab, which plays a role in type of effector function as well as the anatomical distribution of the Ab. Depending on isotype, heavy chains typically have three or four C_H domains while light chains contain one C_L domain. Additionally, depending on Ab isotype, the terminal two or three C_H domains are typically referred to as the Fc region.

For a typical IgG1, these constant domains contain: disulfide bonds, a hinge region, glycosylation sites, effector protein and immune cell binding sites. (50) The disulfide bonds between C_{H1} and C_L hold the heavy and light chains together. The hinge region between the C_{H1} and C_{H2} domains allows the variable domains to flex and bend to improve antigen binding. IgGs have an N-linked glycosylation site in the C_{H2} domain at Asn297, which positions the oligosaccharides in the space between the heavy chains. Full length Igs are usually favored for *in vivo* therapy because they produce the most robust effector responses, and persist in the circulation for much longer periods of time. (50)

1.3.3 Fc-Mediated Functions

The tail of an IgG Ab, containing C_{H2} and C_{H3}, is collectively referred to as the Fc region, and plays a role in signaling effector cells during an immune response. An important response triggered by the Fc region is Antibody Dependent Cell-mediated Cytotoxicity (ADCC), which signals through Fcγ receptors on immune cells to lyse infected cells. ADCC typically involves the release of cytokines and cytotoxic granules when Ab-coated infected cells are crosslinked to FcγRIII (CD16) on the surface of NK cells (51-52). Key binding sites are located throughout C_{H2} and C_{H3} (52), but mutations such as S239D/I332E/A330L can increase ADCC by increasing affinity for the activating Fcγ receptors like FcγRI, FcγRIIa, FcγRIIIa while decreasing affinity for inhibitory receptors like FcγIIb. Increased ADCC response has been correlated with a slower rate of progression to AIDS and are found at higher levels in elite controllers. (53) ADCC is a major mechanism in the defense against viral infection to compliment neutralization of cell-free virus.

The adaptive immune response again overlaps with cell-mediated immunity through interactions called Antibody-Dependent Cell-mediated Virus Inhibition (ADCVI). It does not take into account only the amount of direct cell death, but rather the impact that effector cells in the presence of Ab have on virus production from infected cells. (51) It takes into account many of the Ab-dependent effector functions such as ADCC, phagocytosis, and release of cytokines or chemokines. Original assays developed by Forthal et al analyzed Cr-release in ADCC assays and used reduction in virus infectivity as an endpoint for ADCVI. (54) They also reported that ADCVI has been associated with reduction of viremia during acute HIV infection in rhesus macaques and in human vaccine participants of the Vax 004 trial. (51)

Yet another function of the constant region is Complement-Dependent Cytotoxicity (CDC), which uses the amplification power of C1q to enhance Fc-mediated killing by activating the classical complement pathway at the site of infection. The C1q binding site on C_H2 serves to activate the CDC pathway. Several amino acids in C_H2 near the hinge region at positions D270, K322, P329, and P331 were found to be required for this interaction. (55) CDC accompanies other functions of complement, including opsonization, chemotaxis, and direct cell lysis by increasing sensitivity to invading organisms by utilizing Abs. Opsonophagocytosis of complement coated microbes is enhanced by cooperative interactions between complement and Fc receptors on PMNs and monocytic phagocytes. Complement-coated immune complexes also get scavenged by red blood cells and taken to the spleen for destruction by phagocytes. (56) Activation of this pathway leads to a cascade of effects resulting in inflammation, which causes direct killing or inactivation of the pathogen and enhanced targeting to infected cells. In the case of HIV, CDC-enhancing Abs were found in the blood of infected patients in the late 1980s (57), yet their function is still unclear. There is data to support the beneficial role of some CDC-enhancing Abs by increasing virus inhibition (58); while others have shown that complement deposition enhances infection by binding to Fc γ receptors, which brings virus in close proximity to its cellular receptors (59-60).

The Fc region not only activates antigen-targeting immune cells but also binds to endothelial cells while in circulation. A key *in vivo* function of the Fc region is to increase half-life by recycling Abs in circulation. Salvaging IgG is the responsibility of the neonatal Fc receptor (FcRn) expressed on absorptive epithelial (61), endothelial vessels (62), and immune cells (63) to facilitate trafficking, half life, and phagocytosis. Many have used Hinton's proven method of mutating T250Q and M428L in the constant region of the heavy chain to increase binding to the neonatal Fc receptor (FcRn) at pH=6.0 and double the serum half life of these Abs. (64)

Hessell et al demonstrated the in vivo importance of the Fc region when they reported decreased protection in a macaque model after both complement- and Fc receptor-binding activities were engineered out of IgG1b12, yet no loss of protection was associated with removing only the complement-binding portion. (65) In this study, they reported four out of nine macaques given the engineered Ab became infected while eight out of nine macaques given IgG1b12 were protected after high-dose vaginal challenge. Unfortunately, no one to date has conducted a study to determine how all these mutations may interact with each other. For example, how will an ADCC-enhancing mutation affect the overall function of an Ab if combined with FcRn and CDC mutations? This is currently an area of intense research to determine the best backbone on which to base future clinical Abs. The future design of therapeutic Abs will require an overall framework that takes into account modifications for each of these important functions.

1.4 Therapeutic Antibodies

As of this year, 28 mAbs are approved to treat viral, autoimmune, inflammatory, and oncological disorders (66) while approximately one hundred more are undergoing development and testing. Prior to the explosion of mAbs serum therapy was one of the best treatments available for bacterial and viral diseases, especially toxin-mediated diseases like tetanus and diphtheria. By the 1950s, production techniques and research broadened the range of treatable diseases to viruses like polio, measles, mumps, pertussis, and hepatitis A. (67) Today, it is still used to treat infectious diseases that have confounded vaccinologists, as well as many immunologic and oncologic disorders. Intravenous Ig (IVIG) is a pooled collection of IgG Abs extracted from the plasma of thousands of donors. The wide sampling of individuals creates the broad protective effects seen upon administration. IVIG therapy is licensed to treat wide-ranging conditions like primary immunodeficiency, hypergamma globulinemia, leukemias, and as prophylaxis in stem cell transplants and pediatric HIV/AIDS. (68)

The current state of Ab therapy is dominated by the biological drug market. Each year, new mAbs as well as engineered Ab-like molecules are being testing and approved (Table 1). Several of the top selling mAbs have been approved to treat chronic diseases rather than cancer. For example, anti-TNF therapeutics account for a large part of the drug regimens used against autoimmune and inflammatory disorders. In 2011, the top five anti-TNF biologics (Adalimumab, Etanercept, Infliximab, Golimumab, Certolizumab) accounted for nearly \$25b

in sales. Recently, an Ab to proprotein convertases subtilisin/kexin type 9 (PCSK9), REGN727, has been shown in Phase II trials to significantly reduce LDL-cholesterol levels in patients with familial hypercholesterolemia who fail to reach appropriate levels while on statin therapy. (69) PCSK9 functions to bind LDL receptors, preventing them from removing LDL from the blood. Furthermore, statins are reported to stimulate the production of PCSK9, so for some patients, statins are not the gold standard. Some mAbs were further developed into ICs by linking the Ab to a radionuclide or cytotoxic agent to kill select cells.

Table 1 - List of Most Common mAbs in Clinical Use

Antibody	Year	Target	Disease	Sales
Adalimumab (Humira)	2002	TNF- α signaling	RA, CD, psoriasis	\$7.9b
Basiliximab (Simulect)	1998	IL-2 receptor	Transplant rejection	
Belimumab (Benlysta)	2011	BAF	SLE	
Bevacizumab (Avastin)	2004	VEGF	cancer (colorectal)	\$5.8b
Brentuximab vedotin (Adcetris)	2011	CD30	HL	
Cetuximab (Erbix)	2004	EGFR	cancer (colorectal)	\$3.4b
Infliximab (Remicade)	1998	TNF- α signaling	RA, CD, psoriasis, UC	\$9.0b
Omalizumab (Xolair)	2004	IgE	allergic asthma	\$1.3b
Natalizumab (Tysabri)	2006	α 4-integrin	MS	\$2.6b
Palivizumab (Synagis)	1998	RSV F protein	RSV	\$1.0b
Ranibizumab (Lucentis)	2006	VEGF-A	WMD	\$3.6b
Rituximab (Rituxan)	1997	CD20	NHL, RA	\$6.6b
Trastuzumab (Herceptin)	1998	HER2	Breast cancer	\$5.7b

Source: HENRY et al. (70)

Target Abbreviations: Tumor Necrosis Factor (TNF); B-cell Activating Factor (BAF); Vascular Endothelial Growth Factor (VEGF); Epidermal Growth Factor Receptor (EGFR); Respiratory Syncytial Virus (RSV); Human Epidermal Growth Factor Receptor 2 (HER2).

Disease Abbreviations: Rheumatoid Arthritis (RA); Crohn's Disease (CD); Systemic Lupus Erythematosus (SLE); Hodgkin's lymphoma (HL); Ulcerative colitis (UC); Multiple Sclerosis

(MS); Respiratory Syncytial Virus (RSV); Wet Macular Degeneration (WMD); Non-Hodgkin's lymphoma (NHL)

1.4.1 Antibodies against Infectious Diseases or as Immunomodulatory Agents

Pathogenic organisms are consistently evolving to survive in or on humans at the same time as we are evolving our Ab response to eliminate the pathogen. Some were targeted through vaccination, which led to a dramatic reduction in mortality and morbidity associated with many microorganisms such as *Haemophilus influenzae* or *Poliovirus*. Passive transfer of Abs (IVIG) is also used to treat susceptible pathogens such as hepatitis A or measles (68). To date only one mAb (Palivizumab) has been approved for treatment of infectious disease (RSV). (71) However, not all diseases can be cured with a vaccine and must be treated differently. Also, drug resistance creates the need for new drug development, such as mAbs. Creation of better, multispecific Abs may require engineering to target two different virulence factors of a pathogen to increase avidity or cross-linking. Alternatively, pathways that are initiated by infectious agents could be shut down by targeting two signaling molecules that perform redundant functions.

Improper production of immune mediators and cytokines can lead to inflammatory diseases like multiple sclerosis, rheumatoid arthritis, and inflammatory bowel disease. Adalimumab and Infliximab, Abs to TNF- α , are approved to treat rheumatoid arthritis and Crohn's disease; while Natalizumab, an Ab to α 4-integrin receptor, treats multiple sclerosis. Since cytokines potently drive immune responses, blocking immune signaling is an advantageous way to prevent graft rejection. Basiliximab and Daclizumab are Abs against the IL-2 receptor (CD25) and are used to prevent rejection of transplanted organs, especially kidneys. In fact, the first mAb to be approved by the FDA, Muromonab-CD3 (Orthoclone OKT3), was actually a mouse IgG2a Ab raised against CD3 of the T cell receptor complex that was approved to help reduce the risk of acute organ rejection by blocking or killing activated T cells that would otherwise attack the transplant. (72) It was usually reserved for use in steroid-resistant cases because patients treated multiple times with this drug developed tachyphylaxis, a response characterized by anti-mouse Abs that accelerated elimination and reduced the efficacy of this drug. Furthermore, there was the potential for an anaphylactic response or cytokine release syndrome resulting from using foreign Abs. For these reasons, most mAbs in clinical development today are nearly all chimerized or humanized to be as non-immunogenic as possible.

1.4.2 Antibodies for Treatment of Cancer

Targeted therapy for cancer strives to block growth factor signaling or deliver toxic drugs or death signals only to cancerous cells while reducing adverse effects on healthy cells. Some cancer cells express unique surface receptors to which Abs can easily bind and alter downstream effects. In the case of breast cancer, some types overexpress the growth factor receptor, HER-2. Genetic testing can identify these types and the patients can be treated with a mAb (Trastuzumab) that selectively binds the HER2 receptor, leads to its inactivation, and the cancer cells no longer receive the signal to reproduce uncontrollably. (73) Other examples of this class of drugs are the VEGF inhibitor, Bevacizumab and the EGFR inhibitor, Cetuximab. (74) Aside from inhibiting growth factor signaling, some anti-cancer immunotherapies such as Rituximab (75) bind to cells and lead to a direct killing through caspase 9-directed apoptotic pathways. Thus, mAbs may also utilize ADCC and CDC to produce anti-cancer effects.

1.4.3 Antibody Drug Conjugates (ADC)

ADCs are tripartite drugs comprising a tumor-specific mAb conjugated to a potent cytotoxin via a stable linker (Figure 5). The three components of the ADC together give rise to a powerful oncolytic agent capable of delivering normally intolerable cytotoxins directly to cancer cells or other infected cells like HIV-infected lymphocytes, which then internalize and release the cell-destroying drugs. (76-78) Although the concept of combining a mAb with a cytotoxic drug is fairly old, significant improvement have been made since the first generation of ADCs. (76) The design of ADCs with respect to the choice of target, mAb, linker and cytotoxin (such as ITs) are all very important determinants of whether or not the threshold concentration of the cytotoxic drug is reached within the tumor cell. These factors therefore determine the overall success of an ADC.

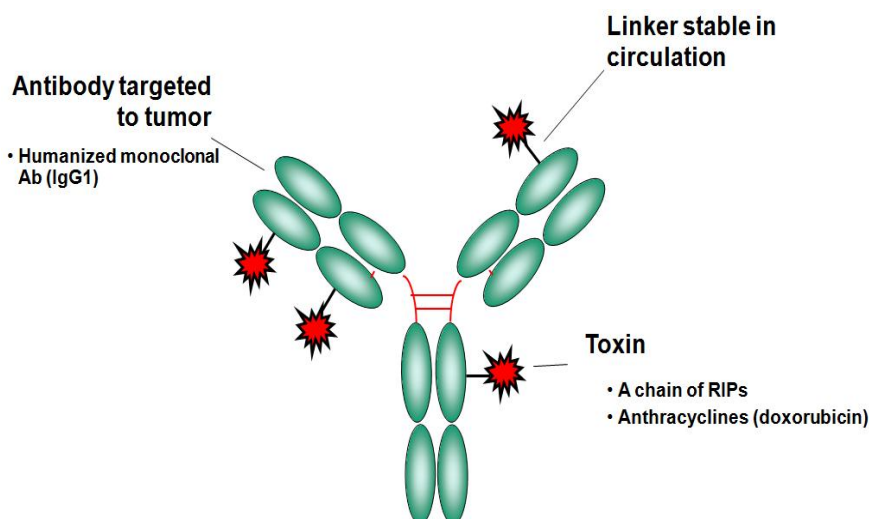


Figure 5 - Schematic structure of Antibody Drug Conjugates¹
Source: By the author.

1.4.4 Antibodies as Immunoconjugates

Most anti-cancer immunotherapies utilize at least one of the above mechanisms, but in some cases, Abs can be made even more powerful by incorporating a toxic moiety. These immunoconjugates (ICs) are able to deliver cytotoxic agents to dysfunctional cells by targeting unique epitopes not commonly found on healthy cells. As they have proven safe and effective in humans, their use is now being explored outside the confines of oncology. (79) Originally, bacterial and plant toxins were conjugated to mAbs, called immunotoxins (ITs), and used to treat cancer and viral infections. Prototypical A-B toxins like ricin are commonly engineered so that the cell-binding domain is removed and only the active subunit is attached to the Ab. This attempts to prevent non-specific killing of healthy, non-target cells. Ab-drug conjugates (ADCs) can also be engineered by linking cytotoxic drugs such as microtubule-inhibiting auristatin drugs to mAbs. A final method conjugates mAbs to radionuclides like Iodine-131 that emit ionizing radiation to kill cells.

These methods all have strengths and weaknesses but all have been used in some manner with success. ICs that incorporate bacterial or plant toxins like *Pseudomonas* exotoxin or ricin toxin may not work after repeated use since Abs against the toxin develop, which drastically

decreases the effect of the treatment. However, if a disease requires long-term administration of therapy, then ICs that exert a “bystander effect” may be preferred. Some cancer drugs and radionuclides can exert their effects on cells near the targeted cell. For cancer, this is a great advantage but if one was trying to attack a small population of cells distributed throughout the body it may not be beneficial.

Currently there are several ICs approved for the treatment of hematologic disorders (Table 2). In 2001, gemtuzumab ozogamicin was approved for AML but was withdrawn due to increase in the fatal toxicity rate. Since then another ADC, brentuximab vedotin, was approved for Hodgkin’s and anaplastic large cell lymphomas by targeting CD30. (80) First developed for non-Hodgkin’s lymphomas but now used for solid organ and gliomas, radioimmunotherapy is very effective at reducing toxicity and increasing concentration in the tumor microenvironment. Targeting CD20 on dysplastic cells can effectively deliver molecules like Yttrium-90 or Iodine-131 (81) to tumors.

Table 2 - General List of Immunoconjugates

Immunoconjugate	Target	Toxin	Disease
*Denileukin difitox	IL-2	DAB	CTCL, CLL, NHL
*Tositumomab	CD20	Iodine-31	NHL
*Ibritumomab tiuxetan	CD20	Yttrium-90	NHL
*Brentuximab vedotin	CD20	Auristatin E	HL, sALCL
DT388-GM-CSF	GM-CSF	DT388	AML
TP38	EGFR:TGF- α	PE38	Glioblastoma
RFB4-dgA	CD22	dgA	NHL, CLL
B43-PAP	CD19	PAP	ALL

* = FDA approved.

Source: SMAGLO et al. (82)

Toxin Abbreviations: truncated diphtheria toxin (DAB₃₈₉ or DT388), truncated *Pseudomonas* exotoxin (PE38), deglycosylated ricin A chain (dgA), pokeweed antiviral protein (PAP).

Disease Abbreviations: cutaneous T-cell lymphoma (CTCL), chronic lymphocytic leukemia (CLL), Non-Hodgkin lymphoma (NHL), Hodgkin’s lymphoma (HL), systemic anaplastic

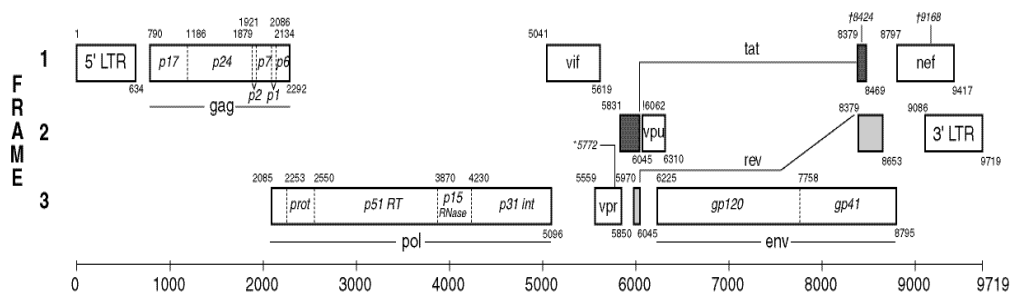
large cell lymphoma (sALCL), acute myelogenous leukemia (AML), acute lymphoblastic leukemia (ALL). (82)

1.5 Human Immunodeficiency Virus

1.5.1 Background and Significance of HIV

It is critical to develop effective treatments to combat the worldwide epidemic of AIDS, which kills nearly 2 million people each year. Since the beginning of the epidemic, more than 70 million people have been infected with the HIV virus and about 35 million people have died of HIV. Globally, 36.7 million people were living with HIV at the end of 2015. An estimated 0.8% of adults aged 15–49 years worldwide are living with HIV, although the burden of the epidemic continues to vary considerably between countries and regions. (83) A member of the Retroviridae family, HIV is an RNA virus that must reverse transcribe its RNA genome into DNA to replicate. The provirus commonly integrates into the host cell's genome, and may remain latent until that cell is activated. It contains several major genes encoding structural proteins (Gag and Env), regulators (Tat, Rev, Vpu, Nef), and enzymes (reverse transcriptase, integrase, protease). The Gag polyprotein is cleaved by the HIV protease into capsid (p24), matrix (p17), and several other peptides. Env is produced as a precursor (gp160), which is cleaved by cellular proteases (furin and furin-like proprotein convertases) into the surface receptor-binding gp120, and the transmembrane gp41, which are non-covalently associated with each other. Env is the only HIV protein expressed intact on the surface of both the virion and infected cells. The figure below shows the organization of the HIV genome and the structure of HIV.

A



(continued)

(continuation)

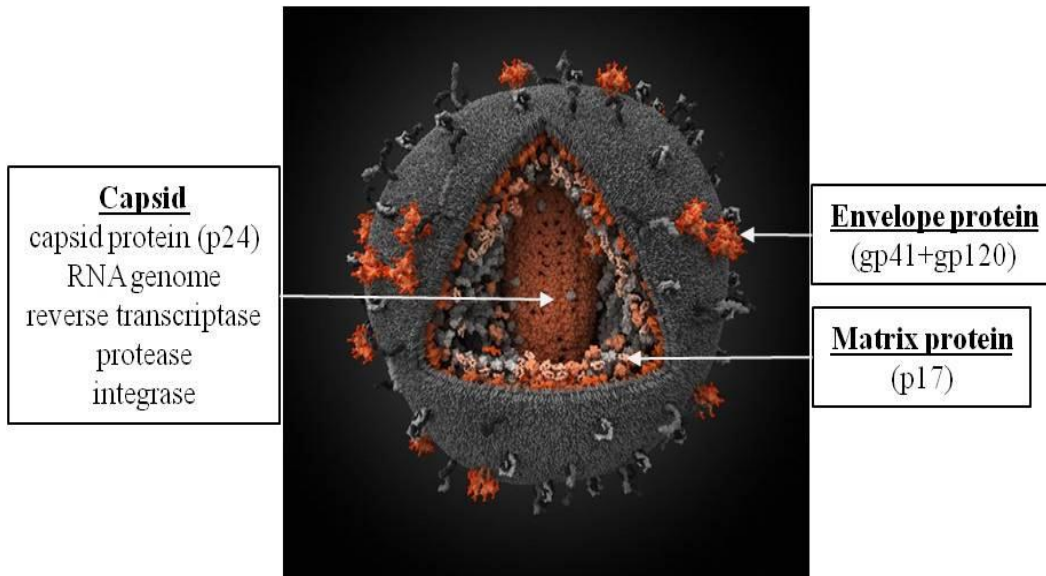
B

Figure 6 - HIV genome organization and virus structure **A**: Genome organization showing major genes of HIV (84). **B**: 3D structure of HIV virions (HIV-derived proteins shown in orange, human in grey) (85). Source: KONSTANTINOV (84-85).

The introduction in 1996 of a drug cocktail containing reverse transcriptase and protease inhibitors, known as highly active anti-retroviral therapy (HAART), has been extremely effective in reducing viral loads and reducing the spread of infection. However, upon cessation of therapy, the provirus can be reactivated in long-lived memory cells. Some estimate it would take over 70 years to exhaust the latent reservoir completely (86), making eradication by HAART unfeasible. There is still a need for further research and innovative concepts to combat drug-resistant escape variants, persistent proviral reservoirs, and patient compliance issues due to multiple daily doses, severe adverse effects, and the high cost of drugs. One approach focuses on Abs as targeting molecules to attack HIV since Abs to the envelope protein provide the neutralizing component necessary for an effective AIDS vaccine. (87) Additionally, passive administration of Abs has been proposed for both the prevention and treatment of HIV infection. Abs were first used as passive immunotherapy by Jackson, who demonstrated p24 clearance and increase in T cell counts in a 1988 clinical trial. (75) Although it is unlikely that the administration of Abs will supplant conventional HAART regimens, there are specific instances where Abs may have a role. One example is the use of

broadly reactive potent neutralizing Abs as post-exposure prophylaxis. Others, including the Pincus lab, focus on using the specificity of Abs to eradicate the latent reservoir of HIV-infected cells in “activate and purge” protocols. (88)

1.5.2 HIV Vaccine (T cell immunity vs. B cell immunity)

For prevention of HIV infection, scientists look to a vaccine that could protect against as many of the worldwide variants of HIV as possible. Unfortunately, attempts at developing protective Abs through vaccination have failed multiple approaches to date. (80,89) Only very recently, after more than 25 years of effort, have there been modest glimpses of success and what might constitute a protective Ab response. (90) The reasons for the lack of effective, naturally-made antibodies are poorly understood, but may be due to extensive glycosylation (91), sequence variability (92), or epitope masking of HIV surface proteins. (93-94) In theory, creating an effective vaccine hinges on the selection of a proper immunogen, or combination of immunogens, and a proper route of delivery that can stimulate both neutralizing Abs (nAbs) and a strong T cell response. In the case of HIV, an effective immunogen continues to elude researchers. Continued research in vaccine delivery methods and vectors may also improve immunogenicity, perhaps by targeting responses to the mucosal tissues or to a specific immune cell lineage. A preventive vaccine may reduce the incidence rate of new infections while a therapeutic vaccine could help to control viral load and decrease risk of transmission by those already infected with HIV.

Experimental vaccines were generated almost as soon as the AIDS epidemic could be linked to HIV; however, the choice of immunogen and/or delivery method was not optimal. Initial studies focused on Env as the immunogen, but failed to elicit protective bnAbs after immunization with more than 35 different vaccine candidates. With those failures, and the demonstration that cell-mediated immunity to HIV immunogens could be elicited more easily, two camps emerged in search of the solution. The first continued to emphasize the important role of Abs in neutralizing the virus and preventing infection. The others emphasized the T cell response, arguing that sterilizing immunity was not achievable, and that once a person is exposed and infected, Abs play no role in curing the disease because CTLs were required to kill infected cells. These two viewpoints were apparent in the choice of immunogens for the advanced vaccine trials. The AIDSVAX trial included Env in the subunit to stimulate nAbs, while the Merck STEP trial utilized an adenovirus encoding Gag, Pol, and Nef, all targets of CTLs, but not Env.

In 1998 rgp120 from the subtype B virus (MN strain) was used in Phase I/II trials, but two vaccines became infected with subtype E viruses. Therefore, for broader coverage, both MN (subtype B) and A244 (subtype E) were included in the lead vaccine candidate for next Phase III trial in Thailand, AIDSVAX B/E. This strategy included MN-rgp120 administered in four 300µg doses at 0, 1, 6, and 12 months. No beneficial effect was seen although HIV-specific Abs could be induced, so the trial was ended in 2003. (95)

The next attempts came with the STEP trials commenced in the Americas in 2004 and in South Africa in 2007, also known as HVTN 502 and 503 respectively. Merck developed a replication-deficient adenovirus containing genes for Gag, Pol, and Nef proteins from HIV, called V520. (96) This method was the first attempt to induce cell-mediated immunity against internal proteins (no Env included) but had vastly different results than expected. There was a trend toward increase rate of infection in men and in vaccinees who had pre-existing humoral immunity to adenovirus type 5, the serotype of the vaccine vector. The trial was closed in 2007 due to higher infection rates in the vaccinated groups when compared to the placebo groups. (96)

The third main clinical trial, known as RV144 or the “Thai trial”, was also conducted in Thailand and contained a combination of a priming canarypox vector expressing Env, Gag, and Pol (ALVAC-HIV, vCP1521) and a booster of the MN/A244-rgp120 protein vaccine (AIDSVAX B/E). This combination approach resulted in a safe, well-tolerated vaccine regimen. (97) With cautious optimism the authors reported, “This ALVAC-HIV and AIDSVAX B/E vaccine regimen may reduce the risk of HIV infection in a community-based population with largely heterosexual risk. Although the results show only a modest benefit, they offer insight for future research.” A very intriguing finding was that induction of IgG Abs against the V2 loop decreased rate of infection by 43%, while induction of IgA Abs to other epitopes increased chance of infection by 54%. (90,98) The results of these trials can be interpreted optimistically since they gave clues as to optimal routes of administration, favorable responses, and effective targets from which researchers can develop future vaccine strategies.

1.5.3 HIV Envelope Protein and the Immune Response

Env is the only protein expressed on surface of virions and infected cells and is target of neutralizing Abs that may prevent infection. Surface exposed gp120 is composed of several variable loops (V1-V5) that aid the virus by targeting the Ab response away from functionally

important conserved epitopes. Gp120 is heavily glycosylated, which acts to block key epitopes from Ab recognition as well. Attachment to target cells requires gp120 binding to the receptor, CD4, and coreceptors CXCR4 or CCR5. Anchoring gp120 to the membrane is gp41. It is made of two sets of heptad repeats brought in close proximity due to a hairpin turn near the middle of gp41. The hairpin turn interacts with gp120 and is also the immunodominant region of gp41, although Abs to this region do not appear to neutralize. On the other hand, Abs directed against the membrane proximal exposed region (MPER) of gp41 are highly effective at neutralizing HIV. (99)

In a natural HIV infection, the immune response creates Abs directed against most HIV proteins; however, nearly all nAbs are made to gp41 or gp120 of the surface Env spikes. These glycoproteins are synthesized as a single precursor, gp160, which is cleaved and glycosylated in the Golgi into its two monomeric subunits, gp41 and gp120. These subunits are held together by weak noncovalent bonds that retain this structure until assembled as trimers on the viral envelope. (100) The trimers are made of the transmembrane gp41 and surface exposed gp120. The three-dimensional viral structure and expression of Env was eloquently described by Zhu et al using cryoelectron microscopy tomography. They were able to determine an average size of 12nm high by 11nm wide at a distribution of roughly 14 trimeric spikes per virion and confirm the tripod-like leg structure of gp41. (101)

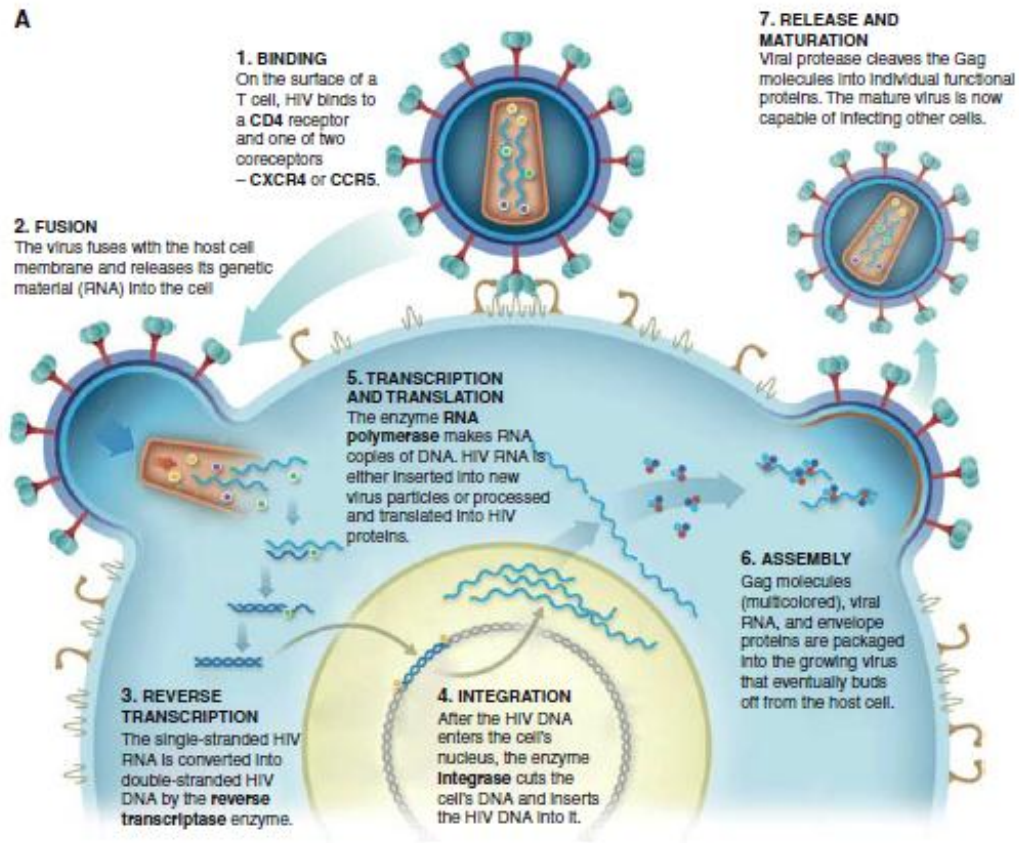


Figure 7 - Illustration of HIV life cycle.

Source: MURPHY. (56)

The figure above shows the life cycle from binding, fusion, and subsequent integration of HIV into cells to reactivation and release of infectious virus (Fig. 7). Cell free virus is the target for most neutralizing Abs, which act to prevent infection from becoming established by blocking binding, fusion, and entry. On the other hand, assembly and budding allow Abs that play a major role in ADCC or delivery of immunoconjugates to identify infected target cells that need to be killed. For infection to take hold, gp120 on the envelope spike must bind to the first domain (D1) of CD4 on a host cell. Abs to the CD4 binding site of gp120 most likely neutralize by blocking this CD4:gp120 interaction on cell-free virus. Upon binding CD4, conformation changes occur in gp120 that expose new regions and allow co-receptor (CXCR4 or CCR5) binding, then dissociation of gp120 from gp41 (102) and exposure of the fusion peptide along with other cryptic epitopes on gp41. CD4 binding- induced (CD4i) epitopes on gp120 are mainly located at and around co-receptor binding sites, yet the majority of Abs made to this region are non-neutralizing. The exception being nAbs like 17b, the prototypic CD4i nAb. (100) The V3 loop of gp120, originally known as the principal neutralizing

determinant (103), has been implicated in CCR5 coreceptor binding and presents epitopes for the bnAb, 447-52D. (104) Other notable regions of gp120 include the V1/V2 loops that are usually associated with strain-specific nAbs. (105) As more Abs are discovered and created, ideas for potential targets based on binding or functional activity are constantly being redefined.

One thing is certain, Abs are not only made against gp120; gp41 is also a potent immunogen that leads to the creation of many Abs. After CD4 binding and shedding of gp120, the hairpin loop is exposed and the fusion peptide inserts into the host membrane. It is during this process that several cryptic epitopes are revealed in the immunodominant region. This region along with the MPER leads to the formation of hundreds of Abs. Some are neutralizing, some act as potent ICs, but most are ineffective at inhibiting the virus. Rarely, potent neutralizing Abs can be isolated from infected patients; however, very few are able to broadly neutralize viruses across different clades.

1.5.4 Early Discovery of Broadly Neutralizing Antibodies

As research began on HIV, the mechanisms responsible for either preventing or controlling infection were poorly understood. But it became apparent that nAbs played a role in controlling the virus, so many studies focused on raising or engineering more bnAbs. These studies were done to understand the human immune response to HIV and help inform the design of immunogens. For many years, anti-Env antibodies were isolated from infected patients; unfortunately, only a handful was shown to be broadly neutralizing. These include the two gp120-binding Abs: 2G12 and b12, and the two gp41-binding Abs: 2F5 and 4E10. (106)

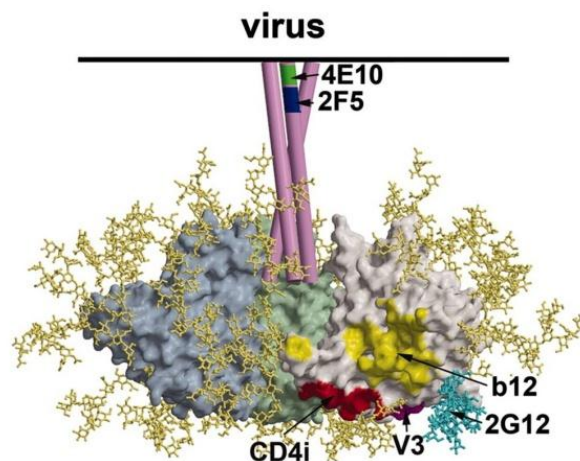


Figure 8 - Env structure with earliest neutralizing antibody epitopes.

Source: DUBRUILLE. (106)

Glycosylation residues show in dark yellow, gp41 trimers in purple and gp120 trimers in blue, green, and grey. CD4-bs in yellow, CD4i epitopes in red, MPER epitopes in dark green and dark blue.

In order to study Ab responses, the structure of both virus proteins and Abs needed to be solved; however, there were major hurdles to overcome. More than half the mass of gp120 is heterogeneous carbohydrate residues. (107) The protein sequence contains five variable regions (V1-V5) that form flexible loops adding conformational variability. Gp41 is noncovalently bound to gp120 so keeping them together as crystals is nearly impossible. The first crystal structure reported by Kwong et al required modifications to a monomeric version of gp120 derived from a laboratory-adapted strain, HXB2, yet he was able to generate crystals of gp120 in complex with CD4 and the CD4-i Fab, 17b. The next structure was determined for a neutralization resistant virus, YU-2, in complex with CD4. These early structures revealed specifics about gp120 including the relatively conserved “inner domain”, a more variable “outer domain”, and a “bridging sheet” separating the two domains. Furthermore, the addition of CD4 and 17b allowed them to examine the overall relationships. These crystal structures exposed conformational changes associated with CD4 binding, determined the interaction sites of the V3 loop and conserved regions with coreceptor binding, and provided insight on mechanisms of immune evasion. (88)

Then in 2001, another advantageous crystal structure was published showing CD4-bound gp120 docked with b12. It identified unique features of the asymmetric IgG1b12. (108) Notably, only the heavy chain of b12 interacted with gp120, with each of the three heavy-chain complementarity-determining regions (CDRs) making extensive contact (Fig. 9). The b12 Ab targets the CD4 binding site through a uniquely long CDR H3 loop and it has been shown to neutralize a broad range of isolates.

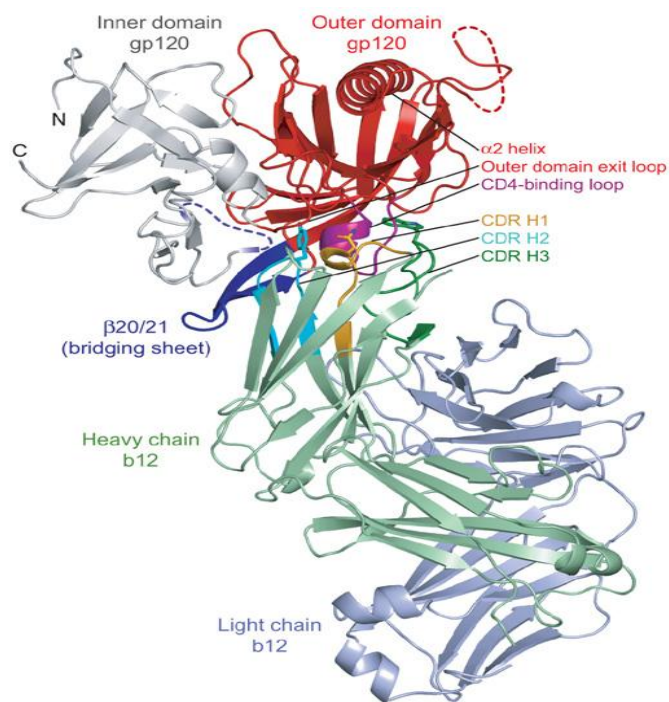


Figure 9 - Crystal structure of b12-Fv bound to gp120; Secondary structures reveal the CDR loops and Ig domain- folds of b12, and the bridging sheet, inner, and outer domains of gp120.
Source: ZHOU; TONGQING. (109)

Yet another intriguing anti-Env nAb is 2G12, which recognizes an N-linked oligomannose epitope on the silent face of the gp120 outer domain. (110) It was also crystallized to reveal a unique, domain-swapped, multivalent antigen-binding fragment, which makes it possible to bind up to four oligomannose sugars. (111) The unique phenomenon of domain swapping occurs when a pair of 2G12 Fabs in close proximity exchange VH domains. The original Fabs remain attached by their CL and CH1 domains but the variable domains swap VL partners, potentially increasing avidity by creating two swapped VH:VL antigen binding sites and one new VH:VH' binding site. (112) These crystallographic and computer modeling experiments give an insight into the interactions between virus and Ab at a molecular level and allow us to engineer Abs that target specific weaknesses in the virus itself.

Unfortunately, gp41 has proven harder to crystallize and study. There are no full-length structures available, but some have been successful at crystallizing portions of the molecule. It is known that gp41 contains about 345 amino acids and is folded in a very specific way so that it can associate with gp120 as trimeric Env on the surface of the virus. Combining crystallographic studies and sequencing data indicated a 15 amino acid fusion domain at the N terminus, followed by a coiled coil formed by a 4-3 heptad of hydrophobic repeats, a loop region responsible for intrachain disulfide bonding, another heptad repeat of about 50 amino

acids, a transmembrane domain, and finally the cytoplasmic tail. (113) Among these sections are highly immunogenic sequences that lie within either the loop containing the disulfide bonds known as immunodominant cluster I, or the C terminal heptad repeat, known as immunodominant cluster II (114). While Abs to this region have anti-viral activity most do not neutralize a broad range of primary isolates, except 2F5, 4E10, and 98-6. (115-116)

A small subset of these nAbs target a region of gp41 exposed near its insertion point at the MPER (Fig. 10). The epitope of 2F5 is slightly more distal from the membrane than 4E10. 4E10 showed the most potency and breadth, yet they both exhibited broad *in vitro* neutralization. (117) These mAbs have been safely administered alone and in combination in a Phase I trial. (110) Most immunotherapy against a swiftly mutating virus like HIV should be most successful when used as combination therapy. This makes even more of an argument for engineering bispecific DVD-Igs.

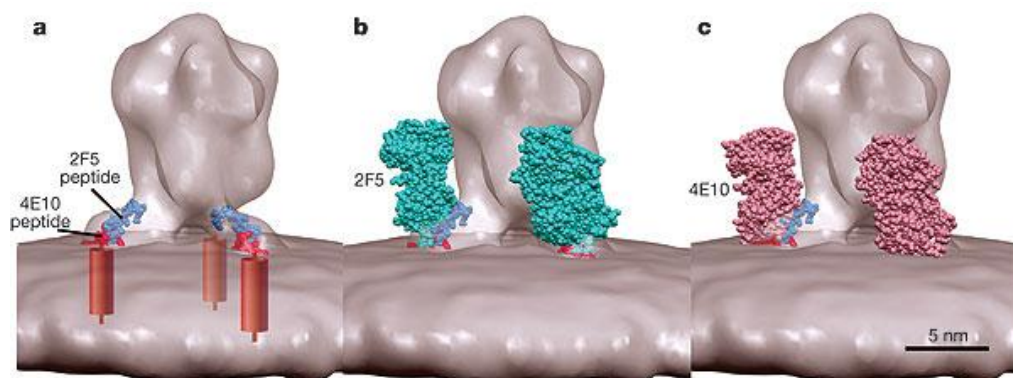


Figure 10 - 2F5 and 4E10 epitopes overlaid on SIV gp160. a, Peptide epitope superimposed on Env shell with gp41 anchor residues shown. b and c, Overlay of Fv structures of 2F5 (b) and 4E10 (c) on peptide epitopes and Env shell.

Source: BARBATO. (118)

1.5.5 Recent Discovery of Broadly Neutralizing Antibodies

The envelope of HIV presents the best target for broadly neutralizing antibodies (bnAbs) to bind and prevent attachment, entry, or even intracellular activity in multiple, susceptible cell types. The reasons for the lack of naturally made, nAbs are poorly understood, but that is not to say that Abs are not generated against the immunogenic proteins, gp41 or gp120. Thousands of Abs have been screened and as Burton's work shows us, it takes over 30,000 B

cell clones from more than 1,800 donors to produce 1 or 2 new bnAbs like PG9 and PG16. (119) Several bnAbs, like 2F5 and 4E10 appear good after *in vitro* studies only to find that they cross-react with molecules like cardiolipin, which may lead to down-regulation *in vivo* and act as an immune evasion mechanism by the virus.

Some Abs made to quaternary epitopes are so specific that they only neutralize a small subset of viruses, as is the case of mAb 2909 made against the SF162 strain of HIV. However, other quaternary epitope Abs like PG16 and PG9 are effective at neutralizing over 70% of circulating isolates tested from clades A, B, or C. (119-120) Other Abs target intermediate conformations that are only exposed during CD4 binding as the virus prepares to enter the cell. Abs like X5 (121), 17b, and 48d (122) are all human Abs against these induced epitopes. Not surprisingly, 17b and 48d cannot neutralize HIV in the absence of CD4, which indicates how restricted these epitopes are in the cell-free virus.

A strategy that had been used years earlier to develop b12 was re-implemented by Dimitrov et al and used bone marrow from long-term nonprogressors to isolate a series of Abs by using competitive antigen panning (CAP) of the immune library derived from these patients. Of these Abs, m44 and m46 were not autoreactive and were able to neutralize most of the primary isolates from different clades better than 2F5 but exhibited a lack of activity against clade A specifically. (123)

Anti-Env Abs targeted to the conserved CD4 binding site (CD4bs) on gp120 have been well characterized to neutralize virus by preventing it from binding CD4 and attaching to cells. CD4 is the cellular receptor for HIV, a high affinity ligand of gp120 (124), and a member of the Ig superfamily. Attached to human Fc domains, CD4 functions both to inhibit spread of HIV infection and as a highly efficient neutralizing Ab. (125) One molecule that received a lot of focus was CD4-IgG2. It is an Ab-like fusion protein with an IgG2 Fc plus hinge region fused to the first two domains of CD4 that act as V-domains. In both *in vitro* assays, *in vivo* assays (126), and in human trials (127), it showed encouraging results and could broadly and potently neutralize primary HIV isolates.

Due to the lack of our current technologies during the 1990s and early 2000s like high throughput screening of genetic libraries or isolating and cloning single B cells from infected patients by antigen trap techniques, only a few anti-Env nAbs were described that were broadly neutralizing. However, in the last few years, the explosion of genetic techniques led to the generation of many more nAbs. Recently promising nAbs have been described, notably the anti-V2 loop PG9 and PG16 (119); the anti-CD4 binding site HJ16, PGV04,

VRC01/VRC03 (128) and a clonal variant NH45-46; the mucosal-derived anti-CD4i CH08 (129); and the anti-V3 glycan PGTs. (92)

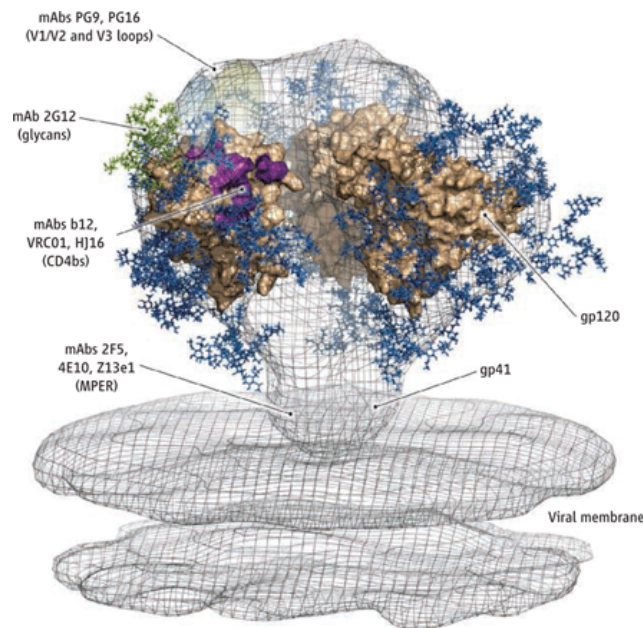


Figure 11 - Shell of gp120 with broadly neutralizing antibody epitopes. Illustration shows a transparent glycosylated Env trimer anchored into viral membrane with binding sites for major recently discovered bnAbs to gp120 and gp41.

Source: BURTON. (130)

1.5.6 Anti-HIV Immunoconjugates

Great progress has been made in the area of controlling HIV due to small molecule drugs, yet there is still no way to eradicate the infection. Using immunoconjugate (IC) techniques developed to target and kill cancer cells it may be possible to target and kill latently infected cells, removing the reservoir that would reseed the infection, and thus cure the patient. Several key regions of the virus have been proposed as potential targets including: CD4 binding site and the variable loops of gp120, especially the V3 loop, and gp41. Instead of attacking the virus directly, others are attempting to target host receptors expressed on cells latently infected with HIV.

Several groups of investigators have studied different approaches for HIV therapy. One of these approaches is to kill persistently HIV-infected cells and each newly HIV-infected cell. It is believed that preventing the production of more infective virions by elimination of HIV-infected cells is crucial in limiting further reduction of CD4-positive cells. (23,131) This approach seems feasible since immunotoxins (ITs) are able to specifically eliminate undesirable cells. ITs are chimeric molecules in which cell-binding ligands are coupled to

toxins chemically or by DNA-fusion techniques. The majority of HIV-infected cells are in the circulation and in the lymphatic system which is encouraging for the treatment of HIV-infection with ITs. This can be concluded from studies in which was shown that malignant lymphoid cells are more responsive to ITs than solid tumors possibly due to the greater accessibility of lymphoid cells. (2,132) An immunotoxin against HIV-infected cells could possibly not only kill HIV-infected cells but also neutralize interactions of cell-free virions with uninfected cells.

Early attempts recognized the importance of CD4 and fused it to the *Pseudomonas* exotoxin A (PE-40) for use as an IC. (130) Berger et al showed that CD4.178-PE40 was active against cells expressing a diverse array of HIV and SIV strains. The in vitro results were so striking that it warranted a Phase I clinical trial; however, it proved to be hepatotoxic, immunogenic, was rapidly cleared from serum, and showed no antiviral effects. (133) After failing a small clinical trial, PE-40 was re-engineered by Bera et al to eliminate cell binding domain as well as other nonessential protein domains. Instead of linking the toxin to CD4, it was conjugated to a 3B3-Fv construct that was previously shown to be more potent than its parent, IgG1b12. (115) This CD4bs Ab acts like CD4 but comes from an HIV-infected individual and was shown to specifically kill gp120-expressing transfected cells as well as HIV-infected lymphocyte cells when conjugated to PE38. (130)

Vitetta et al have used a different approach to target cellular receptors that are expressed on memory T cells, the most likely reservoir of latent virus in humans. Using an anti-CD45RO Ab to deliver deglycosylated ricin A chain to infected cells, they found selective killing of CD45RO⁺ but not CD45RA⁺ cells and that the surviving cells produced no p24 or detectable DNA. (134) Further trials are underway to test models of activation by immune stimulation followed by a purge of infected cells using cell-targeting ICs in the presence of HAART as a means to eradicate infection.

Hamer et al took a more traditional route of using Abs against HIV Env to deliver cytotoxic agents to kill infected cells. Using earlier versions of HY, he characterized the binding and structural relationships between Abs and the CD4 binding site on gp120. Plus, they improved the affinity and biochemical stability through several structural-based mutations and even increased the potency in several cell types by adding a KDEL sequence that retains the IC in the endoplasmic reticulum. (135) This work established ICs as a real potential weapon in the eradication of AIDS.

Subsequently, Pincus et al hypothesized that gp41 might offer better targets than gp120 for ICs. His work focuses on ricin A chain as the toxin of choice, rather than *Pseudomonas*

exotoxin or diphtheria toxin. However, results are similar in terms of cell killing ability. *In vitro* testing showed that Abs to gp41 could be up to 30-fold more cytotoxic with the presence of sCD4 in the media. (136) The marked increase in efficacy most likely results from conformational changes associated with sCD4 binding that expose gp41 epitopes. He confirmed the efficacy of the anti-gp41 ICs *in vivo* in an irradiated NOD/SCID mouse model. By measuring infection using plasma p24 levels and a focal infectivity assay that determined HIV-infected cells, they were unable to show any evidence of HIV infection remaining after treatment with a combination of an anti-gp41 IC and CD4-IgG2. (136)

Currently, many eradication studies are testing immunoconjugates *in vivo* for their ability to target and remove viral reservoirs; however, several key Abs have emerged from these studies as potential therapeutic ICs. This is even more reason to create powerful DVD-Igs by combining two variable domains from potent ICs or combining enhancing domains with IC domains (i.e., CD4 plus 7B2).

1.5.7 Antigenic determinants as target on the HIV-infected cell

The cell-binding carrier proteins of the ITs have to be chosen very carefully. Only a portion of antigenic determinants are suitable targets. Internalization of the ITs and their routing into the cytosol, is dependent on the targeted antigen. An optimal IT will react with different HIV isolates, will be minimally immunogenic, and will possess little nonspecific toxicity. (99,132)

One feature of HIV is the extensive variability between viral genomes. This genetic variability in HIV manifests itself over time not only in different infected individuals but also within each infected individual. This variability might be due to the high mutation rate HIV genome induced by an extremely inaccurately acting RT. Thus, it has been difficult to choose targets that are specifically and broadly present on HIV-infected cells. The cell-binding carriers developed so far have been directed against different sites on the surface of HIV-infected cells, such as *a.* different regions of the HIV envelope glycoprotein (gp120 and gp41) and *b.* surface antigens expressed by CD4-positive cells (Figure 12). (4,132)

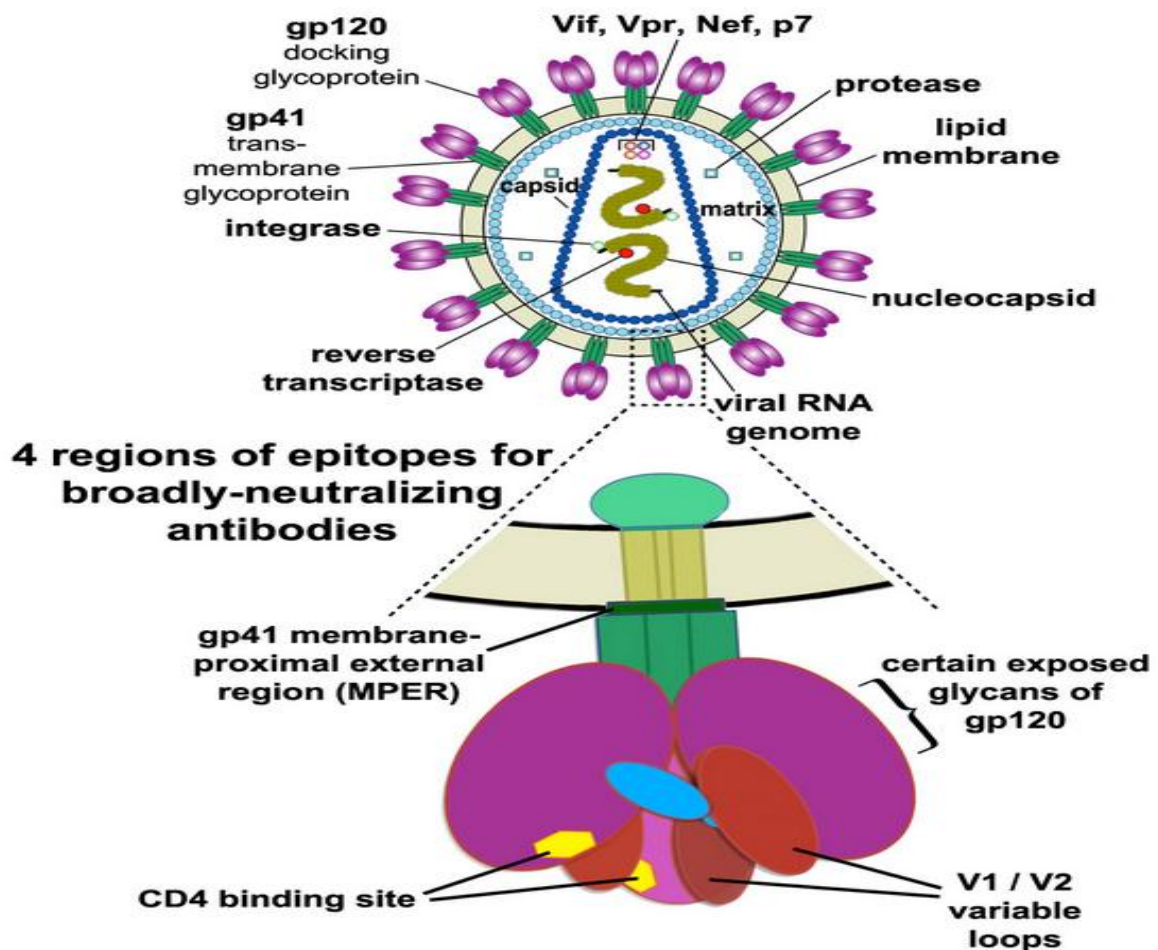


Figure 12 – Organization of the HIV-1 virion. Env consists of two smaller glycoproteins: gp41 forms the stem and gp120 the tip. A great deal of study has focused on one part of the gp120 glycoprotein known as the V3 (variable region #3) loop. The V3 loop is involved in both the virus's infection of host cells and in recognition of HIV by the immune system.

Source: MERK. (4,132)

1.5.8 Anti-HIV IT against HIV gp160

HIV Env (precursor gp160, surface gp120, and transmembrane gp41) is the only virus-encoded protein expressed on infected cells and virions. Native Env is a complex antigen, consisting of trimers of dimers (gp120/gp41), having different conformational states, and mobile within a lipid bilayer. mAbs with different affinities and directed against different epitopes could vary widely in their ability to neutralize virus, bind cells, elicit Fc-mediated effects, or to act as effective immunoconjugates. (99,137)

Most of the genomic diversity is located in the viral envelope gene, however different regions of the HIV envelope have been used as targets for ITs. Although there is some evidence that core proteins may be expressed on the surface of HIV-infected cells, no ITs have been directed to them.

It is presumed that an anti-HIV IT targeted to the envelope of HIV should act via at least two pathways. First, cells actively producing HIV and expressing HIV antigens on their cell surface will be killed by the toxin of the IT. Second, the carrier protein of the IT can neutralize interactions of cell-free virions and infected cells with uninfected cells. (131-132,137) Through these mechanisms the cycle of infection may be decreased and CD4-positive cell decrease may be halted. However, it is expected that extremely high concentrations of IT are needed for neutralizing activity.

The envelope glycoprotein contains well-defined variable and constant regions located on extracellular (gp120) and transmembrane (gp41) domains. The most variable regions have been found in gp120 but between those variable regions, a more conserved sequence has been detected among different viral isolates. This conserved sequence is immuno-dominant and located in the principal neutralizing determinant (PND). The majority of HIV-neutralizing antibodies react with this sequence, though the mechanism of this neutralization is not entirely understood. Nonetheless, these antibodies have been used in several HIV-ITs. (138)

Since HIV-1, HIV-2 and even SIV (simian immunodeficiency virus) use CD4 as the surface receptor to bind to target cells, the amino acid sequence of the putative CD4-binding domain in the carboxy terminal C4 region on gp120 is highly conserved among various HIV isolates. Furthermore, antibodies against gp120 in patient sera, are probably not directed against this binding region suggesting that this region is less immunogenic. For these reasons, soluble recombinant CD4 (srCD4) molecules or antibodies directed against the CD4 binding region on gp120 have been used as toxin carriers. Many parts of gp41 are highly conserved and thus antibodies have been also targeted against these domains. (4,138)

Besides targeting the ITs to different regions of the HIV envelope glycoproteins, several ITs have been targeted to surface antigens expressed by CD4-positive cells. The antigenic targets that have been used are CD4, CD5, CD7, CD25 and Le^y, a cell-surface carbohydrate antigen found on tumor cells and HIV-infected cells. (2,132,137) The use of these antigens has several advantages above HIV-envelope glycoprotein: 1. the HIV envelope glycoprotein is only deposited on the surface of the cell late in the infectious cycle, 2. normal surface antigens are not as variable as envelope glycoproteins, 3. serum of HIV-infected individuals contains anti-envelope antibodies that might compete with ITs directed against the envelope glycoprotein, 4. gp120 might be complexed with sCD4 which might prevent binding of ITs to the envelope protein. (131-132)

However, the possible killing of uninfected cells expressing these antigens is a disadvantage, although ITs with PAP do not kill uninfected cells when used in low doses. Furthermore, HIV-infected monocytes or neural cells do not express these antigens and are not susceptible, except for monocytes that express CD4. Another problem in trying to kill latently infected cells may be that the cytotoxicity of ITs in inactive cells is not as high as in activated cells. (131-132,139)

1.6 HIV-envelope glycoprotein as the best target for Anti-HIV ITs

1.6.1 mAb-IT, directed against PND region on gp120

Hybrid toxins like CD4.178-PE40, composed of two proteins each with a short half-life, are cleared rapidly from the circulation. ITs that have a longer serum half-life could be more beneficial for patients. Conjugation of a toxin to a carrier protein with a long half-life, such as a mAb, can substantially increase the half-life of an IT. The serum half-life of an IT can even be more increased by using a humanized mAb or chimeric mAb. (139)

The mAb G3.519, directed against a putative CD4-binding region on gp120 was coupled to PAP. This IT specifically inhibited H9 cells, infected with three diverse HIV-1 strains (HTLV-IIIb, HTLV-IIIMN, and HTLV-IIIRF) with the ID₅₀ ranging from 1.4×10^{-10} M to 1.7×10^{-9} M, which is rather disappointing. G3.519-PAP prevented syncytia formation and retained the ability to neutralize HIV virions infecting T cells. The mAb 110.1, directed against the highly conserved carboxyl terminus of gp120, neutralized 13 different HIV isolates, but the IT 110.1-Ricin A was relatively ineffective against infected cells. (132,137)

The IT, BAT123-PAP, directed against a peptide segment (amino acid residues 307-317) of the PND region of gp120, was effective in killing H9 cells infected with HTLV-IIIb (ID₅₀ of 4.3×10^{-11} M) or with HTLV-IIIMN (ID₅₀ of 4.7×10^{-10} M), but not with HTLV-IIIRF.

1.6.2 mAb-Ricin A, directed against a CD4-binding region on gp120

The PND region of HTLV-IIIb shares higher degree of homology with HTLV-IIIMN than with HTLV-IIIRF. mAbs directed against the PND region were also coupled to other toxins such as ricin A. The IT 924-Ricin A, directed against amino acids 313-324 of gp120, showed strong reactivity against the HIV-1 NL4-3 strain, a little reactivity against the HIV-1

NY5 strain, and almost no reactivity against cells infected with HTLV-IIIMN, HTLV-IIIRF or HTLV-IIICC. (140) In contrast, F58-Ricin A directed against amino acids 309-317 was broadly reactive. The IT 907-ricin A, directed against amino acids 313-324 of gp120, killed H9 cells infected with the HTLV-IIIB strain. In these experiments, the activity of the IT could be reduced for 70% by blocking antibodies in serum of HIV-infected individuals. These results indicate that binding of the IT does not guarantee that a carrier protein forms a potent IT. The internalization and intracellular routing of the toxin, induced by the interaction between carrier and target antigen, appeared to be even more important. (131)

It has been shown by using 907-ricin A that IT-resistant HIV variants exist. Clones resistant to this IT arose at a frequency of 0.1-1.0%. Two distinct resistant groups could be determined. One group had a truncated gp41 but was still capable of binding to CD4. The other group contained provirus but lacked cell surface CD4 and could not be induced with agents known to activate latent HIV. (141) Both groups could escape from killing by the IT but as they could not produce infectious virus, such resistant cells are not interfering with the IT-therapy.

1.6.3 Human polyclonal /monoclonal Abs coupled to RTA

A human antibody will be less immunogenic for *in vivo* usage than a non-human antibody. Pincus et al. coupled ricin A to a human polyclonal antibody directed against gp160. They purified the antibody from sera of HIV-1-infected individuals by affinity chromatography with recombinant gp160. (131,141) This IT inhibited protein synthesis in H9 cells infected with the NL4-3 strain and was able to prevent infectivity of seven different viral strains. This IT showed a broader specific killing compared with a lot of other ITs. However, it could not prevent infection of cells by Z2, a Zairean isolate, although cells infected with the Z2 isolate showed the highest level of gp160 expression measured by the same antibody. Furthermore, the activity of the IT was strongly inhibited by an HIV-immune globulin pool of antibodies purified from sera of HIV-positive individuals. (131) In general polyclonal antibody preparations have several advantages over mAb, including higher avidity and they react with multiple epitopes on the antigenic target. However, the advantages of this human polyclonal IT must be weighed against potential drawbacks including variability in the source of human antibodies, the possibility of the antibodies cross-reacting with normal human tissues, and of strain-specific neutralizing antibodies when recombinant gp160 derived from a single HIV strain is used as the immobilized antigen.

Two human mAbs to gp41, 50-69 and 98-6, have been shown to be potent ITs when chemically conjugated to dgA. These ITs killed T-cell lines and monocyte lines infected with different variants of HIV-1 (ID50 of 2×10^{-9} M) whereas uninfected cells and Daudi cells were not affected. Furthermore, the presence of anti-gp41 antibody in the serum of patients may not be an insurmountable obstacle to therapy with these ITs, because *in vitro* a 5-fold excess of unconjugated anti-gp41 antibody added to these ITs only partially inhibited their cytotoxicity. When infected U937 cells were treated with the ITs in the presence of 20 μ M of the lysosomotropic amine, chloroquine, cytotoxicity was strongly enhanced up to an ID50 of 4.6×10^{-11} M, probably due to the increase of the lysosomal pH and inhibition of the fusion of endosomes, increasing the intracellular trafficking of the toxin to the cytosol. (142)

The IT 41.1-ricin A, containing a human mAb which binds to amino acids 579-603 of gp41, showed specific cytotoxicity against H9 cells infected with the NL4-3 isolate but only a small inhibitory effect on viral infectivity against a panel of HIV-1 isolates. (131,142) Using a pool of sera from HIV-infected individuals, it was demonstrated that binding of 41.1-ricin A was blocked. The same sera initiated less pronounced blocking of mouse mAb IT 924-ricin A (against the PND of gp120) but stronger blocking of human polyclonal anti-gp160-ricin A. Surprisingly, when tested in the presence of sCD4 the efficacy of anti-gp41, 41.1-ricin A, was enhanced at least 30-fold. This effect was specific for HIV-infected cells and not for uninfected cells, and was seen at concentrations of sCD4 as low as 0.1 μ g/ml. The anti-gp120 ITs were rather marginally inhibited in the presence of sCD4. These results could not be explained by conformational changes in the envelope proteins by sCD4. Flow cytometric analysis revealed that sCD4 increased the expression of gp41 epitopes on the surface of infected cells and increased internalization of gp120 and gp41. (143) These data suggest that sCD4 alters the cellular trafficking of HIV envelope proteins.

1.6.4 Implications for mAb therapies to eradicate HIV infection

There has been a rebirth of interest in the use of MAbs to treat HIV infection. This has resulted in part from the development of better anti-Env mAbs and better modes of delivery of MAb. Perhaps most important are the results of recent studies demonstrating impressive anti-viral activity of MAbs in treating established SHIV infections in macaques. (141)

The persistence of the latent reservoir of HIV is a major barrier to a functional cure of HIV infection. One approach to eliminating the reservoir involves activating the latent virus, maintaining anti-retroviral therapy, and purging the activated cells. Purging may be

accomplished by viral cytopathic effect, by established host defenses, or by actively eliminating cells with passively administered MAbs or Its. (144) We and others have designed ITs targeted to cells expressing HIV Env. These ITs are active against many cell types and clinical HIV isolates. They are also effective in murine models of HIV infection, including a model of latent infection. In a companion publication, we show their effects in SHIV-infected macaques. (144)

2 OBJECTIVES

- We propose to use anti-HIV immunotoxins to eliminate infected cells that serve as the persistent virus reservoir.
- We have sought to test a recently described toxin Pulchellin A chain, and compare it to the standard toxin, Ricin A chain, used for ITs.
- This is the first study on the possible utility of PAC for the design and construction of therapeutic ITs.

3 MATERIALS AND METHODS

3.1 Cells and reagents

H9/NL4-3 cells are laboratory-adapted and persistently infected with the NL4-3 molecular clone of HIV (145; 146) and maintain a productive infection in all cells during passage in tissue culture. Uninfected H9 cells, a human CD4+ lymphoma cell line, were obtained from Dr. M. Reitz (Institute of Human Virology, Baltimore, MD). H9 and H9/NL4-3 cells were maintained at 37°C in 5% CO₂ in RPMI 1640 medium with 10% fetal bovine serum (Gibco Invitrogen, Grand Island NY) as described elsewhere. (147)

293T cell lines stably express clade A clinical isolate 92UG037.8 gp160 as native gp120/gp41 trimers (293T/92UG) (148). 293T cells were used as uninfected control cells. The transfected and non-transfected 293T cells were maintained at 37°C in 5% CO₂ in DMEM medium with 10% fetal bovine serum (Gibco Invitrogen, Grand Island NY). In this paper, Env-transfected cells refer to the 293T cells stably transfected with 92UG037.8 gp160.

3.2 Production of Antibodies

MAb 924 was produced from a mouse immunized with a vaccinia virus recombinant containing a gene encoding the HIV gp160, as described elsewhere. (11) This IgG1 antibody reacts with the V3 loop of HIV gp120 of LAV/HTLV-III B isolate. MAb 7B2 (Genbank accession numbers JX188438 and JX188439) is a human IgG1 which binds HIV gp41 at AA 598–604 (CSGKLLIC) in the helix-loop-helix region. MAb 7B2 was secreted by hybridoma cells in tissue culture using IgG-depleted FCS. (136,143) HY (Genbank accession numbers JX188440 and JX188441), an affinity matured version of the anti-CD4 binding site Ab b12. HY-IgG was produced by transient transfection in 293T cells using the 293Fectin reagent. (149) Murine and chimeric version of anti-ricin A chain MAb RAC18 and Alexa 488-conjugated RAC18 have been described elsewhere. RAC MAb 18 has a common motif of QXXWXXA on the structure of RAC (150), as has the isotype control 924 Mab. (151) MAbs were purified from hybridoma supernatant on Protein A agarose beads (Invitrogen) and eluted with 0.1 M glycine, pH 2.5, immediately neutralized, and dialyzed vs PBS. Two types of soluble CD4 were used to observe CD4-mediated effects (143); CD4-183 contains the first two domains of CD4 including the region in domain 1 that binds the HIV coat protein gp120.

CD4-IgG2 is a tetrameric fusion protein comprising human IgG2 in which the Fv portions of both heavy and light chains have been replaced by the V1 and V2 domains of human CD4. Goat anti-human IgG (Invitrogen) was conjugated to either alkaline phosphatase (AP) or fluorescein isothiocyanate (FITC). Goat anti-mouse IgG (Biacore) (heavy + light chains) secondary antibody was conjugated to Alexa-488.

3.3 Cloning, expression and purification of recombinant toxin A chains

Recombinant pulchellin A-chain (rPAC) was generated by PCR using the pulchellin cDNA isoform PII (27), accession number EU008736.1, as template. In our previous study, the rPAC had a 6xHis-tag at its N-terminal end. (27,29) In this experiment, we designed a new construct containing a tobacco etch virus protease (TEV) cleavage site for proteolytic removal of the 6xHis-tag after purification. Specific primer sequences were the following: rPAC-forward (5' CCCCATGGCTAGCGAGGACCGCC) and rPAC-reverse (5'GTGCTCGAGTTAATTTGGCGGATTGC), including the restriction sites for *NcoI* and *XhoI*, respectively. PCR products were cloned into the pGEM-T (Promega) vector and its sequence was confirmed using an ABI Prism 377 automated DNA sequencer (Genescript). Recombinant RAC was produced in BL21(DE3)RIL cells (Novagen) from plasmid pETtrx, which encodes *E. coli* thioredoxin and a TEV protease-cleavable 6xHis affinity tag in frame with and N-terminal to the RAC coding sequence. The target sequences of RAC and PAC were subcloned into pET28a(+) vector (Novagen). (Figure 13)

For expression and purification of PAC and RAC. briefly, the recombinant PAC and RAC were produced in *E. coli* Rosetta (DE3), and purified by HisTrap Nickel column. The His-tag was cleaved with TEV protease, and the tag-less toxin A chain was purified on a HiPrep 26/60 Sephacryl S-200 column.

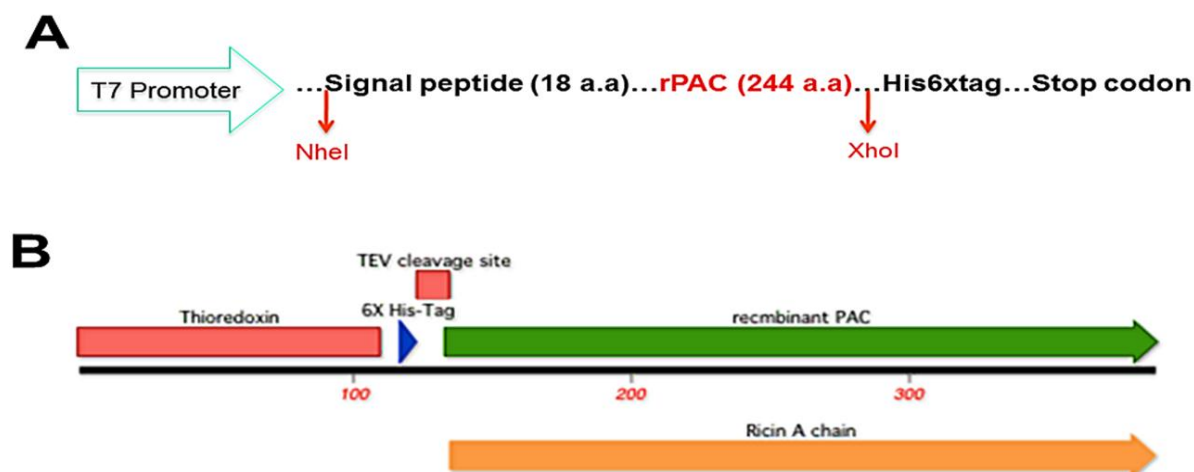


Figure 13 – A. Schematic picture of the sequence of rPAC after generation by PCR. Herein, the target sequence was subcloned into pET28a(+) vector (Novagen). B. Schematic constructs of rPAC and rRAC, demonstrating the position of Thioredoxin and TEV in pET28a(+) vector.

Source: By the author.

3.4 Conjugation of Abs to RAC and PAC

HIV MAbs 924 and 7B2 were conjugated separately to PAC and RAC by using a modification of the protocol described elsewhere. (11,147) Optimization of the concentration of heterobifunctional cross-linking reagent succinimidyl 6-[3(2-pyridyldithio) propionamido] hexanoate (SPDP, Pierce) was carried out for conjugation between amino groups (on lysine and at the N-terminus) on antibody and the single free cysteine on A-chain toxin (152-153) by applying three different concentrations of LC-SPDP biolinker (10, 20, and 40X molar excess relative to MAb). After 2 hr of incubation at room temperature, the MAbs and SPDP were separated on a Zeba desalting column (Pierce) equilibrated with PBS. (Figure 14)

PAC and RAC (0.5 mg/ml), which were stored at -80°C in reduced form, were desalted on Zeba column. The RAC/PAC and MAb-SPDP were mixed separately, concentrated to 0.5 ml and incubated overnight at 4°C . Individual fractions were analyzed by microcapillary electrophoresis (Agilent Bioanalyzer, GE Healthcare). After the conjugation reaction, the removal of unreacted A-chain toxin and holotoxins were achieved by passing from an Amicon Ultra-100K centrifugal filter (Millipore). The concentrations were measured by bicinchoninic acid protein assay (Pierce, Rockford, IL) and confirmed using OD280 reading by Nanovue UV Spectrophotometer (GE Healthcare, Piscataway, NJ), before and after passing from filter.

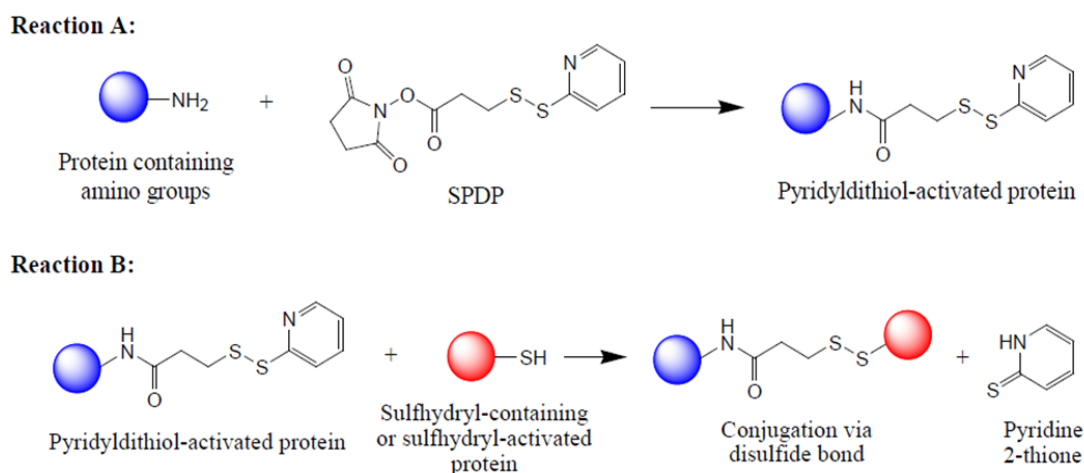


Figure 14 – Two PAC-to-mAb conjugation strategies involving SPDP Reagents; As PAC already contains sulfhydryl groups, so only mAb must be modified by the SPDP reagent (Reaction A). Then the two proteins are conjugated together (Reaction B).

Source: DOSIO. (153)

3.5 ELISA

ELISAs were performed for Ag-binding specificity analysis and titration of purified MAbs and ITs in wells coated with antigen (1 $\mu\text{g/ml}$), as described elsewhere. (140) The gp41 antigen was a linear peptide HIV-1 consensus clade B sequence [LGIWGCSGKLICTT] representing the epitope of 7B2. Gp120 antigen was a recombinant protein expressed in mammalian cells. Recombinant gp120 antigen represented HIV isolate IIIB (gift from Genentech, S. San Francisco, CA). The synthetic V3 loop peptide represented the V3 sequence of strain IIIB (amino acids AA 297-330; numbering according to reference (154), TRPNNNTRKSIRIQRGPGRAFVTIGKIGNMRQAH. Binding of antibody to the antigen was detected with AP-conjugated secondary antibodies: goat anti-mouse IgG (H+L chain specific) for HIV MAb 924 as well as 924 based-ITs; or goat anti-human IgG (H+L chain specific) for HIV MAb 7B2 as well as 7B2 based-ITs (all from Zymed Laboratories, South San Francisco, CA). Data are reported as optical density at 405 nm and represent means of triplicate values with three independent experiments.

3.6 Immunofluorescence assay

We used indirect immunofluorescence and flow cytometry to analyze binding of immunotoxins to either persistently infected H9/NL4-3 cells, or Env-transfected 293T cells. 8×10^4 cells were added to IT to reach the final concentrations of 5 ng/ml to 5 $\mu\text{g/ml}$. Cells

were incubated 1 hr at room temperature. Cells were washed, and then stained with Alexa488-conjugated goat anti-mouse IgG secondary antibody (2 μ g/ml) for 924 based-ITs; or FITC conjugated goat anti-human IgG secondary antibody (2 μ g/ml) for 7B2 based-ITs for 1–4 hr, washed twice and fixed in 100 μ l of 2% paraformaldehyde. After a minimum of 4 hr, 150 μ l of PBS was added. Cells (10,000) were studied on a Becton-Dickson LSR II with HTS plate reader, analyzed by Flow-Jo software (Treestar Inc). Forward scatter (FSC) and side scatter (SSC) gated data are represented as either overlaid histograms or as graphs of mean fluorescence. The conjugates or MAbs did not bind to uninfected H9 cells nor untransfected 293T cells.

3.7 Alexa Fluor 488 labeling of ITs

Labeling was carried out by mixing 1 ml of each IT at ~1 mg/ml, in sodium phosphate buffer 50 mM, pH 7.5, NaCl 0.1 M, with 100 μ g Alexa Fluor 488 as N-hydroxysuccinimide (NHS) salts (Invitrogen Molecular Probes, Eugene, OR). The reaction was maintained for one hour in the dark at room temperature with continuous stirring. Labeled protein was separated from unconjugated dye on Zeba 7KD cutoff desalting columns (Pierce, Rockford, IL). The degree of labeling was determined by measuring the A280 and A495 of the conjugates. ITs were characterized before and after labeling, with aforesaid protocols.

3.8 Measurement of internalization by flow cytometry

Env-transfected 293T cells (1.5×10^5) were placed in 100 μ l in round-bottom 96 well plates (Costar, Lowell, MA) in the presence or absence of 0.05% NaAz for studying, respectively, the binding or internalization of ITs by flow cytometry. Cells were stained with 1.0 μ g/ml Alexa488-labeled ITs in the presence of 1.0 μ g/ml sCD4-183 in serum-free medium for 4 hr at 4°C. As negative controls, two wells either were stained by ChRAC18 or were left unstained. Cells were washed twice then 250 μ l of PBS was added, in the presence or absence of 0.05% NaAz. The percentage of cell viability was analyzed by optical microscopy by incubating with 0.4% Trypan Blue (TB, Sigma) solution diluted in PBS to perform the TB exclusion test with counting in a Neubauer chamber. In order to confirm internalization of ITs to the cells, we used a modification of the protocol described elsewhere. (155-157) An increasing concentration of Trypan Blue from 1 to 3 mg/ml was used to quench the extracellular fluorescence. Cells were analyzed under a Becton-Dickson LSR II (BD, Franklin

Lakes, NJ) both prior and 2 min after TB addition. 10000 events were collected and data analyzed by Flow-Jo software (Treestar, Ashland, OR). Green fluorescence (FL1) of internalized Alexa488-labeled ITs was collected using a 530 ± 30 band-pass filter; red fluorescence emitted from TB bound to Alexa488-labeled ITs on the cell surface (FL3) was collected by using a 650 ± 13 band-pass filter. The data were collected using linear amplification for FSC and SSC, and logarithmic amplification for FL1 and FL3.

3.9 Live confocal imaging

Live cell imaging was performed as described elsewhere (151). All the images, including those used for quantitative analyses, were obtained with an inverted Zeiss LSM 510 microscope, a 63X 1.4 NA oil-immersion objective, and Zeiss LSM software. Heated (37°C) stages and objectives were used on microscope. One day prior to imaging, 10^4 Env-transfected 293T cells were seeded into 35 mm culture dishes with 0.17 mm thickness glass bottom (MatTek, Ashland, MA). In parallel, 293T cells were seeded as a control. Cells were cultured at 37°C in DMEM, 10% FCS, puromycin $1\ \mu\text{g}/\text{ml}$. The following day, cells were placed into 1 ml incomplete RPMI w/o Phenol red at pH 7.4 with 25 mM HEPES/1% BSA and transferred to the heated (37°C) stages for confocal microscopy imaging. 7B2-PAC-Alexa488 and sCD4-183 were added to final concentrations of $1\ \mu\text{g}/\text{ml}$ each. Taking images of different cells started after the addition of Abs, generally 50 observations during the 90 min period. Pinhole settings were such that an optical slice was less than $1\ \mu\text{m}$. The intracellular location of Alexa-labeled IT was confirmed by quenching the Alexa488 bound on the surface (155). After 90 min of imaging, one specific region was analyzed before and after adding $3\ \text{mg}/\text{ml}$ TB. The excitation was at 488 nm and Alexa488 fluorescence emission was detected by 530 ± 30 band-pass filter. TB emission was detected by 650 ± 13 band-pass filter.

3.10 Confocal microscopy for cell binding and internalization

In one day before confocal experiment, 4×10^4 cell per well of two cell lines, 293T and Env-transfected-293T cells, were seeded on a multiple-chamber slide (Nalge Nunc International). The next day, in order to block the IT internalization, the media of two control wells were replaced with PBS/BSA/0.01% sodium azide (PBA) $400\ \mu\text{l}$ per well for 45 min in RT. Then, cells were treated by $1\ \mu\text{g}$ Ab/IT in $500\ \mu\text{l}$ PBS or PBA, incubated 60 min in RT. The antibodies were 7B2-Alexa488, 7B2-PAC-Alexa488 and 7B2-RAC-Alexa488 in the

presence of 1 μg sCD4-IgG2). The controls were chRAC18 and sCD4-IgG2-Alexa488. One well was left without adding antibody. BFA-bodipy (250 ng/ml) was added to cells to demonstrate rapid accumulation of toxins in Golgi and ER. BFA-bodipy was tested to determine that at the concentration used there was minimal effect of the BFA on the cytotoxicity of ITs. (151) After 2X washing with PBA, the cells were fixed in 2% paraformaldehyde/PBS in 45 min. We took out the solution, and removed the slide box, added one drop SlowFade Gold Mountant DAPI (Life Technologies) and covered it by slide glass. Images were obtained with an inverted Zeiss LSM 510 microscope, a 63X 1.4 NA oil-immersion objective, and Zeiss LSM software. For each cell, a Z-stack with 1 μm steps was imaged.

3.11 Cytotoxicity measurements for immunoconjugates

A cytotoxicity assay was performed to analyze the cell killing ability of ITs. The target H9/NL4-3 cells or Env-transfected 293T cells (or their uninfected/untransfected parents as controls) were plated in triplicate in Complete RPMI (Supplement RPMI-1640 medium with 10% FCS and 1% sterile antibiotic) or DMEM plus 10% FCS, respectively, in 96 well flat-bottom tissue culture plates (Costar). Controls included: no cells (background) and cells in the absence of IT or in the presence of naked antibody. Serial dilutions of ITs, including the Alexa-labeled and unlabeled versions, were incubated with cells for 3 days. The incubation of 7B2-based ITs (not 924-based ITs) were in the presence or absence of 300 ng/ml of sCD4. For the final 6 hr of incubation, MTS/PMS substrate (Promega, Madison, WI) was added to each well and plates read hourly at 490 nm. Results represent the mean and SEM of triplicate samples (representative of three independent experiments), and are plotted as A_{490} with the no cell background subtracted (Figure 15). The percentage of cell viability was quantified by calculating the ratio below:

$$\% \text{ of cell viability} = \text{OD}_{490 \text{ nm}} (\text{antibody treated cells}) / \text{OD}_{490 \text{ nm}} (\text{negative control cells}) \times 100\%.$$

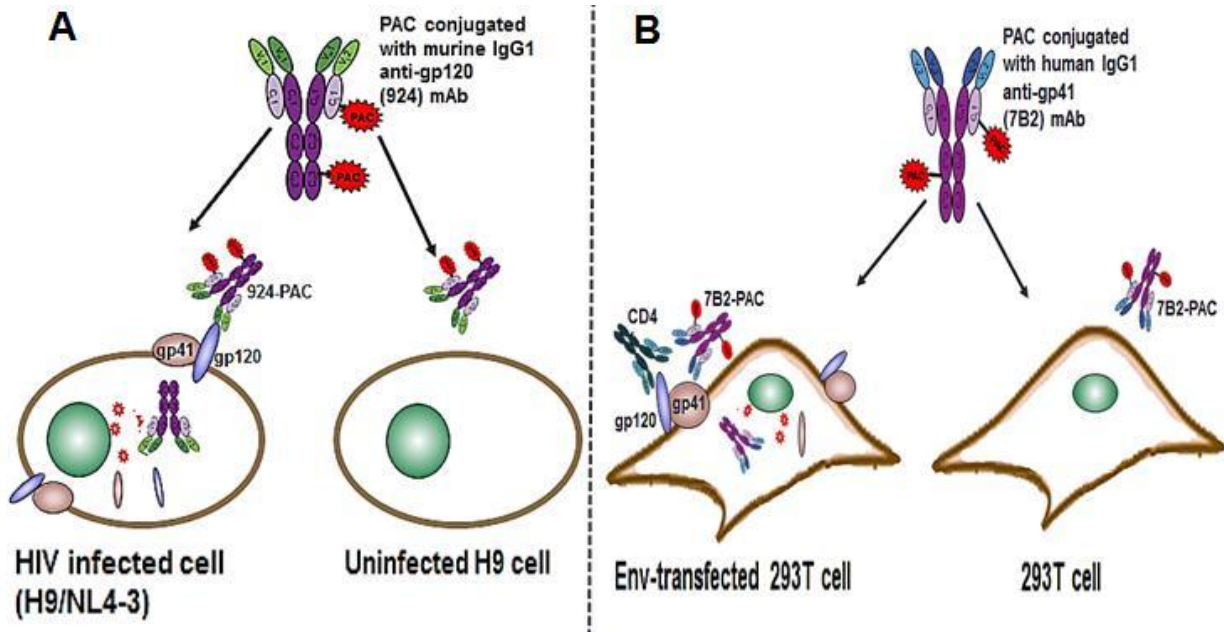


Figure 15 – Schematic representation of the delivery of cytotoxic immunotoxins based on pulchellin A chain to the relevant antigens. The overall structures of two antibodies conjugated to PAC are shown. Cell lines are depicted in different morphology representing suspension H9 lymphoma cells (**A**) and adherent 293T (**B**) cells. **A.** 924 MAb specifically targets HIV infected cells expressing native Env on the surface. After internalization of 924-PAC, the toxin compartment has separated from MAb, and PAC kills the cell. **B.** 293T cell lines are stably transfected with gp160, expressing gp120 and gp41 on the surface. Anti-gp120 (CD4) has a positive cooperativity on the binding of 7B2-PAC to the hairpin loop of gp41. Neither ITs nor CD4 bind to non-transfected 293T cells.

Source: By the author.

3.12 Statistical analyses

Statistical analyses were performed using GraphPad Prism, v5.0. Data are shown as mean and SEM of the indicated number of replicate values. If no error bar appears present, the error bars are smaller than, and obscured by, the symbol. The method for statistical comparison is by unpaired two-tailed Student's t-test, unless specifically indicated otherwise.

4 RESULTS

4.1 Production, characterization and conjugation of toxin A chains to MAbs

PAC and RAC, produced in *E. coli*, were purified on a 5-ml HisTrap column, eluted by adding increasing concentrations of imidazole, and collected. The 6xHis-tag was removed by TEV protease cleavage, dialyzed, concentrated and purified on a HiPrep 26/60 Sephacryl S-200 column (GE Healthcare). Figure 16 demonstrates the SDS-PAGE analysis of purified His6 tag-removed products after cleavage by TEV protease by Sephacryl S-200 column (Fig. 16). Fractions containing purified either PAC or RAC were reduced in 2mM B-mercaptoethanol, pooled, and concentrated to 2 mg/ml and stored at -80°C .

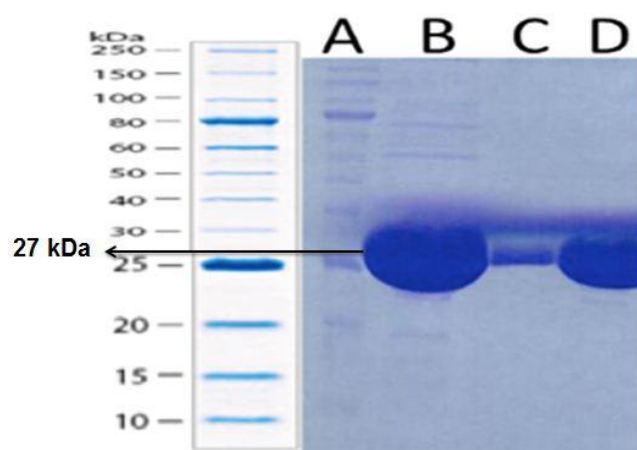


Figure 16 – SDS-PAGE analysis of purified His6 tag-removed products of PAC (B) and RAC (D) after cleavage by TEV protease by Sephacryl S-200 column; lane A, Protein marker; lane B, PAC; lane C, Control RAC; lane D, RAC. The arrow indicates the similar molecular weight of 27 kDa for both PAC and RAC.

Source: By the author.

In order to optimize the biolinker concentration, HIV mAb 924 (1 mg) in 0.5 ml PBS, pH 8.0, was mixed separately with 10, 20 and 40-fold molar excess of LC-SPDP biolinker. After 2 hr incubation at room temperature, they were passed from Zeba columns equilibrated in PBS. At the same time, RAC and PAC (1 mg in 0.5 ml) were reduced for 30 min in 50 mM dithiothreitol, then were passed from Zeba columns equilibrated in PBS. The two products, RAC and PAC were mixed separately with 10, 20 or 40-fold molar excess of Antibody-biolinker, concentrated to 0.5 ml and incubated overnight at 4°C . The six individual fractions were analyzed by Microcapillary Electrophoresis and bicinchoninic acid protein assay to find

the optimum conjugation. Figure 17 demonstrates that the conjugates with 40-fold molar excess of biolinker can harbor more A chain toxin.

After purification of 6xHis tag-removed product by Sephacryl S-200 column, fractions containing purified PAC or RAC were concentrated to 2 mg/ml. MAbs were produced in tissue culture supernatants and purified on Protein A agarose beads. MAbs and toxin A chains were tested for purity and size by microcapillary electrophoresis (Fig. 17). Results demonstrate the appropriate size for full length MAbs (H and L chain) with approximately 150 and 157 kDa for 924 and 7B2 MAbs, respectively. Both RAC and PAC are 27 kDa. We optimized the conjugations of RAC and PAC to MAbs 924 and 7B2, in parallel, by applying different concentrations of LC-SPDP bifunctional cross linker (10, 20 and 40-fold molar excess of LC-SPDP). The results of microcapillary electrophoresis analysis under reducing and non-reducing conditions of the 924-ITs and 7B2-ITs are shown in figure 17. The conjugates with 40-fold molar excess of LC-SPDP biolinker gave major bands of the predicted molecular weights for one and two toxin A chains per antibody molecule (approximate MW, 180,000 and 210,000, respectively) and a minor band of MW 240,000 representing three toxin A chains per antibody molecule. Under reducing conditions, the conjugates showed three characteristic bands corresponding to light and heavy chains, and the toxin A chains.

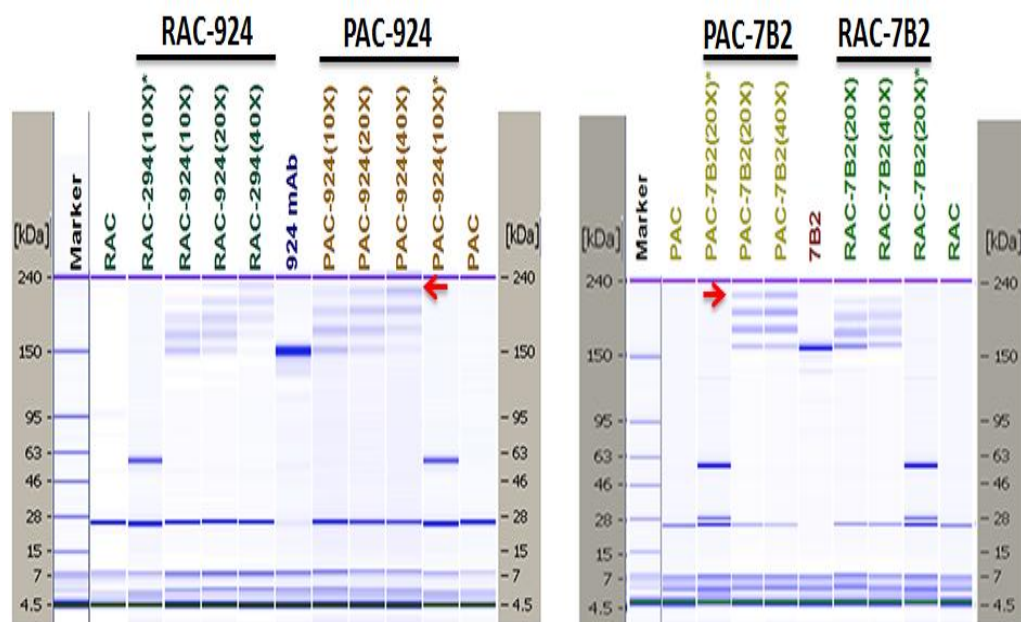


Figure 17 – Microcapillary electrophoresis of reduced and non-reduced protein preparations with 10, 20 or 40-fold molar excess of antibody-biolinker. Results show the conjugates with 40-fold molar excess of LC-SPDP biolinker give major bands of the predicted molecular weights for one, two and three toxin A chains per antibody molecule. Red arrows indicate the conjugate harboring three toxin A chains. The star symbol (*) means under reducing conditions by using 2-Mercaptoethanol.

Source: By the author.

By comparing toxin A chains, both RAC and PAC were conjugated equally to 924, however with 7B2 we obtained a superior conjugation with PAC (Fig. 18). Then, the conjugates with 40-fold molar excess of biolinker passed from Ultra-100K centrifugal filter. As Fig.18C shows, by 40-fold molar excess of cross-linker, we could reach to optimum IT with almost eliminated free MAb. In Fig.18D, the Electropherogram of ITs (40 x ones) shows the total protein mass of RAC and PAC ICs were containing only 3.9% and 2.7% free 924 MAb, respectively. After labeling the conjugates with Alexa488, the conjugation of 924-PAC were confirmed by comparing with 924-Alexa, by using fluorescence correlation spectroscopy (FCS). (Figure 19)

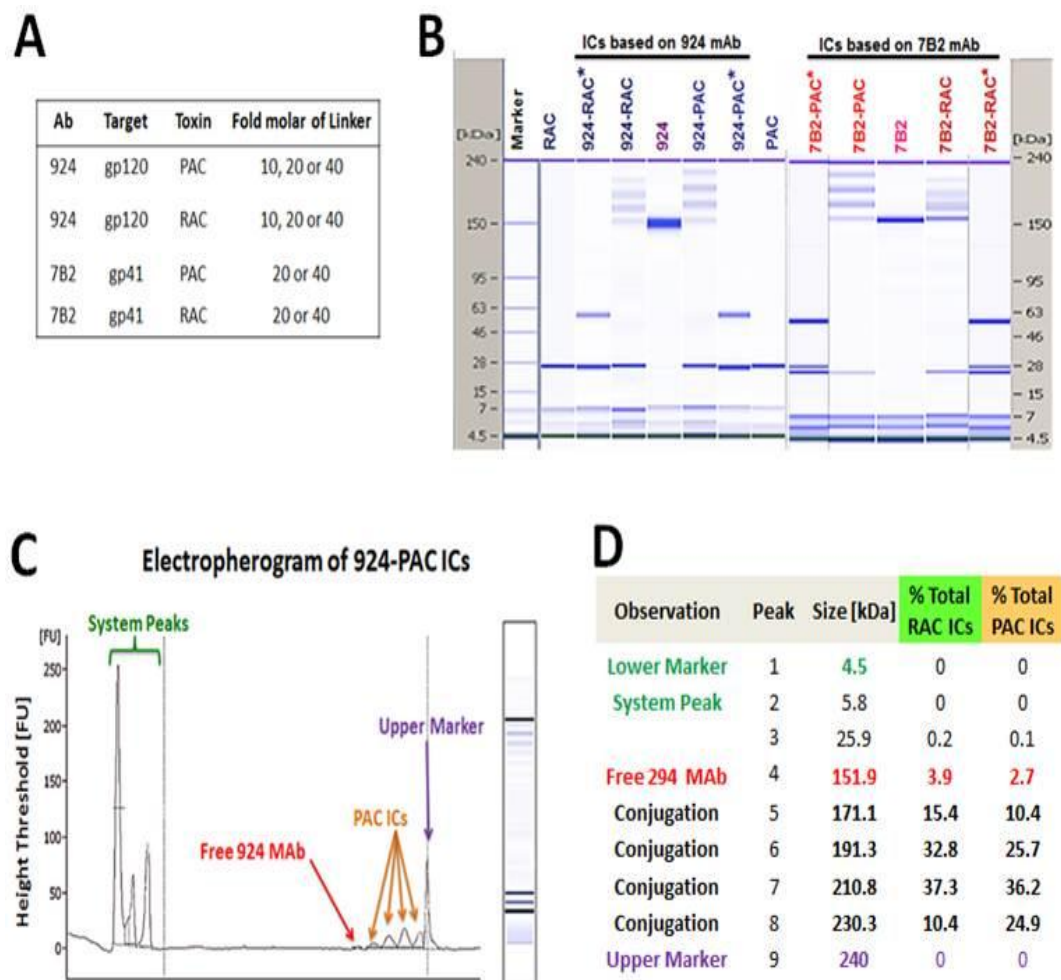


Figure 18 – Characterization of immunoconjugates (ICs). **A.** The table shows components of ICs with different concentrations of LC-SPDP biolinker. The final products include 10 ICs as well as 2 conjugates with irrelevant MAb, as control. **B.** Microcapillary electrophoresis of reduced and non-reduced ICs. Results are displayed in the familiar format of a coumassie stained gels. Size standards are indicated on the side of each “gel”. PAC, RAC and light chain of 924 MAb represent the same molecular size on the gel. The star symbol (*) means under reducing conditions by using 2-Mercaptoethanol. The ICs represent the conjugation with 40-fold molar excess of LC-SPDP biolinker. **C.** Electropherogram of 924-PAC IC, after passing from Ultra-100K centrifugal filter, demonstrates the negligible presence of free MAb as well as MABs conjugated with 1, 2, 3 or even 4 PAC. **D.** Peak table of RAC and PAC ICs show the percentage of MABs conjugated with A chains.

Source: By the author.

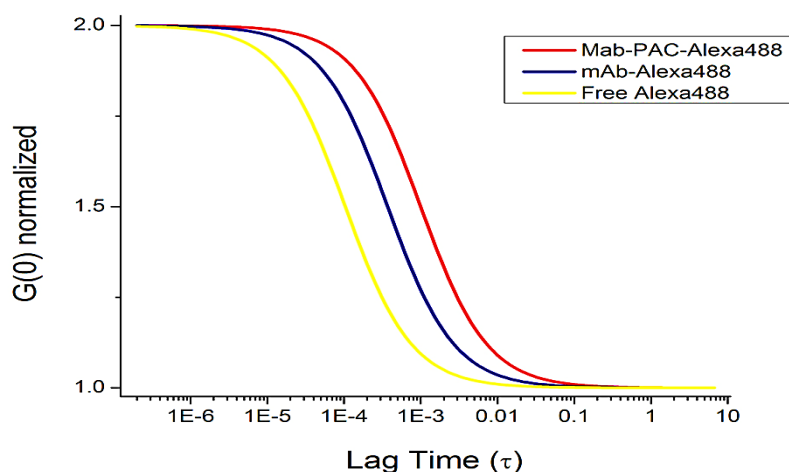


Figure 19 – Fluorescence correlation spectroscopy (FCS) to confirm the conjugation of 924-PAC with Alexa Fluor 488. Red line shows a significant shift to the right side, as a result of labeling between mAb-PAC and Alexa Fluor 488.

Source: By the author.

4.2 Binding of immunotoxins to recombinant antigen

By using an indirect ELISA, we tested the ability of purified MAb 924 and 924-based ITs to bind recombinant gp120(IIIB) antigen and V3 loop peptide. In parallel, the binding ability of MAb 7B2 and 7B2-based ITs were examined by using the gp41 loop peptide antigen. In figures 20A and 21, all the purified MAbs and conjugates bound to the appropriate antigens, while the isotype controls (MAbs and MAb-RAC) and negative control (plate coated with unrelated control ligand) did not, demonstrating that immunologic specificity of the antibodies in the ITs was unaffected by the conjugation process. Besides, we examined the ability of anti-ricin A chain MAb RAC18 to bind recombinant RAC (rRAC) and recombinant PAC (rPAC). As has previously been reported (151), RAC MAb18 bound to rRAC, with no binding to the isotype control MAb 924. Interestingly, RAC MAb18 showed a binding ability to rPAC as much as rRAC. (Figure 20B)

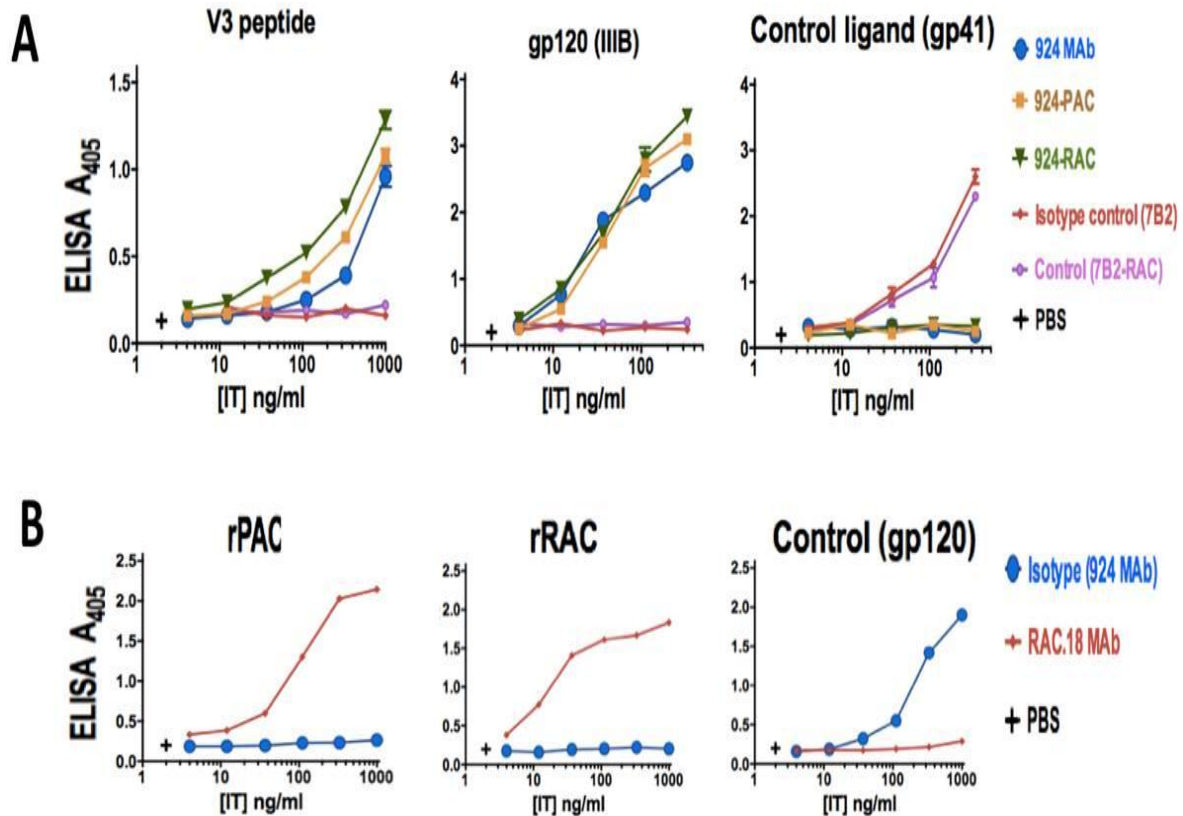


Figure 20 – 924 based-ITs bind to recombinant antigens and native antigens on the HIV infected cells. **A.** ELISA plates are coated with a synthetic V3 loop peptide, recombinant gp120 and gp41 peptide as a control ligand. The results show the binding of 924 MAb and 924-ICs to the either gp120 or V3 peptide, but not the unrelated isotype controls. **B.** ELISA plates are coated with recombinant RAC, PAC and recombinant gp120 as a control ligand. The results demonstrate the binding of anti-ricin A chain MAb (RAC18) to rPAC and rRAC, but not the unrelated isotype control. In panels **A** and **B**, the Ab binding is detected with AP-conjugated goat anti-mouse IgG. Where no error bars are visible they are obscured by the symbol. Results are representative of means of duplicate values with at least three different assays (varying by Ab, ITs, or Ag tested).

Source: By the author.

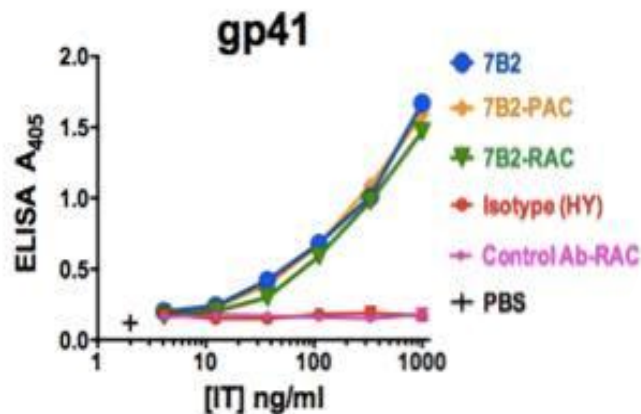


Figure 21 – Binding ability of 7B2 based-ITs to gp41 antigen by using ELISA and flow cytometry. **A.** ELISA plates coated with gp41 Ag, as a peptide representing 7B2's epitope. Binding of the 7B2 based-ITs is detected by AP-conjugated goat anti-human IgG. Results are representative of means of triplicate values with three individual experiments.

Source: By the author.

Moreover, the binding ability with different concentration of LC-SPDP (10x, 20x, 40x) were analyzed and compared side by side (Figure 22). The optimization results show that the concentration of biolinker does not have a significant effect on the binding ability of MABs. The results demonstrate that the different concentrations of biolinker did not significantly affect the function of the conjugated MAB.

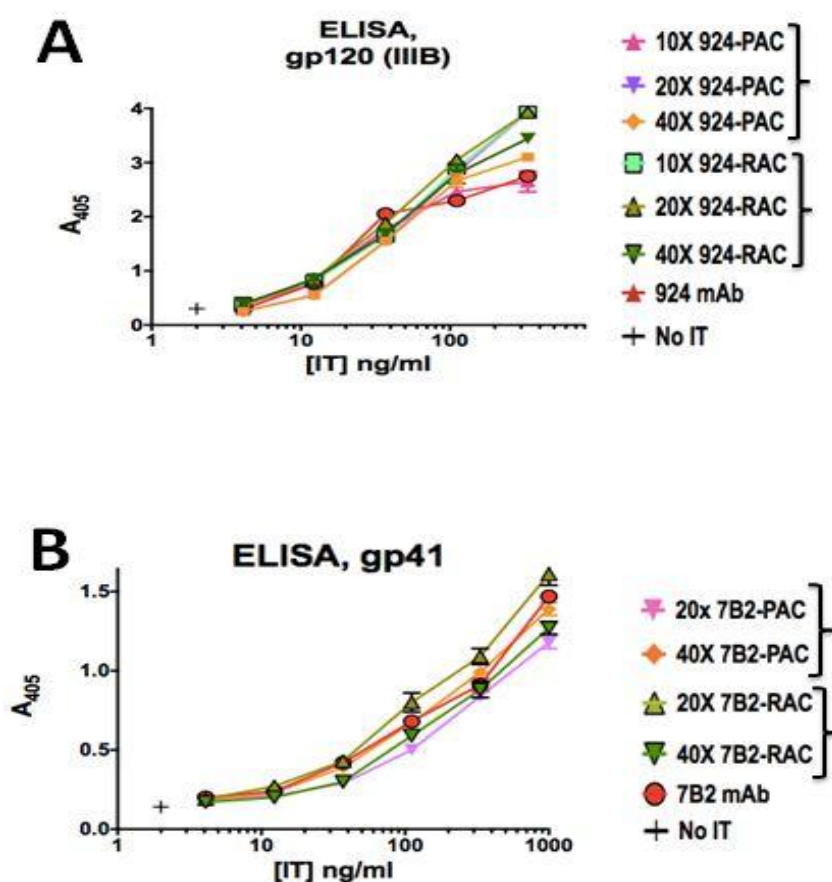


Figure 22 – The concentration of LC-SPDP biolinker did not have a significant effect on the antigen binding ability of immunoconjugates. The graphs show ELISA assay of the conjugates based on either 924 MAb (A) or 7B2 MAb (B) with different fold molars of biolinker (10X, 20X or 40X). **A.** ELISA binding of 924-ITs to recombinant gp120 antigen were compared side by side. **B.** 7B2-ITs with 10X or 20X molar excess of biolinker were compared for binding ability to gp41 antigen. Results are representative of at least three independent experiments.

Source: By the author.

4.3 ITs bind to Env expressed on the surface of infected and transfected cells

We examined binding to native Env by flow cytometry, using FITC conjugated goat anti-human or Alexa488 conjugated goat anti-mouse IgG secondary antibody to detect IT binding. 924-based ITs bound to persistently infected H9/NL4-3 cells. (Fig. 23) 7B2-based ITs bound to H9/NL4-3 cells (136) as well as to 293T cells transfected with 92UG037.8 gp160 (Fig

24A-C). ITs did not bind uninfected H9 or 293T cells, confirming the specific cell binding of ITs. Addition of sCD4-183 enhanced binding of 7B2-based ITs to Env-transfected 293T cells (Fig. 24A), as has previously been reported for RAC-7B2. (140,143) We directly labeled ITs to Alexa488 for later experiments. Figure 24C shows direct fluorescence with the ITs and naked 7B2 after Alexa488 labeling.

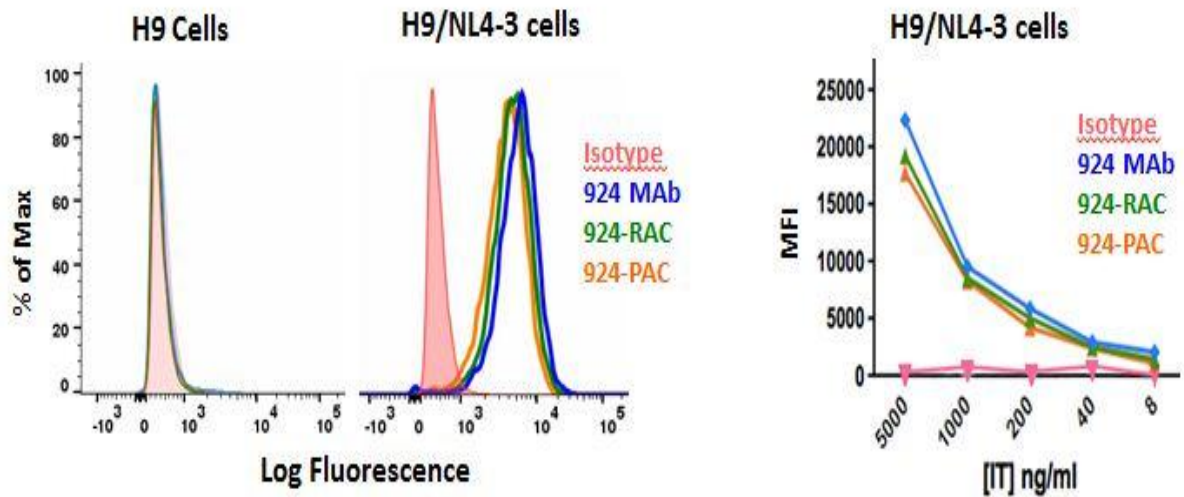


Figure 23 – Flow cytometry histograms for binding of 924 MAb and 924 based-ITs to uninfected H9 cells, as control, and persistently-infected H9/NL4-3 cells. Binding was detected with Alexa488 conjugated goat anti-mouse IgG. On the right, IT binding to H9/NL4-3 cells are plotted as median fluorescence versus IT concentration. The results are representative of three independent experiments. Isotype control is shown as red shaded histogram.

Source: By the author.

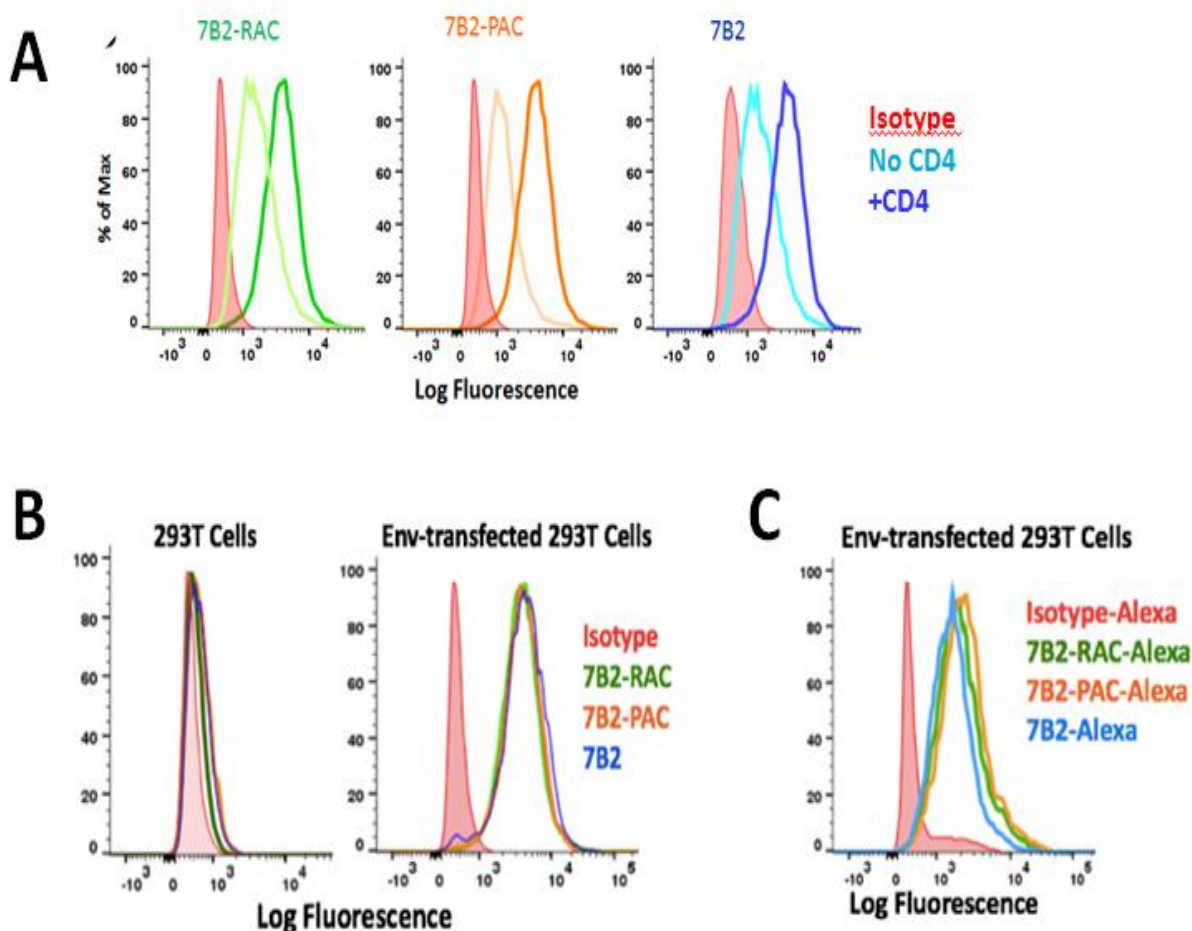


Figure 24 – **A.** Using FITC-secondary immunofluorescence, we detect binding of ITs to Env-transfected 293T cells in the presence (**darker line**) or absence (**lighter line**) of sCD4 (CD4-183). Isotype control is shown as red shaded histogram. **B.** IT binding to 293T cells and transfected 293T cells with 92UG037.8 gp160 (293T/92UG) was detected by using FITC-secondary immunofluorescence. Results are representative of at least three independent experiments. **C.** The flow cytometry histogram of Alexa488-labeled ITs by using Env-transfected 293T cells incubated in PBS +1% BSA+sodium azide (0.2%). Results are representative of three individual experiments. Isotype control (chimeric RAC18-alexa488) is shown as red shaded histogram.

Source: By the author

4.4 Cell binding and internalization of immunotoxins

To quantify the internalization of ITs by flow cytometry, the Env-transfected 293T cells were incubated with Alexa-labeled ITs in the presence or absence of 0.05% sodium azide (NaAz). Prior to cytometry external fluorescence was quenched with trypan blue (TB). Given that TB enters dead cells and may interfere with the fluorescent analysis, we confirmed high cell viability (96%). In the presence of NaAz, ITs cannot be internalized, they only bind to antigens on the cell surface. The addition of an increasing concentration of TB showed that 3 mg/ml of TB was sufficient to quench extracellular fluorescence (Fig. 25A). However in the absence of NaAz this concentration of TB caused no quenching (Fig. 25A), indicating the

Alexa-labeled ITs were internalized, although we cannot rule out a small amount was bound to the cell surface. Figure 25B demonstrates the population of cells in the absence of TB, with 7B2-PAC-Alexa488, either bound to the cell membrane or internalized. We also observed a negligible population of cells without Alexa-labeled ITs. After addition of TB, the green fluorescence emission was not quenched, signifying the 7B2-PAC-Alexa was internalized. Moreover, the upshift of cell population corresponded to the cells with damaged membrane (dead cells) and Alexa-labeled ITs adherent to the membrane which emitted red fluorescence after quenching. Figure 25C shows the same results for 7B2-RAC-Alexa488.

4.5 Live imaging of ITs during binding and internalization

Internalization of ITs was confirmed by live confocal microscopy of Env-transfected cells with 7B2-PAC-Alexa488. After the addition of IT, live imaging included approximately 50 observations during the 90 min period. In figure 25D, after 15 min of incubation, the IT was observable on the cell surface, and after 30 min, was identified intracellularly as small vesicles. Following 90 min, the imaging of one specific region before and after TB addition demonstrated quenching of the green fluorescence on the cell surface and emitting red fluorescence. (shown by white arrow in Fig. 25D)

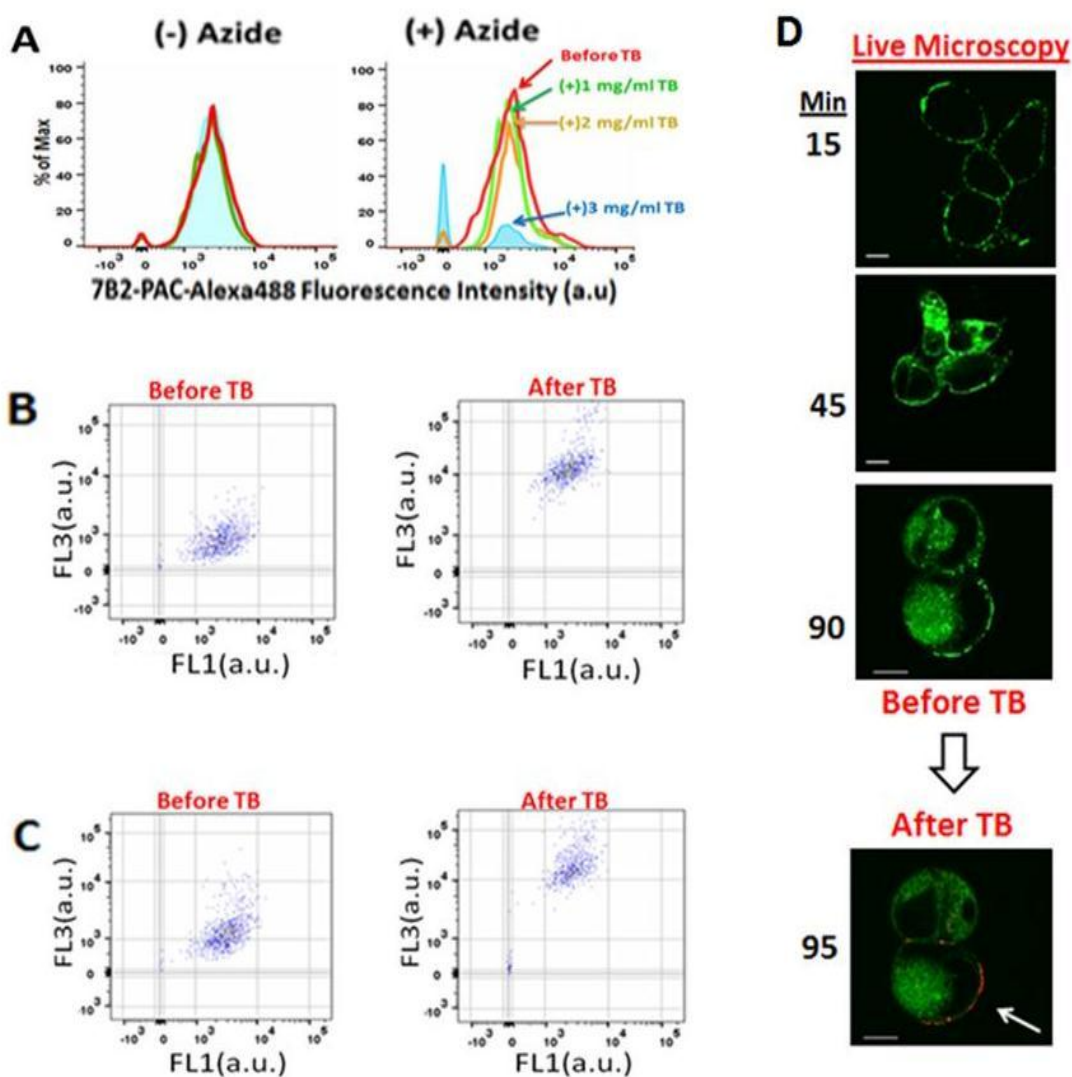


Figure 25 – Distinguishing the internalized ITs from those bound on the cell surface by using quenching effect of Trypan Blue (TB). All the flow cytometry and microscopic experiments are in the presence of sCD4-183 (300 ng/ml) **A.** Before incubation with ITs, the viability of cells was 96%. The diagrams show percentage of 7B2-PAC-Alexa488 that remained fluorescent after the addition of an increasing concentration of TB (1, 2 and 3 mg/ml). In the presence of NaAz, 7B2-PAC can only attach to the cell membrane, without cell internalization. As the right diagram demonstrates, the addition of an increasing concentration of TB shows that a concentration of 3 mg/ml of TB is sufficient to quench the extracellular fluorescence. In the absence of NaAz, due to the IT internalization, the fluorescence intensity of ITs remain intact from quenching by TB (**B**, **C**). Dot plots of cells incubated with 7B2-PAC-Alexa488 (**B**) or 7B2-RAC-Alexa488 (**C**) in the absence of NaAz, analyzed by flow cytometry before TB addition and 2 hr after that. Before TB addition, the dot plots of the cell population incubated with Alexa-ITs, either adherent to plasma membrane or internalized, are emitting green fluorescence (FL1). TB cannot enter the live cells, therefore, after TB addition the green fluorescence emission (FL1) is not quenched, while we observe the upshift of cell population corresponding to the cells with damaged membrane (ie. 4% dead cells) and Alexa-ITs adherent to the membrane which emitted red fluorescence (FL3) after quenching. Results are representative of two independent experiments. (**D**) Live confocal microscopy by taking images from a series of different regions started with time after the addition of Abs, generally 50 observations during the 90 min period. Live cells incubated with 7B2-PAC-Alexa488 demonstrate the presence of IT on the cell surface after 15 min. Following 90 min, 7B2-PAC is observable both internalized and on the cell surface. By imaging the same region, after 5 min TB addition, only the green fluorescence on the cell surface is quenched and emitting red fluorescence (shown by white arrow). The green and red fluorescences are detected by band-pass filters 530±30 nm and 650±13 nm, respectively.

Source: By the author

4.6 Confocal microscopy of binding, internalization and intracellular localization of Its

The localizations of 7B2-PAC and 7B2-RAC were studied by non-quantitative confocal microscopy. Env-transfected 293T cells were incubated with Alexa488-ITs and BFA-bodipy under physiologic conditions, or in the cold with sodium azide to block the entry of IT into the cell. Serial vertical sections are shown in figure 26. In the presence of azide (Fig. 26A), ITs only bound to the cell surface, whereas under physiologic conditions 7B2-PAC or 7B2-RAC were observed on the cell surface and internalized. The areas of yellow signal demonstrate the colocalization of internalized IT (green signal) on the ER and Golgi colored by BFA-bodipy (red signal).

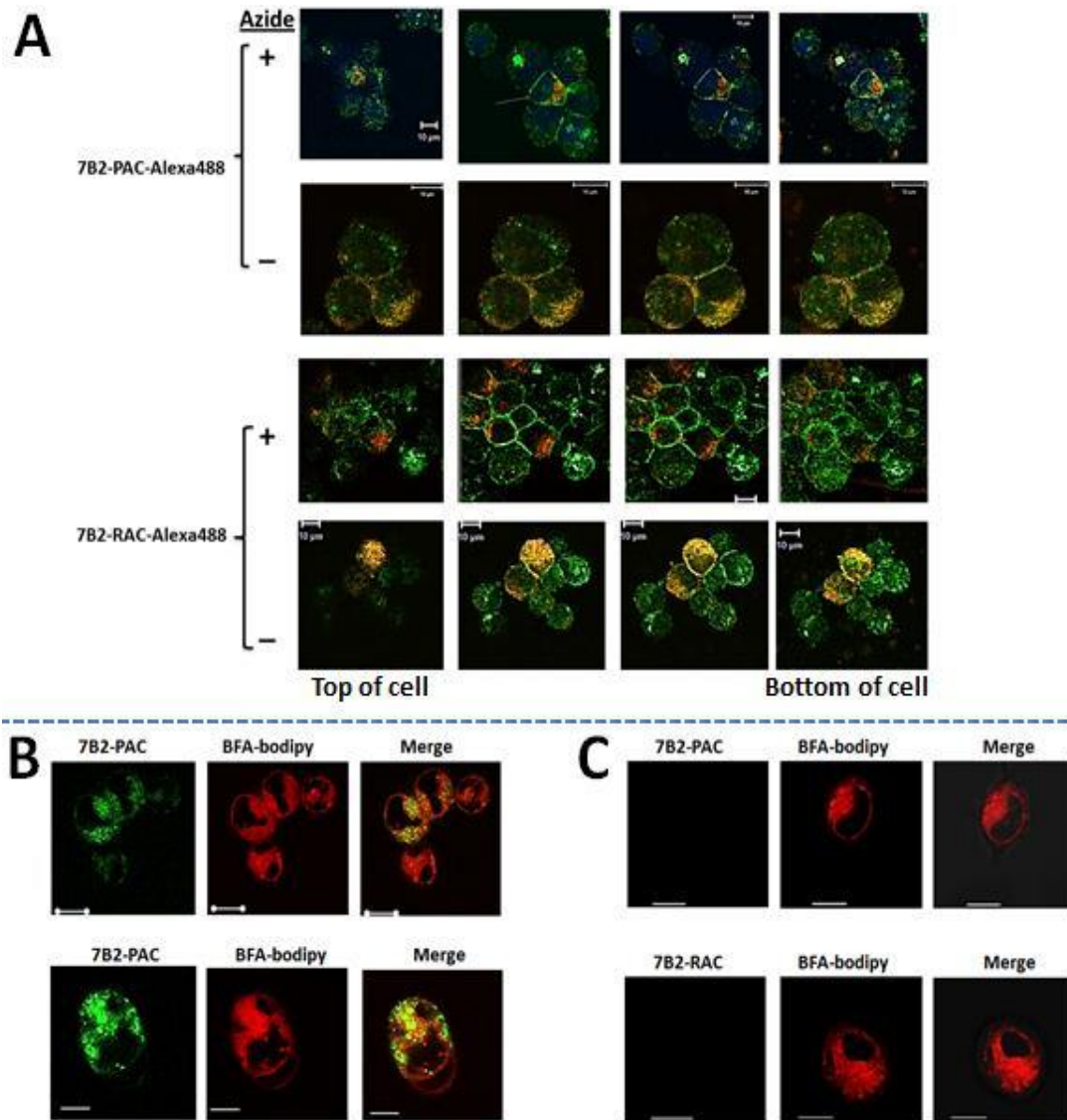


Figure 26 – Binding, internalization and intracellular localization of fluorescent ITs. (A). Env-transfected 293T cells were incubated with cold PBS in the presence or absence of 0.02% sodium azide. 45 min later, Alexa488-ITs were separately added to each set of slides in the presence of sCD4-IgG2. The slides were counterstained with BFA-bodipy, incubated an additional 60 min under the same conditions. Five min later, cells were washed 3X with cold PBS in the presence or absence of azide. The cells were fixed in 2% paraformaldehyde or one drop SlowFade Gold Mountant DAPI. Cells were observed with a 62X oil-immersion objective. Z-stack images collected at 1 μ m sections. The bottom of cells represents the closest plane to the slide. ITs are green, ER and Golgi are red. Some samples have nuclei stained with Hoechst Dye (Blue). Colocalization of red and green dyes appears yellow. The white bar indicates 10 μ m. (B,C). A comparison between Env-transfected 293T cells (B) and 293T cells (C) incubated with the same description in panel (A) but in the absence of sodium azide, in order to show the specific targeting the transfected cells. BFA-bodipy was used to demonstrate accumulation of ITs on the ER and Golgi.

Source: By author

4.7 Immunotoxins based on PAC effectively and specifically kill infected/transfected cells

To test biological activity of ITs, we used a direct cytotoxicity assay in two experiments: In the first experiment, we used H9/NL4-3 infected T cells to test the cytotoxicity of 924-based ITs. In the second, we assayed the cytotoxicity of 7B2-based ITs, including Alexa-labeled and unlabeled versions, to Env-transfected 293T cells in the presence or absence of sCD4. In each experiment, the cells were incubated with differing concentrations of ITs or MAbs as control. The other controls included; no cells (background) and cells in the absence of IT. Cell viability was measured after 3 days by MTS dye reduction, with a decrease in A_{490} indicating cell death (figures 27). The results demonstrate the efficacy and specificity of each IT for the infected cells, but not uninfected cells. Although 924-PAC appeared less efficacious than 924-RAC, these results were not observed with 7B2-PAC and 7B2-RAC. The cytotoxicity of ITs used in imaging analyses was unaffected by Alexa conjugation (Fig. 27C).

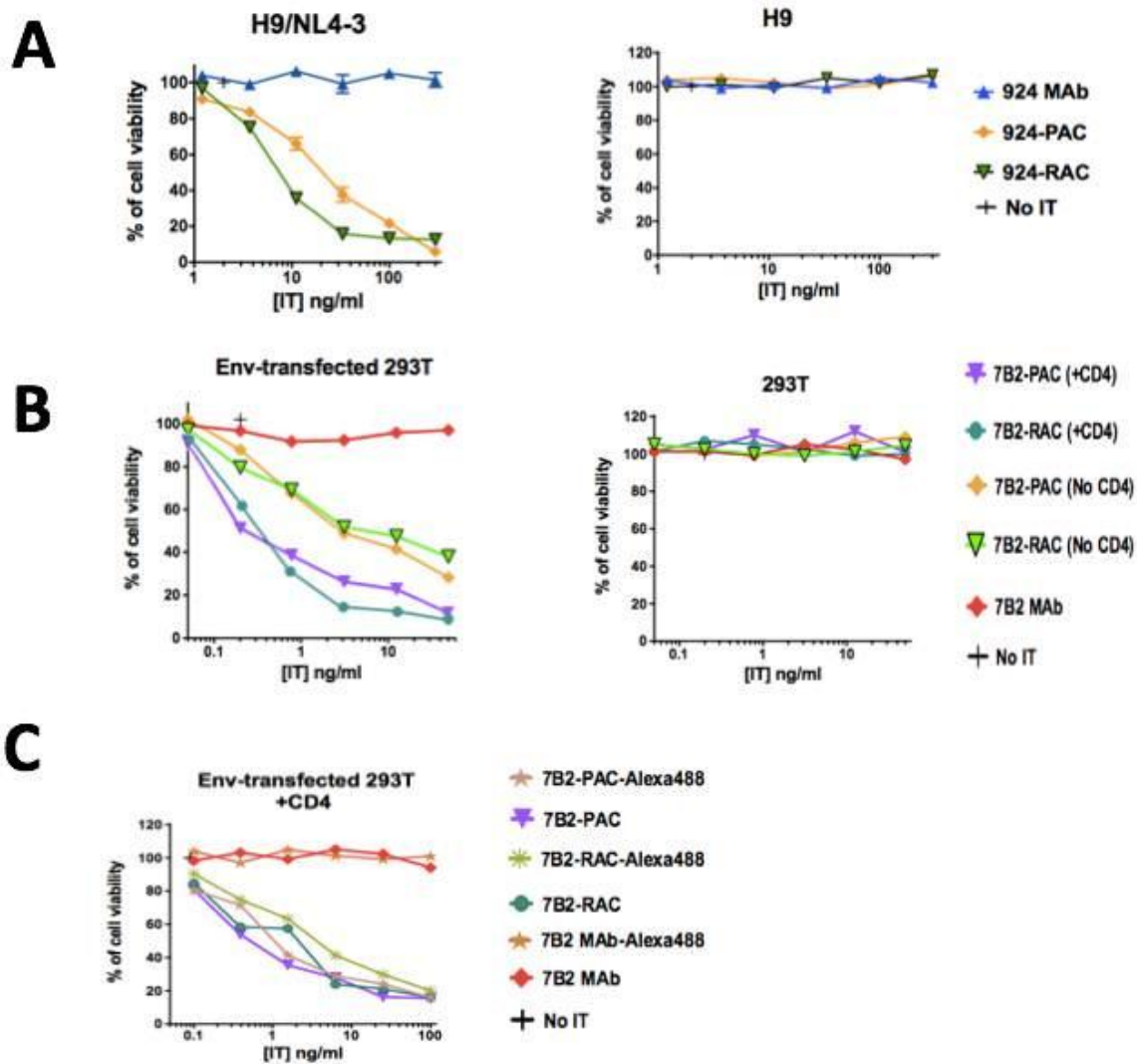


Figure 27 – Comparing the cytotoxicity and targeting of ITs by direct cytotoxicity assay. A. The cytotoxicity of 924-based ITs was assayed by using persistently-infected H9/NL4-3 cells. 924-RAC appears more cytotoxic than 924-PAC. ITs did not have cytotoxicity on T-cell lymphoma (H9) cells, signifying ITs have specific targeting. **B.** The cytotoxicity of 7B2-based ITs to Env-transfected 293T cells (293T/92UG) in the presence or absence of sCD4 (anti-gp120) was assayed. The results show that 7B2-RAC and 7B2-PAC had equivalent cytotoxicity. The presence of soluble CD4 (300 ng/ml) had a significant enhance on the cytotoxicity of ITs. **C.** The cytotoxicity of ITs was compared before and after labeling in the presence of sCD4 (300 ng/ml). Results show mean and standard error of triplicate samples. Results are representative of three individual experiments. Where no error bars are visible they are obscured by the symbol.

Source: By the author

5 DISCUSSION & CONCLUSION

To develop improved ITs, different toxic domains have been used, aiming for higher toxic efficacy or fewer undesired effects. (158) Pulchellin toxin is a type II RIP, structurally similar to ricin. (28,159) Moreover, the A chains of both ricin and pulchellin contain only one cysteine residue for forming an interchain disulfide bridge. (27,29) In spite of the similarities in the structure of ricin and pulchellin, the anti-viral and anti-tumor activities of RAC have been studied well (21,160-161), while there are no published data to exploit the feasibility of using PAC in targeted therapy. Here we have explored the function of PAC as an IT candidate, when coupled to MAbs to the HIV envelope, the only intact virus protein expressed on the surfaces of virions and infected cells.

We have conjugated two different anti-Env Abs to RAC and PAC, then tested their cytotoxic activity on either persistently infected or transfected cell lines. The results clearly indicate the efficacy of PAC-containing Immunoconjugates. The comparative efficacy of PAC vs the well-studied toxic moiety RAC is not fully resolved, with one set of experiments using 924 MAb showing PAC to be slightly less efficacious than RAC, but the set of experiments with 7B2 ITs showing no difference. Within the range we tested, the concentration of bifunctional crosslinker did not appear to have a significant effect on the binding ability of the conjugates. (Figure 17) A disulfide bridge is usually thought to be essential for maximal cytotoxicity. Most type 1 RIPs do not have any free cysteine residues, which implies the need for modification of both antibody and RIP with chemical agents to produce the disulfide bond. But, fortunately there is only one free cysteine on PAC (Cys247) which reacts with MAb-linker rapidly in high yield without diminishing biological activity of toxin. Regarding the immune-therapeutic use of immunotoxins, an important consideration for immunoconjugate assembly is the nature of the linkage between antibody and RIP. Although several alternative methods for the preparation of antibody-A chain conjugates have been described, the SPDP method is probably the easiest, most popular and most reproducible method to use. As there is a unique free cysteine on A-chain toxin, with the realization that thiols are very nucleophilic, which react rapidly in high yield without diminishing biological activity of toxin. SPDP can crosslink with primary amino groups (on lysine and at the N-terminus) on the MAb. Using this approach, a stable but intracellularly cleavable disulfide linkage may obtain. This may not affect the A-chain toxicity, due to the singularity of free cysteine on the toxin. But, it may

affect the Ab binding ability, while we have shown by ELISA and FACS which is not affected. It has been observed that the location of the conjugated toxin is not as important as the stoichiometry of A-chain toxin attachment. (152-153)

After the conjugation reaction, the removal of unreacted A-chain toxin and holotoxins were achieved by using an Amicon Ultra-100K centrifugal filter. As Fig.18B shows, by 40-fold molar excess of cross-linker, we could reach to optimum IC with almost eliminated free MAb. In Fig.18D, the Electropherogram of ICs (40 x ones) showed less than 4% of total protein mass contains free MAb, that is negligible. Therefore, the abscissas of Fig. 20A, Fig. 21 and Fig. 22 represent concentrations of only ITs (40 x ones), with negligible free MAb.

For most chemically linked antibody-toxin conjugations, the purification procedures are primarily based on removal of unreacted payloads. Poor antibody separation from ICs may result in significant naked antibody contaminations devoid of any cytotoxic activity. Hence, we showed in figure 18.C that the percentage of free unreacted antibodies is negligible in comparison with reacted ones. Regarding the interspecies heterogeneity, most ITs are chemically heterogeneous with one to four linked A-chains, and their large size (usually for payloads more than 4 toxins) may hinder them from penetrating targeted cells. To study this, IT internalization was analyzed based on the quenching effect of trypan blue by using flow cytometry and confocal microscopy. Furthermore, the peak table in figure 18.D, demonstrates a stoichiometric similarity between PAC and RAC ICs, regarding in the number and percentage of the linked A-chains. This similarity of stoichiometric heterogeneity may not affect the interpretation of the cytotoxicity assay during comparison between RAC and PAC ICs, as our major aim of this study. For the next study on this novel PAC-IT, we suggest the generation of genetically engineered HIV MAbs which allows stoichiometric and site-directed PAC attachment to the MAb. This strategy may result in highly homogeneous PAC ICs.

In this study we tested the 924 ITs on persistently infected H9/NL4-3 cells. The Env expressed by this virus is the prototypical laboratory strain IIIB, and MAb 924 binds uniquely to the tip of the V3-loop of this isolate. MAb 7B2 binds a well conserved epitope in the helix-loop-helix region of gp41. The peak table in figure 18D, demonstrates a stoichiometric similarity between PAC and RAC ICs, regarding in the number and percentage of the linked A-chains. This similarity of stoichiometric heterogeneity may not affect the interpretation of the cytotoxicity assay during comparison between RAC and PAC ICs. The efficacy of 7B2-

RAC ITs has been studied extensively in a variety of HIV infected cells, and more recently in Env-transfected 293T cells. The efficacy of 7B2 ITs has been demonstrated in vivo(136,162). Here we have used cells stably transfected to express fully functional envelope (gp160, gp120 and gp41) from HIV clade A clinical isolate gp160 (293T/92UG) (148) and shown that 7B2-RAC and 7B2-PAC are equivalently cytotoxic. As we have observed previously (143), soluble CD4 enhances epitope exposure and IT efficacy. By comparing the susceptibility of these two cell lines, as we have shown before (146), 293T/92UG cells are significantly more sensitive to the IT than H9/NL4-3 cells. These differences in IT-mediated killing, between transfected 293T/92UG cells and infected H9/NL4-3 cell lines, are unrelated to the binding of the MAb to the target cells. As we have explained previously (146), discrepancies among these two cell lines may reflect differences resulting from transfection versus infection and/or laboratory-adapted versus clinical isolates.

In this study, we demonstrate that PAC stands out as feasible candidate for the design and construction of effectively specific ITs. In this case, the immunogenicity of PAC will be a matter of great interest; whereas the development of anti-pulchellin Abs will be a major limitation for pulchellin-based immunotoxins. RAC MAb 18 has a common motif of QXXWXXA on the structure of RAC (150) and PAC which fold into part of the enzyme active site. Overlaying this sequence on the three-dimensional structure of PAC and RAC provides a best fit with Q160, A165, W198, for PAC with its counterpart Q173, A178, W211, for RAC, which fold into part of the enzyme active site. (27) We have demonstrated that RAC MAb 18 binds to not only RAC also PAC (Fig. 20B). This finding helps us for our future study on the immunogenicity of PAC.

Our previous microscopy studies have revealed the intracellular localization and trafficking of whole pulchellin and ricin toxins. Briefly, the plant toxin binds exposed galactosyls at the cell surface of target mammalian cells, and, following endocytosis, is transported in vesicular carriers to the endoplasmic reticulum (ER). Subsequently, the cell-binding B chain and the catalytic A chain (RAC or PAC) are separated reductively, RAC/PAC embeds in the ER membrane and then retrotranslocates (or dislocates) across this membrane. The protein conducting channels used by RAC/PAC are usually regarded as part of the ER-associated protein degradation system (ERAD) that removes misfolded proteins from the ER for destruction by the cytosolic proteasomes. Finally, cytosolic RAC/PAC folds into a catalytic conformation that inactivates its target ribosomes. (31,151) We assumed this process may happen for PAC conjugated with mAb. Herein, we have used flow cytometry and confocal microscopy to study cell binding, uptake, and intracellular localization of 7B2-PAC. We have

used Env-transfected 293T cells for microscopic study, because these cells are adherent in compare to suspension H9 lymphoma cells. (163) We have shown that 7B2-PAC binds to the cell surface and is internalized, possibly localizing to ER and Golgi, within one hour. We suggest studying the intracellular trafficking of PAC immunotoxins for the next study.

Herein, we have shown the presence of CD4 have a synergic effect on 7B2-ITs. Previously, our partner, Prof. Seth Pincus, demonstrated that the gp41 heptad repeat (HR) and loop region were the best targets for cytotoxic ITs when used in conjunction with soluble CD4 (sCD4) (143). The addition of sCD4 destabilizes the gp120-gp41 interaction, resulting in greater exposure of this otherwise partially obscured epitope. Others have also targeted this region. A different group of investigators has focused on the CD4-binding site (CD4bs) as the target of choice.

Previous studies have identified the two target epitopes most effective for the delivery of cytotoxic immunoconjugates the CD4-binding site of gp120, and the hairpin loop of gp41 (140). Hence, we suggest designing double variable domain immunoglobulin molecules (DVD-Igs) that bind to both epitopes, containing both 7B2 and HY parental antibody.

We conclude that pulchellin A chain can function effectively within an IT. PAC-IT toxicity appears somewhat less than RAC-IT, the standard for comparison. This is the first demonstration that PAC may have utility for the design and construction of therapeutic ITs, highlighting the potential role for specific cell targeting not only for AIDS also cancer treatment.

6 PUBLICATIONS EXTRACTED FROM THIS STUDY:

MOHAMMAD SADRAEIAN, FRANCISCO EDUARDO GONTIJO GUIMARÃES, ANA PAULA ULIAN DE ARAÚJO, SETH H. PINCUS, DAVID K. WORTHYLAKE. Selective cytotoxicity of a novel immunotoxin based on Pulchellin A chain towards HIV infected or transfected cells. **Nature, Sci Rep**, 2017; 7(1),7579

M. SADRAEIAN, F. M. TSUTAE, H. H. T. MOREIRA, A. P. U. ARAUJO, F. E. G. GUIMARÃES, S. H. PINCUS. Preparation of HIV monoclonal antibody-conjugated pulchellin in order to study its intracellular trafficking pathway in HIV-infected cells by confocal microscopy. **SPIE 9531, Biophotonics South America**, 953117 (June 19, 2015); doi:10.1117/12.2181011

Title of patent: Immunotoxins based on Pulchellin for HIV immunotherapy, **Patent type:** Grant, **Inventors:** MOHAMMAD SADRAEIAN, FRANCISCO EDUARDO GONTIJO GUIMARÃES*, ANA PAULA ULIAN DE ARAÚJO, SETH H. PINCUS, **Filed:** August 22, 2017, **Assignee:** University of Sao Paulo.

7 ACKNOWLEDGMENT:

Special thanks to Prof. Bing Chen from the Department of Pediatrics, Harvard Medical School for the generous gift of 293 T cell lines stably transfected with 92UG037.8 gp160s. We acknowledge Children's Hospital of New Orleans, CAPES and CNPq for the financial support to carry out this research. The authors acknowledge the support provided by: FAPESP (Sao Paulo Research Foundation) –grant numbers: 2013/07276-1(CEPOF – CEPID Program), 2009/54035-4 (EMU). S.H. Pincus was supported by NIH grant U54 GM104940 (Louisiana Clinical and Translational Science Center). We also thank NIH AIDS Research and Reference Reagent Program for supporting the reagent related to HIV.

REFERENCES

- 1 CONSULTATION, W. H. O. et al. Animal models for HIV infection and AIDS: memorandum from a WHO meeting. **Bulletin of the World Health Organization**, v. 66, n. 5, p. 561–574, 1988.
- 2 DOLIN, R. Human studies in the development of human immunodeficiency virus vaccines. **Journal of Infectious Diseases**, v. 172, n. 5, p. 1175–1183, 1995.
- 3 BARTON F HAYNES. NIH Public Access. **Expert Review of Vaccines**, v. 29, n. 6, p. 997–1003, 2006.
- 4 MERK, A.; SUBRAMANIAM, S. HIV-1 envelope glycoprotein structure. **Current Opinion in Structural Biology**, v. 23, n. 2, p. 268–276, 2013.
- 5 STIRPE, F. Ribosome-inactivating proteins. **Toxicon**, v. 44, n. 4, p. 371–383, 2004.
- 6 SANDVIG, K.; VAN DEURS, B. Transport of protein toxins into cells: pathways used by ricin, cholera toxin and Shiga toxin. **FEBS Letters**, v. 529, n. 1, p. 49–53, 2002.
- 7 STIRPE, F. Ribosome-inactivating proteins: from toxins to useful proteins. **Toxicon**, v. 67, p. 12–16, 2013. doi: 10.1016/j.toxicon.2013.02.005.
- 8 DE VIRGILIO, M. et al. Ribosome-inactivating proteins: From plant defense to tumor attack. **Toxins**, v. 2, n. 11, p. 2699–2737, 2010.
- 9 PURI, M. et al. Ribosome-inactivating proteins: current status and biomedical applications. **Drug Discovery Today**, v. 17, n. 13–14, p. 774–783, 2012.
- 10 SADRAEIAN, M. et al. Induction of antitumor immunity against cervical cancer by protein HPV-16 E7 in fusion with ricin B chain in tumor-bearing mice. **International Journal of Gynecological Cancer**, v. 23, n. 5, p. 809–814, 2013.
- 11 PINCUS, S. H. et al. In vitro efficacy of anti-HIV immunotoxins targeted by various antibodies to the envelope protein. **Journal of Immunology**, v. 146, n. 12, p. 4315–4324, 1991.
- 12 STIRPE, F. Ribosome-inactivating proteins. In: WILEY, R. G.; LAPPI, D. A. (Ed.) **Molecular neurosurgery with targeted toxins**, Totowa: Humana Press, 2005. p. 9–29.
- 13 SANDVIG, K. et al. Ricin transport into cells: studies of endocytosis and intracellular transport. **International Journal of Medical Microbiology**, v. 290, n. 4–5, p. 415–420, 2000.
- 14 BONNESS, M. S. et al. Pokeweed antiviral protein inactivates pokeweed ribosomes; implications for the antiviral mechanism. **Plant Journal**, v. 5, n. 2, p. 173–183, 1994.

15 SANDVIG, K. et al. Retrograde transport from the Golgi complex to the ER of both Shiga toxin and the nontoxic Shiga B-fragment is regulated by butyric acid and cAMP. **Journal of Cell Biology**, v. 126, n. 1, p. 53–64, 1994.

16 TOO, P. H. M. et al. The C-terminal fragment of the ribosomal P protein complexed to trichosanthin reveals the interaction between the ribosome-inactivating protein and the ribosome. **Nucleic Acids Research**, v. 37, n. 2, p. 602–610, 2009.

17 CHOI, A. et al. Structures of eukaryotic ribosomal stalk proteins and its complex with trichosanthin, and their implications in recruiting ribosome-inactivating proteins to the ribosomes. **Toxins**, v. 7, n. 3, p. 638–647, 2015.

18 SANDVIG, K. et al. Ricin transport in brefeldin A-treated cells: correlation between Golgi structure and toxic effect. **Journal of Cell Biology**, v. 115, n. 4, p. 971–981, 1991.

19 SADRAEIAN, M. et al. Prevention and inhibition of TC-1 cell growth in tumor bearing mice by HPV16 E7 protein in fusion with shiga toxin b-subunit from shigella dysenteriae. **Cell journal**, v. 15, n. 2, p. 176–81, 2013.

20 SADRAEIAN, M. et al. Modification in media composition to obtain secretory production of STxB-based vaccines using Escherichia coli. **Virologica Sinica**, v. 28, n. 1, p. 43–48, 2013.

21 RUDOLPH, M. J. et al. Crystal structures of ricin toxin's enzymatic subunit (RTA) in complex with neutralizing and non-neutralizing single-chain antibodies. **Journal of Molecular Biology**, v. 426, n. 17, p. 3057–3068, 2014.

22 HASSETT, K. J. et al. Stabilization of a recombinant ricin toxin A subunit vaccine through lyophilization. **European Journal of Pharmaceutics and Biopharmaceutics**, v. 85, n. 2, p. 279–286, 2013.

23 MANSOURI, S. et al. Suppression of human T-cell leukemia virus I gene expression by pokeweed antiviral protein. **Journal of Biological Chemistry**, v. 284, n. 45, p. 31453–31462, 2009.

24 SADRAEIAN, M. et al. Extraction, cloning and expression of RTB, as a vaccine adjuvant/carrier. **Iranian Journal of Pharmaceutical Sciences**, v. 7, n. 4, p. 247–254, 2011.

25 _____. Cloning and expression of CtxB-StxB in Escherichia coli: a challenge for improvement of immune response against StxB. **Iranian Journal of Pharmaceutical Sciences**, v. 7, n. 3, p. 185–190, 2011.

26 CASTILHO, P. V. et al. Isolation and characterization of four type 2 ribosome inactivating pulchellin isoforms from Abrus pulchellus seeds. **FEBS Journal**, v. 275, n. 5, p. 948–959, 2008.

27 SILVA, A. L. C. et al. Pulchellin, a highly toxic type 2 ribosome-inactivating protein from Abrus pulchellus: Cloning, heterologous expression of A-chain and structural studies. **FEBS Journal**, v. 272, n. 5, p. 1201–1210, 2005.

- 28 GOTO, L. S. et al. Abrus pulchellus type-2 RIP, pulchellin: Heterologous expression and refolding of the sugar-binding B chain. **Protein Expression and Purification**, v. 31, n. 1, p. 12–18, 2003.
- 29 REYES, L. F. et al. The role of the C-terminal region of pulchellin A-chain in the interaction with membrane model systems. **Biochimica et Biophysica Acta - biomembranes**, v. 1818, n. 1, p. 82–89, 2012.
- 30 GOTO, L. S. et al. Endocytosis of pulchellin and its recombinant B-chain into K-562 cells: binding and uptake studies. **Biochimica et Biophysica Acta**, v. 1770, n. 12, p. 1660–6, 2007.
- 31 GOTO, L. S. et al. Endocytosis of pulchellin and its recombinant B-chain into K-562 cells: Binding and uptake studies. **Biochimica et Biophysica Acta - general subjects**, v. 1770, n. 12, p. 1660–1666, 2007.
- 32 VON BEHRING, E. K. The mechanism of diphtheria immunity and tetanus immunity in animals. **Molecular Immunology**, v. 28, n. 12, p. 1317, 1319–20, 1991.
- 33 BEHRING, E. **The nobel prize in physiology or medicine 1901**. Available from: <http://www.nobelprize.org/nobel_prizes/medicine/laureates/1901>. Accessible at: 23 Jan. 2016.
- 34 EHRLICH, P. On immunity with special reference to cell life. **Proceedings of the Royal Society of London**, v. 66, p. 424–448, 1900.
- 35 TISELIUS, A.; KABAT, E. A. Electrophoresis of immune serum. **Science**, v. 87, n. 2262, p. 416–7, 1938.
- 36 SLATER, R.J.; WARD, S. M.; KUNKEL, H. G. Immunological relationships among the myeloma proteins. **Journal of Experimental Medicine**, v. 101, n. 1, p. 85–108, 1955.
- 37 HARBOE, M. et al. Genetic characters of human gamma-globulins in myeloma proteins. **Journal of Experimental Medicine**, v. 116, p. 719–738, 1962.
- 38 EDELMAN, G. M. et al. Structural differences among antibodies of different specificities. **Proceedings of the National Academy of Sciences**, v. 47, n. 11, p. 1751–8, 1961.
- 39 PORTER, R. R. The structural basis of antibody specificity. **Bulletin de la Societe de Chimie Biologique**, v. 50, n. 5, p. 991–995, 1968.
- 40 _____. The hydrolysis of rabbit γ -globulin and antibodies with crystalline papain. **Biochemical Journal**, v. 73, n. 1, p. 119–126, 1959.
- 41 WEIR, R. C.; PORTER, R. R. Comparison of the structure of the immunoglobulins from horse serum. **Biochemical Journal**, v. 100, n. 1, p. 63–68, 1966.
- 42 POLJAK, R. J. Three-dimensional structure, function and genetic control of immunoglobulins. **Nature**, v. 256, n. 5516, p. 373–376, 1975.

- 43 DWEK, R. A. et al. Structure of an antibody combining site by magnetic resonance. **Nature**, v. 266, n. 5597, p. 31–37, 1977.
- 44 HOZUMI, N.; TONEGAWA, S. Evidence for somatic rearrangement of immunoglobulin genes coding for variable and constant regions. **Proceedings of the National Academy of Sciences**, v. 73, n. 10, p. 3628–3632, 1976.
- 45 VAN HAUWERMEIREN, F.; VANDENBROUCKE, R. E.; LIBERT, C. Treatment of TNF mediated diseases by selective inhibition of soluble TNF or TNFR1. **Cytokine & Growth Factor Reviews**, v. 22, n. 5, p. 311–319, 2011.
- 46 RICE, G. P.; HARTUNG, H. P.; CALABRESI, P. A. Anti-alpha4 integrin therapy for multiple sclerosis: mechanisms and rationale. **Neurology**, v. 64, n. 8, p. 1336–1342, 2005.
- 47 WALDMANN, T. A. Immunotherapy: past, present and future. **Nature Medicine**, v. 9, n. 3, p. 269–277, 2003.
- 48 UNIVERSITY OF ARIZONA. **Immunology**. Available from: <<http://www.biology.arizona.edu/immunology/immunology.html>>. Accessible at: 23 Jan. 2017.
- 49 PETERMANN, M.L.; PAPPENHEIMER, A .M. J. The action of crystalline pepsin on horse anti-pneumococcus antibody. **Science**, v. 93, n. 2419, p. 458, 1941.
- 50 MURPHY, K.; TRAVERS, P.; WALPORT, M.; JANEWAY, C. Janeway's immunobiology. 8th ed. London : Garland Science, 2012.
- 51 FORTHAL, D. N. et al. Recombinant gp120 vaccine-induced antibodies inhibit clinical strains of HIV-1 in the presence of Fc receptor-bearing effector cells and correlate inversely with HIV infection rate. **Journal of immunology**, v. 178, n. 10, p. 6596–6603, 2007.
- 52 BECK, A. et al. Strategies and challenges for the next generation of therapeutic antibodies. **Nature Reviews Immunology**, v. 10, n. 5, p. 345–352, 2010.
- 53 BAUM, L. L. et al. HIV-1 gp120-specific antibody-dependent cell-mediated cytotoxicity correlates with rate of disease progression. **Journal of Immunology**, v. 157, n. 5, p. 2168–2173, 1996.
- 54 FORTHAL, D. N. et al. Antibody from patients with acute human immunodeficiency virus (HIV) infection inhibits primary strains of HIV type 1 in the presence of natural-killer effector cells. **Journal of Virology**, v. 75, n. 15, p. 6953–6961, 2001.
- 55 IDUSOGIE, E. E. et al. Mapping of the C1q binding site on rituxan, a chimeric antibody with a human IgG1 Fc. **Journal of Immunology**, v. 164, n. 8, p. 4178–4184, 2000.
- 56 MURPHY, K.; TRAVERS, P.; WALPORT, M.; JANEWAY, C. **Janeway's immunobiology**. 8th ed. London : Garland Science, 2012.

57 TOTH, F. D. et al. Complement-dependent cytotoxicity of antibodies reactive with HIV-induced cell surface antigens in HIV-carrying haemophiliacs. **Acta Virologica**, v. 33, n. 6, p. 521–526, 1989.

58 AASA-CHAPMAN, M.M. et al. Detection of antibody-dependent complement-mediated inactivation of both autologous and heterologous virus in primary human immunodeficiency virus type 1 infection. **Journal of Virology**, v. 79, n. 5, p. 2823–2830, 2005.

59 ROBINSON, W. E. et al. Complement-mediated antibody-dependent enhancement of HIV-1 infection requires CD4 and complement receptors. **Virology**, v. 175, n. 2, p. 600–604, 1990.

60 BECK, Z.; PROHASZKA, Z.; FUST, G. Traitors of the immune system-enhancing antibodies in HIV infection: their possible implication in HIV vaccine development. **Vaccines**, v. 26, n. 24, p. 3078–3085, 2008.

61 ISRAEL, E. J. et al. Expression of the neonatal Fc receptor, FcRn, on human intestinal epithelial cells. **Immunology**, v. 92, n. 1, p. 69–74, 1997.

62 GHETIE, V. et al. Abnormally short serum half-lives of IgG in beta 2-microglobulin-deficient mice. **European Journal of Immunology**, v. 26, n. 3, p. 690–696, 1996.

63 ZHU, X. et al. MHC class I-related neonatal Fc receptor for IgG is functionally expressed in monocytes, intestinal macrophages, and dendritic cells. **Journal of Immunology**, v. 166, n. 5, p. 3266–3276, 2001.

64 HINTON, P. R. et al. Engineered human IgG antibodies with longer serum half-lives in primates. **Journal of Biological Chemistry**, v. 279, n. 8, p. 6213–6216, 2004.

65 HESSELL, A.J. et al. Fc receptor but not complement binding is important in antibody protection against HIV. **Nature**, v. 449, n. 7158, p. 101–104, 2007.

66 ACTIP. mAb review. Available from: < <http://www.actip.org/products/human-vaccines-produced-with-animal-cell-technology-status-2012/>>. Accessible at: 23 Jan. 2016.

67 EIBL, M. M. History of immunoglobulin replacement. **Immunology and Allergy Clinics of North America**, v. 28, n. 4, p. 737–764, 2008.

68 KRAUSE, I. et al. In vitro antiviral and antibacterial activity of commercial intravenous immunoglobulin preparations--a potential role for adjuvant intravenous immunoglobulin therapy in infectious diseases. **Transfusion Medicine**, v. 12, n. 2, p. 133–139, 2002.

69 STEIN, E. A. et al. Effect of a monoclonal antibody to PCSK9 on LDL cholesterol. **New England Journal of Medicine**, v. 366, n. 12, p. 1108–1118, 2008.

70 CAI, H. Therapeutic monoclonal antibodies approved by FDA in 2016. **MOJ Immunology**, v. 5, n. 1, 2017. doi: 10.15406/moji.2016.05.00145.

71 ROBINSON, K. A.; ODELOLA, O. A.; SALDANHA, I. J. Palivizumab for prophylaxis against respiratory syncytial virus infection in children with cystic fibrosis. **Cochrane Database of Systematic Reviews**, n. 7, n. 1, p. 1–10, 2016.

72 TRUVEN HEALTH ANALYTICS, I. Orthoclone OKT3. Available from: <<https://www.drugs.com/cons/orthoclone-okt-3.html>>. Accessible at: 21 Sept. 2017.

73 HUDIS, C. A. Trastuzumab--mechanism of action and use in clinical practice. **New England Journal of Medicine**, v. 357, n. 1, p. 39–51, 2007.

74 BONNER, J. A. et al. Radiotherapy plus cetuximab for squamous-cell carcinoma of the head and neck. **New England Journal of Medicine**, v. 354, n. 6, p. 567–578, 2006.

75 EEVA, J. et al. The involvement of mitochondria and the caspase-9 activation pathway in rituximab-induced apoptosis in FL cells. **Apoptosis**, v. 14, n. 5, p. 687–698, 2009.

76 SOCHAJ, A. M.; ŚWIDERSKA, K. W.; OTLEWSKI, J. Current methods for the synthesis of homogeneous antibody-drug conjugates. **Biotechnology Advances**, v. 33, n. 6, 2015. doi: 10.1016/j.biotechadv.2015.05.001.

77 GOSWAMI, S. et al. Developments and challenges for mAb-Based Therapeutics. **Antibodies**, v. 2, n. 3, p. 452–500, 2013.

78 TRAIL, P. Antibody drug conjugates as cancer therapeutics. **Antibodies**, v. 2, n. 2, p. 113–129, 2013.

79 HAMLIN, A. Developmental therapeutics meeting. in therapeutic immunoconjugates in the treatment of hematological malignancies. In: CONFERENCE STATE-OF-THE-ART AND FUTURE STRATEGIES. **Anais...**2010

80 FRANCISCO, J. A. et al. cAC10-vcMMAE, an anti-CD30-monomethyl auristatin E conjugate with potent and selective antitumor activity. **Blood**, v. 102, n. 4, p. 1458–1465, 2003.

81 JACENE, H. A. et al. Comparison of 90Y-ibritumomab tiuxetan and 131I-tositumomab in clinical practice. **Journal of Nuclear Medicine**, v. 48, n. 11, p. 1767–1776, 2007.

82 SMAGLO, B. G. et al. The development of immunoconjugates for targeted cancer therapy. **Nature Reviews Clinical Oncology**, v. 11, n. 11, p. 637–648, 2016.

83 WORLD HEALTH ORGANIZATION. Global Health Observatory data. **HIV/AIDS** . Available from: <<http://www.who.int/gho/hiv/en/>>. Accessible at: 23 Jan. 2017.

84 LOS ALAMOS HIV DATABASES. **HIV molecular immunology database: tools & links**. Available from: <<https://www.hiv.lanl.gov/content/immunology/tools-links.html>>. Accessible at: 23 Jan. 2017

85 KONSTANTINOV, I. et al. Visualization challenge 2010 - illustration. **SCIENCE**, v. 331, n. 6019, p. 848–849, 2011.

- 86 SILICIANO, J. D. et al. Long-term follow-up studies confirm the stability of the latent reservoir for HIV-1 in resting CD4+ T cells. **Nature Medicine**, v. 9, n. 6, p. 727–728, 2003.
- 87 MOSSMAN, S. P. et al. Protective immunity to SIV challenge elicited by vaccination of macaques with multigenic DNA vaccines producing virus-like particles. **AIDS Research and Human Retroviruses**, v. 20, n. 4, p. 425–434, 2004.
- 88 HAMER, D. H. Can HIV be cured? mechanisms of HIV persistence and strategies to combat it. **Current HIV Research**, v. 2, n. 2, p. 99–111, 2004.
- 89 SEKALY, R. P. The failed HIV Merck vaccine study: a step back or a launching point for future vaccine development? **Journal of Experimental Medicine**, v. 205, n. 1, p. 7–12, 2008.
- 90 HAYNES, B.F. et al. Immune-correlates analysis of an HIV-1 vaccine efficacy trial. **New England Journal of Medicine**, v. 366, n. 14, p. 1275–1286, 2012.
- 91 WEI, X. et al. Antibody neutralization and escape by HIV-1. **Nature**, v. 422, n. 6929, p. 307–312, 2003.
- 92 WALKER, L.M. et al. Broad neutralization coverage of HIV by multiple highly potent antibodies. **Nature**, v. 477, n. 7365, p. 466–470, 2011.
- 93 KWONG, P. D. et al. HIV-1 evades antibody-mediated neutralization through conformational masking of receptor-binding sites. **Nature**, v. 420, n. 6916, p. 678–682, 2002.
- 94 KWONG, P. D. et al. Structure of an HIV gp120 envelope glycoprotein in complex with the CD4 receptor and a neutralizing human antibody. **Nature**, v. 393, n. 6686, p. 648–659, 1998.
- 95 FLYNN, N. M. et al.. Placebo-controlled phase 3 trial of a recombinant glycoprotein 120 vaccine to prevent HIV-1 infection. **Journal of Infectious Diseases**, v. 191, n. 5, p. 654–665, 2005.
- 96 PRIDDY, F. H. et al. Safety and immunogenicity of a replication-incompetent adenovirus type 5 HIV-1 clade B gag/pol/nef vaccine in healthy adults. **Clinical Infectious Diseases**, v. 46, n. 11, p. 1769–1781, 2008.
- 97 PITISUTTITHUM, P. et al. Safety and reactogenicity of canarypox ALVAC-HIV (vCP1521) and HIV-1 gp120 AIDSVAX B/E vaccination in an efficacy trial in Thailand. **PLoS ONE**, v. 6, n. 12, p. 27837, 2011.
- 98 CALLAWAY, E. Clues emerge to explain first successful HIV vaccine trial. **Nature**, v. 523, n. 7017, 2011. doi:10.1038/news.2011.541.
- 99 PARREN, P. W. H. I. et al. Relevance of the antibody response against human immunodeficiency virus type 1 envelope to vaccine design. **Immunology Letters**, v. 58, n. 2, p. 105–112, 1997.
- 100 WYATT, R.; SODROSKI, J. The HIV-1 envelope glycoproteins: fusogens, antigens, and immunogens. **Science**, v. 280, n. 5371, p. 1884–1888, 1998.

101 ZHU, P. et al. Cryoelectron tomography of HIV-1 envelope spikes: further evidence for tripod-like legs. **PLoS Pathogens**, v. 4, n. 11, p. 1000203, 2008.

102 MOORE, J. P. et al. Dissociation of gp120 from HIV-1 virions induced by soluble CD4. **Science**, v. 250, n. 4984, p. 1139–1142, 1990.

103 RIZZUTO, C. D. et al. Conserved HIV gp120 glycoprotein structure involved in chemokine receptor binding. **Science**, v. 86, n. 17, p. 6768–6772, 1989.

104 CONLEY, A. J. et al. Neutralization of primary human immunodeficiency virus type 1 isolates by the broadly reactive anti-V3 monoclonal antibody. **Journal of Virology**, v. 68, n. 11, p. 6994–7000, 1994.

105 HAIGWOOD, N. L. et al. Importance of hypervariable regions of HIV-1 gp120 in the generation of virus neutralizing antibodies. **AIDS Research and Human Retroviruses**, v. 6, n. 7, p. 855–869, 1990.

106 DUBRUILLE, R. et al. Specialization of a Drosophila capping protein essential for the protection of sperm telomeres. **Current Biology**, v. 20, n. 23, p. 2090–2099, 2010.

107 LEONARD, C. K. et al. Assignment of intrachain disulfide bonds and characterization of potential glycosylation sites of the type 1 recombinant human immunodeficiency virus envelope glycoprotein (gp120) expressed in Chinese hamster ovary cells. **Journal of Biological Chemistry**, v. 265, n. 18, p. 10373–10382, 1990.

108 SAPHIRE, E. O. et al. Crystal structure of a neutralizing human IGG against HIV-1: a template for vaccine design. **Science**, v. 293, n. 5532, p. 1155–1159, 2001.

109 ZHOU, T. et al. Structural definition of a conserved neutralization epitope on HIV-1 gp120. **Nature**, v. 445, n. 7129, p. 732–737, 2007.

110 ARMBRUSTER, C. et al. Passive immunization with the anti-HIV-1 human monoclonal antibody (hMAb) 4E10 and the hMAb combination 4E10/2F5/2G12. **Journal of Antimicrobial Chemotherapy**, v. 54, n. 5, p. 915–920, 2004.

111 WALKER, L. M. et al. Broad and potent neutralizing antibodies from an African donor reveal a new HIV-1 vaccine target. **Science**, v. 326, n. 5950, p. 285–289, 2009.

112 CALARESE, D. A. et al. Antibody domain exchange is an immunological solution to carbohydrate cluster recognition. **Science**, v. 300, n. 5628, p. 2065–2071, 2003.

113 GORNY, M. K.; ZOLLA-PAZNER, S. Recognition by human monoclonal antibodies of free and complexed peptides representing the prefusogenic and fusogenic forms of human immunodeficiency virus type 1 gp41. **Journal of Virology**, v. 74, n. 13, p. 6186–6192, 2000.

114 XU, J. Y. et al. Epitope mapping of two immunodominant domains of gp41, the transmembrane protein of human immunodeficiency virus type 1, using ten human monoclonal antibodies. **Journal of Virology**, v. 65, n. 9, p. 4832–4838, 1991.

115 TRKOLA, A. et al. Cross-clade neutralization of primary isolates of human immunodeficiency virus type 1 by human monoclonal antibodies and tetrameric CD4-IgG. **Journal of Virology**, v. 69, n. 11, p. 6609–6617, 1995.

116 D'SOUZA, M. P. et al. Evaluation of monoclonal antibodies to human immunodeficiency virus type 1 primary isolates by neutralization assays: performance criteria for selecting candidate antibodies for clinical trials. AIDS clinical trials group antibody selection working group. **Journal of Infectious Diseases**, v. 175, n. 5, p. 1056–1062, 1997.

117 CORTI, D., LANGEDIJK, J.P., HINZ, A., SEAMAN, M.S., VANZETTA, F. Analysis of memory B cell responses and isolation of novel monoclonal antibodies with neutralizing breadth from HIV-1-infected individuals. **PLoS One**, v. 5, n. 1, p. 8805, 2010.

118 BARBATO, G. et al. Structural analysis of the epitope of the anti-HIV antibody 2F5 sheds light into its mechanism of neutralization and HIV fusion. **Journal of Molecular Biology**, v. 2836, n. 3, p. 1101–1115, 2003.

119 WALKER, L. M. et al. Broad and potent neutralizing antibodies from an African donor reveal a new HIV-1 vaccine target. **Science**, v. 326, n. 5950, p. 285–289, 2009.

120 WU, X. et al. Immunotypes of a quaternary site of HIV-1 vulnerability and their recognition by antibodies. **Journal of Virology**, v. 85, n. 9, p. 4578–4585, 2011.

121 MOULARD, M. et al. Broadly cross-reactive HIV-1-neutralizing human monoclonal Fab selected for binding to gp120-CD4-CCR5 complexes. **Proceedings of the National Academy of Sciences of the United States of America**, v. 99, n. 10, p. 6913–6918, 2002.

122 THALI, M., MOORE, J.P., FURMAN, C., CHARLES, M., HO, D. D. Characterization of conserved human immunodeficiency virus type 1 gp120 neutralization epitopes exposed upon gp120-CD4 binding. **Journal of Virology**, v. 67, n. 7, p. 3978–3988, 1993.

123 CHOUDHRY, V. et al. Cross-reactive HIV-1 neutralizing monoclonal antibodies selected by screening of an immune human phage library against an envelope glycoprotein (gp140) isolated from a patient (R2) with broadly HIV-1 neutralizing antibodies. **Virology**, v. 363, n. 1, p. 79–90, 2007.

124 MADDON, P. J. et al. The T4 gene encodes the AIDS virus receptor and is expressed in the immune system and the brain. **Cell Journal**, v. 47, n. 3, p. 333–348, 1986.

125 PINCUS, S. H. et al. A modified SCID mouse model of HIV infection with utility for testing anti-HIV therapies: Comparative activity of antibodies and immunotoxins. **AIDS Research and Human Retroviruses**, v. 19, p. 901–909, 2003.

126 GAUDUIN, M.C. et al. CD4-immunoglobulin G2 protects Hu-PBL-SCID mice against challenge by primary human immunodeficiency virus type 1 isolates. **Journal of Virology**, v. 72, n. 4, p. 3475–3478, 1998.

127 SHEARER, W. T. et al. Recombinant CD4-IgG2 in human immunodeficiency virus type 1-infected children: phase 1/2 study. the pediatric AIDS clinical trials group protocol 351 study team. **Journal of Infectious Diseases**, v. 182, n. 6, p. 1774–1779, 2000.

- 128 WU, X. et al. Rational design of envelope identifies broadly neutralizing human monoclonal antibodies to HIV-1. **Science**, v. 329, n. 5993, p. 856–861, 2010.
- 129 FRIEDMAN, J. et al. Isolation of HIV-1-Neutralizing Mucosal Monoclonal Antibodies from Human Colostrum. **PLoS One**, v. 7, n. 5, p. e37648, 2012.
- 130 BURTON, D. R.; WEISS, R. A. AIDS/HIV. a boost for HIV vaccine design. **Science**, v. 329, n. 5993, p. 770–773, 2010.
- 131 PINCUS, S. H. et al. Variants selected by treatment of human immunodeficiency virus-infected cells with an immunotoxin. **Journal of Experimental Medicine**, v. 172, n. 3, p. 745–757, 1990.
- 132 _____. In vitro effects of anti-HIV immunotoxins directed against multiple epitopes on HIV type 1 envelope glycoprotein 160. **AIDS Research and Human Retroviruses**, v. 12, n. 11, p. 1041–1051, 1996.
- 133 ASHORN, P.; MOSS, B.; BERGER, E. A. Activity of CD4-pseudomonas exotoxin against cells expressing diverse forms of the HIV and SIV envelope glycoproteins. **Journal of Acquired Immune Deficiency Syndromes**, v. 5, n. 1, p. 70–77, 1992.
- 134 SAAVEDRA-LOZANO, J. et al. An anti-CD45RO immunotoxin kills latently infected human immunodeficiency virus (HIV) CD4 T cells in the blood of HIV-positive persons. **Journal of Infectious Diseases**, v. 183, n. 3, p. 306–314, 2002.
- 135 MCHUGH, L. et al. Increased affinity and stability of an anti-HIV-1 envelope immunotoxin by structure-based mutagenesis. **Journal of Biological Chemistry**, v. 277, n. 37, p. 34383–34390, 2002.
- 136 PINCUS, S. H. et al. In vivo efficacy of anti-glycoprotein 41, but not anti-glycoprotein 120, immunotoxins in a mouse model of HIV infection. **Journal of Immunology**, v. 170, n. 4, p. 2236–2241, 2003.
- 137 PINCUS, S. H. et al. Vaccine-specific antibody responses induced by HIV-1 envelope subunit vaccines. **Journal of Immunology**, v. 158, n. 7, p. 3511–3520, 1997.
- 138 KOCH, M. et al. Structure-based, targeted deglycosylation of HIV-1 gp120 and effects on neutralization sensitivity and antibody recognition. **Virology**, v. 313, n. 2, p. 387–400, 2003.
- 139 RAMAKRISHNAN, S.; HOUSTON, L. L. Comparison of the selective cytotoxic effects of immunotoxins containing ricin A chain or pokeweed antiviral protein and anti-Thy 1.1 monoclonal antibodies. **Cancer Research**, v. 44, n. 1, p. 201–208, 1984.
- 140 CRAIG, R. B. et al. Anti-HIV double variable domain immunoglobulins binding both gp41 and gp120 for targeted delivery of immunoconjugates. **PLoS One**, v. 7, n. 10, p. 1–13, 2012.
- 141 PINCUS, S. H. et al. In vivo efficacy of anti-glycoprotein 41, but not anti-glycoprotein 120, immunotoxins in a mouse model of HIV infection. **Journal of Immunology**, v. 170, n. 4, p. 2236–2241, 2003.

142 RASO, V. et al. Monoclonal antibody-ricin A chain conjugate selectively cytotoxic for cells bearing the common acute lymphoblastic leukemia antigen. **Cancer Research**, v. 42, n. 2, p. 457–464, 1982.

143 PINCUS, S. H.; MCCLURE, J. Soluble CD4 enhances the efficacy of immunotoxins directed against gp41 of the human immunodeficiency virus. **Proceedings of the National Academy of Sciences of the United States of America**, v. 90, n. 1, p. 332–336, 1993.

144 BAROUCH, D. H. et al. Therapeutic efficacy of potent neutralizing HIV-1-specific monoclonal antibodies in SHIV-infected rhesus monkeys. **Nature**, v. 503, n. 7475, p. 224–8, 2013.

145 PINCUS, S. H.; WEHRLY, K. AZT Demonstrates Anti-HIV-1 Activity in Persistently Infected Cell Lines: Implications for Combination Chemotherapy and Immunotherapy. **Journal of Infectious Diseases**, v. 162, n. 6, p. 1233–1238, 1990.

146 PINCUS, S. H. et al. Identification of Human Anti-HIV gp160 Monoclonal Antibodies That Make Effective Immunotoxins. **Journal of Virology**, v. 91, n. 3, p. JVI.01955-16, 2017.

147 PINCUS, S. H.; WEHRLY, K.; CHESEBRO, B. Treatment of HIV tissue culture infection with monoclonal antibody-ricin A chain conjugates. **Journal of Immunology**, v. 142, n. 9, p. 3070–3075, 1989.

148 KOVACS, J. M. et al. Stable, uncleaved HIV-1 envelope glycoprotein gp140 forms a tightly folded trimer with a native-like structure. **Proceedings of the National Academy of Sciences of the United States of America**, v. 111, n. 52, p. 18542–7, 2014.

149 MCHUGH, L. et al. Increased affinity and stability of an Anti-HIV-1 envelope immunotoxin by structure-based mutagenesis. **Journal of Biological Chemistry**, v. 277, n. 37, p. 34383–34390, 2002.

150 MADDALONI, M. et al. Immunological characteristics associated with the protective efficacy of antibodies to ricin. **Journal of Immunology**, v. 172, n. 10, p. 6221–6228, 2004.

151 SONG, K. et al. Antibody to ricin a chain hinders intracellular routing of toxin and protects cells even after toxin has been internalized. **PLoS One**, v. 8, n. 4, 2013.

152 VUGHT, R. VAN; PIETERS, R. J.; BREUKINK, E. Site-specific functionalization of proteins and their applications to therapeutic antibodies Abstract : protein modifications are often required to study structure and function relationships . instead of the random labeling of lysine residues, methods ha. **Computational and Structural Biotechnology**, v. 9, n. 14, p. 1–13, 2014.

153 DOSIO, F. D.; BRUSA, P.; CATTEL, L. Immunotoxins and anticancer drug conjugate assemblies: The role of the linkage between components. **Toxins**, v. 3, n. 7, p. 848–883, 2011.

154 DICKEY, C. et al. Murine monoclonal antibodies biologically active against the amino region of HIV-1 gp120: Isolation and characterization. **DNA and Cell Biology**, v. 19, p. 243–252, 2000.

155 BUSETTO, S. et al. A single-step, sensitive flow cytometric assay for the simultaneous assessment of membrane-bound and ingested *Candida albicans* in phagocytosing neutrophils. **Cytometry Part A**: the journal of the international society for analytical cytology, v. 58, n. 2, p. 201–206, 2004.

156 PATIÑO, T. et al. Surface modification of microparticles causes differential uptake responses in normal and tumoral human breast epithelial cells. **Scientific Reports**, v. 5, p. 11371, 2015.

157 AVELAR-FREITAS, B. A. et al. Trypan blue exclusion assay by flow cytometry. **Brazilian Journal of Medical and Biological Research**, v. 47, n. 4, p. 307–315, 2014.

158 AKBARI, B. et al. Immunotoxins in cancer therapy: review and update. **International Reviews of Immunology**, v. 0, n. 0, p. 1–13, 2017.

159 RAMOS, M. V. et al. Isolation and partial characterisation of highly toxic lectins from *Abrus pulchellus* seeds. **Toxicon**, v. 36, n. 3, p. 477–484, 1998.

160 OLSNES, S.; KOZLOV, J. V. Ricin. **Toxicon**, v. 39, n. 11, p. 1723–1728, 2001.

161 SŁOMIŃSKA-WOJEWÓDZKA, M.; SANDVIG, K. Ricin and ricin-containing immunotoxins: insights into intracellular transport and mechanism of action in vitro. **Antibodies**, v. 2, n. 2, p. 236–269, 2013.

162 PINCUS, S. H. et al. Design and In Vivo Characterization of Immunoconjugates Targeting HIV gp160. **Journal of Virology**, v. 91, n. 3, p. 1–15, 2017.

163 GOOTENBERG, B. Y. J. E.; RUSCETTI, F. W.; MIER, J. W. T Cell Lymphoma And And Leukemia Cell Lines Produce Respond To T Cell Growth Factor. **Journal of Experimental Medicine**, v. 154, p. 1403–1418, 1981.